2014

In Utero Exposure To Second-Hand Smoke Aggravates Adult Responses To Inhaled Irritants

Rui Xiao
Louisiana State University and Agricultural and Mechanical College

IN UTERO EXPOSURE TO SECOND-HAND SMOKE AGGRAVATES ADULT RESPONSES TO INHALED IRRITANTS

A Dissertation

Submitted to the Graduate Faculty of the
Louisiana State University and
Agricultural and Mechanical College
in partial fulfillment of the
requirements for the degree of
Doctor of Philosophy

in

The Department of Comparative
Biomedical Sciences

by
Rui Xiao
B. S., Shanghai Jiao Tong University, 2008
May 2014

ACKNOWLEDGEMENTS

The entire faculty and office staff in the CBS Department of the LSU SVM have been extremely helpful to my educational experience at LSU. Inside our laboratory, like a warm family, there have been a number of people who contributed greatly to the work described within this manuscript and each one deserves acknowledgement and recognition for their effort---Zakia Perveen, Lindsey Clemones, Lisa Earl, Dr. Alexandra Noel and Dr. Md Hasanuzzaman.

Within the School of Veterinary Medicine, Dr. Daniel Paulsen and Dr. Viviana Le Donne, from the PBS Department, provided their histopathology expertise for the project while Dr. Rodney Rouse, formerly of CBS, now of the US Food Drug Administration, laid down the research foundation of *in utero* smoke exposures and ovalbumin challenge protocol, which are essential to the success of these studies. We also had help from further outside collaborators, including Paula Polk (LSUHSC-Shreveport) with microarray processing and Dr. Namasivayam Ambalavanan (UAB) with lung morphometric analysis. Thanks also go to my committee members, including Dr. David Horohov, Dr. Shisheng Li, Dr. Kevin Kleinow and Dr. Craig Hart (Dean's Representative), for their time serving on my committee as well as their helpful advice over the years.

Finally, I would like to express my deepest gratitude to my major advisor Dr. Arthur Penn, who has generously offered me his time, knowledge and resources. Along the last few years, he has taught me so much about scientific research as well as the American culture and has given me numerous opportunities to work on interesting projects and present new findings at research conferences. Without his support and guidance, these projects and myself would not have come this far. I am proud to call him a great mentor and a dear friend.

TABLE OF CONTENTS

LIST OF TABLES

LIST OF FIGURES

LIST OF ABBREVIATIONS

AHR.....airway hyperresponsiveness

AIR .....HEPA-filtered air

BALF .....bronchioalveolar lavage fluid

COPD.....chronic obstructive pulmonary disease

ED..... external diameter

f..... breathing frequency

FDR ..... false discovery rate

IPA.....Ingenuity Pathway Analysis

miRNA..... microRNA

MLI.....mean linear intercept

mRNA.....messenger RNA

OVA.....ovalbumin

RAC ..... radial alveolar count

WT ..... wall thickness

SHS.....second-hand smoke

ABSTRACT

In utero exposure to second-hand smoke (SHS) has modulatory effects on adult lung responses to various irritants. To further elucidate diverse responses with different inhaled irritants and to understand how long the effects persist, we have focused on two environmentally-relevant and asthma-associated irritants--SHS and ovalbumin (OVA)--for adult mice that had been exposed *in utero* to SHS.

We hypothesized that *in utero* SHS exposure aggravates lung responses to various inhaled irritants, including SHS and OVA, in adult mice beyond the age of 15 weeks; and that the responses will likely exhibit a sex bias.

Pregnant BALB/c mice were exposed (days 6-19 of pregnancy) to SHS (10 mg/m3) or HEPA-filtered air (AIR). The lung responses of 15-week-old male offspring were examined after daily exposure from 11-15 weeks of age to either SHS or AIR. Another set of lung responses were assessed on 23-week-old mice, both females and males, after OVA sensitization and challenge from 19-23 weeks of age. The assessments focused on pulmonary function, bronchoalveolar lavage fluid (BALF), histopathology, and lung transcriptome screening (mRNAs and miRNAs).

In utero SHS exposure significantly aggravates lung responses in synergy with recurring SHS to 15-week-old male mice, shown by increased airway hyper-responsiveness (AHR) and BALF pro-inflammatory cytokines. Additional morphometric analysis and transcriptome screening indicated that *in utero* exposure resulted in enlarged air spaces and arteries in adult mice regardless of adult irritants. In the case of recurring (adult) SHS exposure, pro-fibrotic genes were activated. This also was evident by increased collagen deposition in the lungs. On the other hand, *in utero* SHS exposure also aggravated lung responses to OVA in 23-week-old

mice, as indicated by further increased lung inflammation, AHR, BALF Th2 cytokines, and pro-asthmatic gene expression changes, with the majority of responses being more pronounced in males than in females. Furthermore, the additional miRNA expression screening identified overexpressed miRNAs that are oncogenic; 16 tumor suppressor genes, as targets of these miRNAs, were found to be down-regulated.

In conclusion, *in utero* SHS exposure elicits deleterious effects on adult mice challenged with inhaled irritants, and may promote and predispose affected individuals to certain respiratory diseases.

CHAPTER 1.
LITERATURE REVIEW

1.1 Short-term and Long-term Effects of Air Pollutants

Highly toxic air pollutants at relatively high doses often trigger acute lung responses and/or drastically exacerbate respiratory diseases in humans shortly after the initial exposure, and may even result in premature death. In the winter of 1952, the Great Smog in London killed 4,000 people and made 100,000 more ill within a week because of the smog's effects on the human respiratory system (Bell and Davis 2001; U.K. Ministry of Health 1954). In the case of Yokkaichi Asthma (1960-1972), an environmental disaster in Japan, the combustion products of petroleum and crude oil containing sulfur heavily polluted ambient air and induced severe cases of COPD, chronic bronchitis, pulmonary emphysema, and bronchial asthma among the local inhabitants, especially for those over the age 50 (Guo et al. 2008; Yoshida 1984).

In other cases, where environmental exposures only occurred at relatively low doses, immediately noticeable changes were not elicited; instead, such exposures have the ability to potentiate future lung responses and/or to accelerate the progression of chronic respiratory diseases, especially after a prolonged period of exposure (MacNee 2009). Therefore, a lag time exists between initial exposure and disease incidence or mortality. In the case of lung cancer, as shown in Figure 1-1, the increased numbers of premature deaths in the past hundred years was preceded by a dramatic elevation in cigarette consumption with a time lag of ~20 years.

A similar approximate 20-year lag may be expected between years of smoke exposure and the onset of other respiratory diseases, e.g., COPD, which is more common among people >65 years old than in younger people (Centers for Disease Control and Prevention 2011).

Asthma, another serious respiratory disease, is frequently diagnosed in children, especially below the age of 18 (Centers for Disease Control and Prevention 2011)

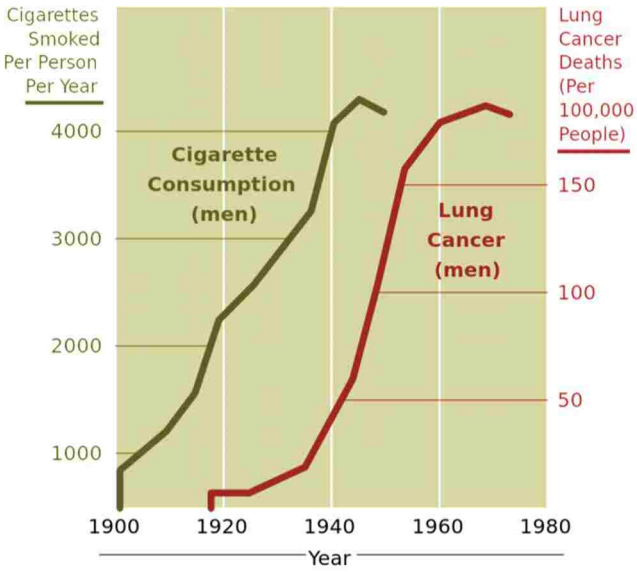

Figure 1–1. Correlation between smoking and lung cancer in US males, showing a 20-year time lag between increased smoking rates and increased incidence of lung cancer (NIH.gov).

The incidence and prevalence of asthma have been increasing dramatically in the past fifty years both in the United States (Mannino et al. 2002) and world-wide (Pearce et al. 2000). The global burden of asthma has been estimated to be as high as 300 million people (Masoli et al. 2003). On the other hand, in the United States, cigarette consumption has being decreasing (Figure 1-2) and air quality has been improving (Table 1-1) over the past 30 years, according to the official data.

If environmental stressors play a role in the increased asthma incidence, could there also be a considerable time-lag between exposure to the stressor and clinical appearance of the disease? If we assume there was also a many-years lag, this could put the time frame of initial impact even before the asthma-prone children were born, i.e., within the *in utero* environment. Although cigarette consumption in the US has decreased in the past 30 years, 25% of adults

continue to smoke on a regular basis (Matthews 2001), and 10.7% of pregnant females smoke during last 3 months of pregnancy (Centers for Disease Control and Prevention 2010). This suggested that the *in utero* exposure to cigarette smoke could be a contributing factor for increased asthma prevalence in children.

Table 1–1. Decreases in concentrations of common pollutants indicated that air quality has improved nationally since 1980 (EPA.gov).

Percentage change (%)	**1980vs2012**	**1990vs2012**	**2000vs2012**
Carbon Monoxide (CO)	-83	-75	-57
Ozone (O_3) (8-hr)	-25	-14	-9
Lead (Pb)	-91	-87	-52
Nitrogen Dioxide (NO_2) (annual)	-56	-50	-38
Nitrogen Dioxide (NO_2) (1-hour)	-60	-46	-29
PM_{10} (24-hr)	---	-39	-27
$PM_{2.5}$ (annual)	---	---	-33
$PM_{2.5}$ (24-hr)	---	---	-37
Sulfur Dioxide (SO_2) (1-hour)	-78	-72	-54

Figure 1–2. The trend of cigarette consumption in the U.S. plateaued between 1950s and 1980s (CDC.gov). Adult per capita cigarette consumption and major smoking and health events in the

United States from 1900 to 1999. Reprinted from The US Surgeon General's Report for the Year 2000.

1.2 Early Onset of Adult Respiratory Diseases

Early development of the mouse lung is a complex, multistage process which begins on E9 (embryonic day 9; week 3-4 in humans), when the lung buds appear and branching starts. As illustrated in Figure 1-3, other than the final stage, alveolar maturation, which takes place in the early postnatal environment, the early stages of lung development, including pseudoglandular, canalicular and saccular stages, occur in the *in utero* environment.

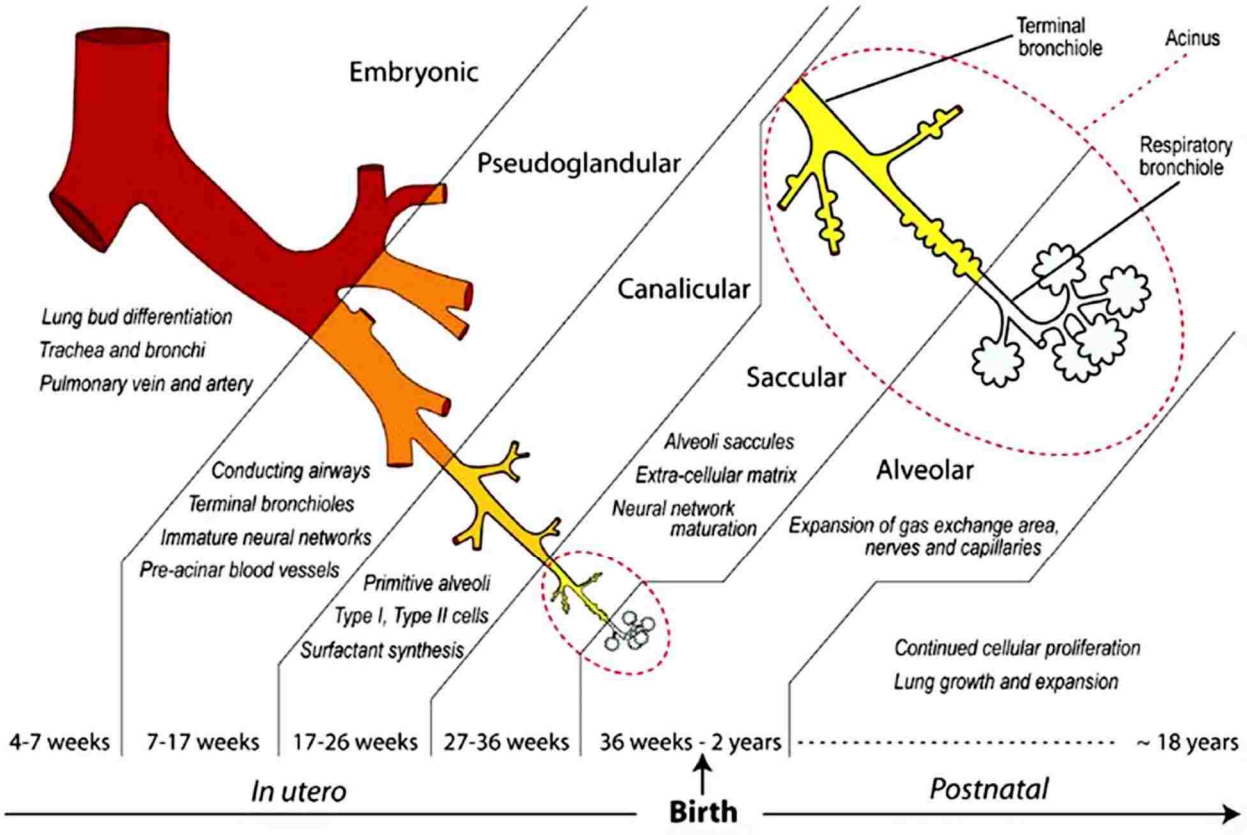

Figure 1–3. Lung development stages in humans. Equivalent time periods in mouse: embryonic, E 9-12; pseudoglandular, E 12-15; Canalicular, E 15-17; Saccular, E 17-Birth; Alveolar, Birth-PN 20. E, embryonic day. PN, postnatal day. The figure was adapted from (Kajekar et al. 2007).

In the pseudoglandular stage, major conducting airways are formed and airway branching reaches the level of the acinus, which is a collective term for the respiratory zone of the lung. The canalicular stage that follows is characterized by completion of the airway branching pattern, which marks the early stages of the future gas-exchange region. The saccular stage is characterized by coordinated growth of the pulmonary parenchyma and maturation of the neural network, while the alveoli, the gas-exchange units of the adult lung, are not yet fully developed. The final stage, alveolar maturation, takes places in the postnatal environment. During this final stage, gas exchange area, nerves and capillaries are fully expanded and matured.

Epidemiological studies have associated exposure to *in utero* stressors with intrauterine growth restriction and increased risk of respiratory problems and reduced lung function in infants, children and adults. In humans, the lungs are constantly undergoing progressive and irreversible increases in alveolar diameter, together with degradation of pulmonary structural proteins, leading to a reduction in the surface area available for gas exchange (Cotes et al. 1997). These changes predispose small airways to narrowing during expiration. Therefore, lung health and lung function during later life are dependent on the architecture of lung parenchyma that is laid down in the critical development period in early life (Figure 1-4).

In animal models, restricted growth *in utero* has been linked to reduction of internal surface area relative to lung volumes (Harding et al. 2000) and impaired growth of bronchial walls, which may have implications for airway compliance in later life (Wignarajah et al. 2002).

Not only is the *in utero* environment crucial for fetal lung development, uterine life is also critical for epigenetic programming, when environmental factors have the most potential to modulate subsequent lung responses to inhaled irritants and contribute to the susceptibility of adult diseases and disorders (Durham et al. 2010; Ho 2010).

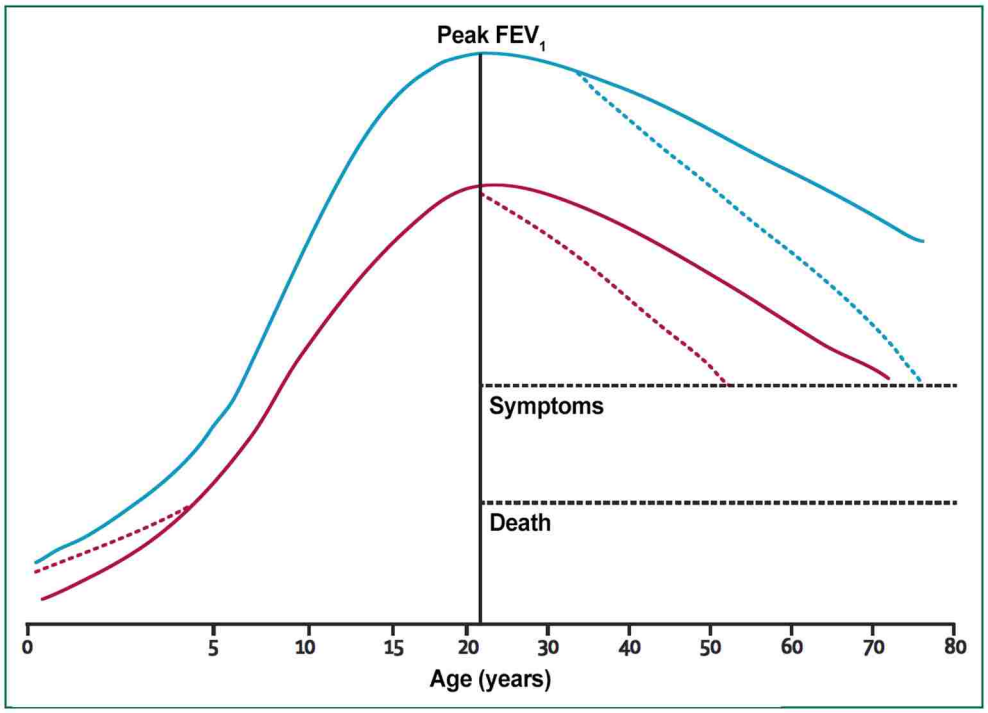

Figure 1–4. Early origins of adult lung disease. The blue line indicates healthy people (normally reaching maximum lung function at 22 years of age); red line represents people with suboptimal lung function. The dashed red line on the left represents those people with hindered lung development at an early age; the dashed red & blue lines on the right indicate people experiencing accelerated decline of lung function. The figure was adapted from (Stocks et al. 2013).

The programming effects *in utero* are believed to be primarily epigenetic, because of the stable nature of the genome (Jirtle and Skinner 2007; Szyf 2007). Since the majority of environmental factors and toxicants do not alter DNA sequence or promote genetic mutations, the epigenetic modifications are defined as the molecular factors and processes around DNA that regulate genome activity independent of DNA sequence and that are mitotically stable; as shown in Figure 1-5, these modification includes small non-coding RNAs, DNA methylations and histone modifications (Skinner and Guerrero-Bosagna 2009). These changes have the potential to explain the abnormal adult phenotypes or diseases that originated from early-life exposures (Hanson and Gluckman 2008).

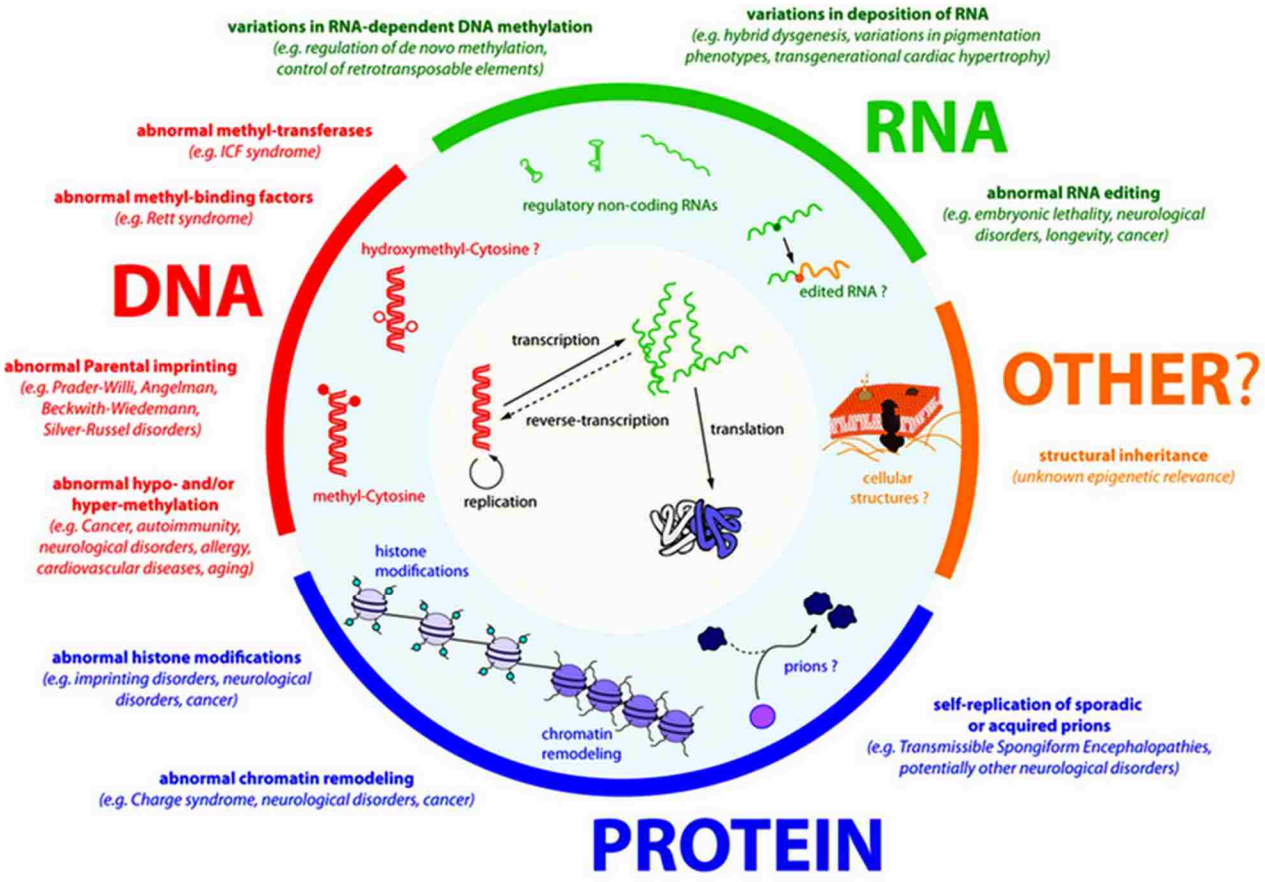

Figure 1–5. The multidimentional nature of epigenetics. DNA: hyper/hypo-methylation; RNA: regulatory/edited RNA; PROTEIN: histone modification, chromatin remodeling and prion. This figure was adapted from (Chahwan et al. 2011).

DNA methylation is an adaptable epigenetic mechanism that, in mammals, modifies genome function through the addition of methyl groups to cytosine. The methylation marks are largely established early in life (Feinberg 2007; Gluckman et al. 2008) and may ensure stable regulation that mediates persistent changes in biological and behavioral phenotypes over the lifespan (Miller and Ho 2008; Weaver et al. 2002; Wright 2010). DNA methylation is a crucial epigenetic modification of the genome that is involved in regulating many cellular processes, such as embryonic development, transcription, X chromosome inactivation and genomic imprinting.

miRNAs which are short double stranded RNA that mediate the post-transcriptional regulation of gene expression, are among the most characterized non-coding RNAs,. Bioinformatics studies suggest that up to a third of all known genes may be regulated by miRNA through RNA interference (Williams et al. 2007). Previous studies have implicated active roles for miRNAs in the course of development (Williams et al. 2006), aging processes (Boehm and Slack 2005) and the induction of diseases, including cancer (McManus 2003).

Histone proteins play a key role in chromosome assembly in the formation of nucleosomes. Amino-terminal tails of core histones are susceptible to a variety of enzyme-catalyzed posttranslational modifications, including acetylation, methylation, phosphorylation, etc. These modifications have long-term effects on chromatin assembly and regulate gene expression. So far, the most well understood histone modification is acetylation of H3 and H4. Generally, increased acetylation is associated with increased transcriptional activity and vice versa. But effects of other modifications are less clear. Furthermore, histone modification may interact with DNA methylation, participating in chromatin remodeling (Henckel et al. 2009; Tamaru and Selker 2001).

Emerging evidence has suggested that epigenetics is involved in the ability of environmental experiences to regulate the genome and to develop stable alterations in phenotype (Jirtle and Skinner 2007). During immune system maturation, an important determinant for developing allergic asthma, T-cell differentiation is under epigenetic regulation (Janson et al. 2009; Fields et al. 2002) and directly influenced by various maternal stimuli, including microbial exposure (Djuardi et al. 2011; Inman et al. 2010), dietary methyl donors (Miller 2008; Hollingsworth et al. 2008) and cigarette smoke (Breton et al. 2009; Murphy et al. 2012).

1.3 *In Utero* Smoke Exposure Studies and the Current Experimental Design

Second-hand smoke (SHS), previously called environmental tobacco smoke, is comprised of approximately 85-90% sidestream smoke and 10-15% exhaled mainstream smoke. Sidestream smoke arises from the burning end of the cigarette. This smoke, which does not pass through the cigarette filter, is more toxic to human lungs than mainstream smoke (Schick and Glantz 2005), and its toxicity is further increased with aging (Schick and Glantz 2006). By convention, sidestream smoke routinely has been generated as a surrogate for SHS.

It has been established that maternal exposure to cigarette smoke can affect fetal lung development (Blacquiere et al. 2009), contributing to an increased risk of subsequent asthma and respiratory disease (Hylkema and Blacquière 2009).

SHS has been examined by many researchers and has been associated with exacerbation of adult asthma and allergy symptoms (Jaakkola et al. 2003; Lajunen et al. 2013). Studies have evaluated the role of SHS in initiation of allergic asthma in the perinatal period (DiFranza et al. 2004; Hong et al. 2003; Jaakkola et al. 2006). The synergistic effects of *in utero* SHS exposure and various adult irritants, including house dust mite (Raherison et al. 2008) and *A. fumigatus* (Singh et al. 2011), have been revealed by different researchers.

From the vast majority of our previously conducted experiments, *in utero* SHS exposure of mice, by itself, does not particularly elicit lung responses different from those of the control group mice. However, a second challenge of adult mouse lungs to inhaled irritants, particularly ovalbumin (OVA), induced significantly aggravated effects in 15-week old mice that had been exposed *in utero* to SHS (Penn et al. 2007; Rouse et al. 2007).

There also are human studies that identified epigenetic changes due to *in utero* smoke exposures. Alterations on global and gene-specific DNA methylation were found in the buccal

cells of children exposed *in utero* to SHS (Breton et al. 2009). Similarly, there were differentially methylated CpG islands, which were mapped to key genes, including AHRR and CYP1A1, in the aryl hydrocarbon receptor signaling pathway within cord blood of newborns in relation to maternal smoking during pregnancy (Joubert et al. 2012). Cigarette smoke also contributes to reduced histone deacetylase activity, which results in differential activation of NF-kB and the expression of pro-inflammatory cytokines IL-6 and IL-8 in peripheral lung tissue (Rahman and Adcock 2006). In pregnancy, the induction of inflammatory genes can influences placental function and fetal programming (Osei-Kumah et al. 2006).

We hypothesize that a) *in utero* SHS exposure disturbs early development and disrupt normal epigenetic regulatory effects on mouse lungs and b) that these alterations remain detectable in adult lungs and continue to modulate lung responses to various inhaled irritants. To test this hypothesis, we conducted *in utero* exposures of pregnant mice to SHS and challenged their offspring with inhaled irritants, including (recurring) SHS and OVA (Figure 1-6).

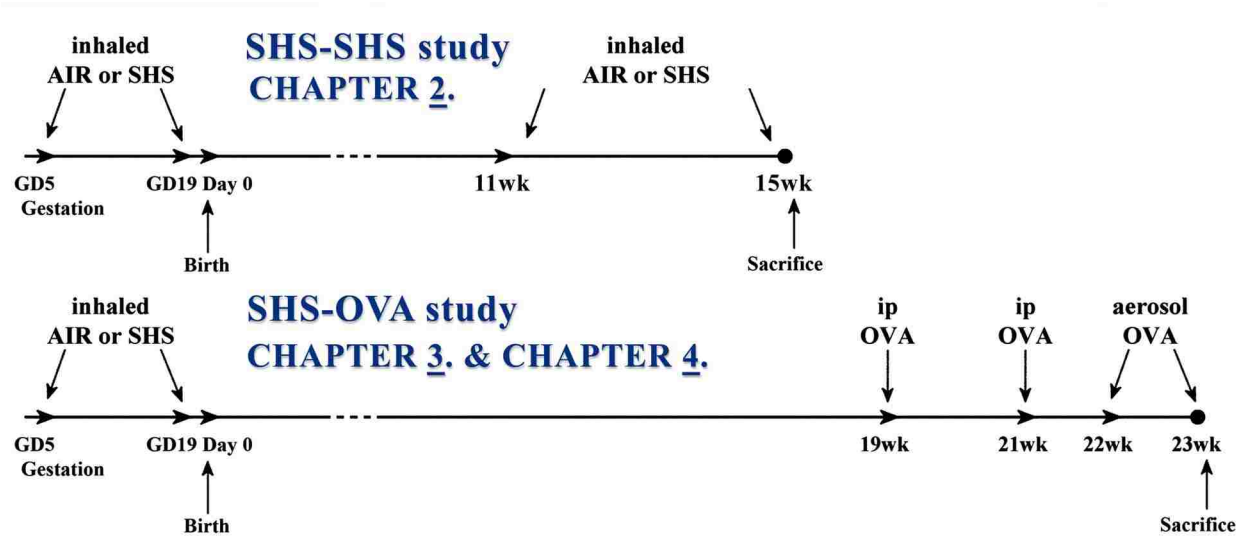

Figure 1–6. Overall experimental plan for the SHS-SHS and the SHS-OVA studies.

This dissertation describes studies involving SHS exposure *in utero* and the subsequent irritant challenge on lung function and other lung responses in the adult offspring. The dissertation is divided into five chapters. Chapter 1 is this introductory chapter. Chapter 2 addresses the lung function and responses of male offspring that had been exposed *in utero* to SHS after re-exposure to SHS, as adults. Chapter 3 further explores the duration of the *in utero* SHS effect as well as sex-specific differences in response to adult OVA challenge, in a mouse asthma model. Chapter 4 extends the findings of Chapter 3, but in addition, examines one of the well-characterized RNA-based epigenetic regulatory factors, miRNA, in OVA-challenged adult mice that had been exposed *in utero* to SHS. Chapter 5 is the concluding chapter that summarizes the advantages of recent technology that has been implemented in the studies described here, re-addresses important findings, and provides critical and forward-looking remarks based on these studies.

The majority of this information has been published previously in peer-reviewed journals as two manuscripts, one covering the information from Chapter 2 (Xiao et al. 2012) and the other detailing the information from Chapter 3 (Xiao et al. 2013). Chapter 4 has been submitted for publication and is presently under review.

CHAPTER 2.
IN UTERO EXPOSURE TO SECOND-HAND SMOKE AGGRAVATES ADULT RESPONSES TO IRRITANTS: ADULT SECOND-HAND SMOKE[1]

2.1 Introduction

In utero exposure to second-hand smoke (SHS), which exerts striking effects on lung function (Lindfors et al. 1999), has been associated with exacerbated asthmatic responses in children (Lindfors et al. 1999; Mannino et al. 2001). Altered lung function, increased asthma risk, and persistent lung function deficits in children have been linked with *in utero* and postnatal exposure to SHS (Gilliland et al. 2003; Gilliland et al. 2000; Gilliland et al. 2001; Li et al. 2000; Zlotkowska and Zejda 2005). The synergistic effects of *in utero* smoke exposure with various non-tobacco allergens also have been reported. Mild *in utero* SHS exposure exacerbates responses of BALB/c mice exposed to ovalbumin (OVA) from 11-15 weeks of age (Penn et al. 2007). These functional, histological and inflammatory responses are accompanied by distinct changes in lung gene expression (Rouse et al. 2007). Children exposed *in utero* to maternal smoking have a higher risk of sensitization to house dust mite (Raherison et al. 2008). A recent study in mice, found that *in utero* smoke exposure promotes Th2 polarization and induces allergic asthma in response to *A. fumigatus* sensitization (Singh et al. 2011). Whether and how *in utero* SHS exposure potentiates subsequent adult physiological and transcriptome responses to SHS exposure without any other irritant challenge, are not fully understood.

There also is evidence that exposure to environmental pollutants, such as SHS, during crucial periods of prenatal and/or postnatal development alters the course of lung morphogenesis

---

[1] Reprinted with permission of the American Thoracic Society. Copyright © 2014 American Thoracic Society. Xiao R, Perveen Z, Paulsen D, Rouse R, Ambalavanan N, Kearney M, Penn AL. *In utero* exposure to second-hand smoke aggravates adult responses to irritants: Adult second-hand smoke. Am J Respir Cell Mol Biol 2012;47(6):843-851.
Official Journal of the American Thoracic Society.

and maturation, potentially resulting in long-term changes that affect the function and structure of the respiratory system (Kajekar 2007). Persistent adult SHS exposure is strongly associated with development of COPD, accounting for more than 80% of COPD cases in the United States (Sethi and Rochester 2000). The effects of relatively brief SHS exposures *in utero* on the lung structure and pathogenesis of COPD have received little attention.

In the experiments described here we tested the hypothesis that *in utero* exposure to SHS will aggravate lung responses of young adult mice re-exposed to SHS. We asked whether *in utero* and/or adult exposures to SHS have significant effects on mouse lungs with regard to:

- lung inflammation; pro-inflammatory cytokine production
- lung morphology (airway, vasculature)
- lung function, including airway hyperresponsiveness (AHR) and breathing patterns
- gene expression patterns.

We focused particularly on whether mice exposed *in utero* or as adults to SHS respond differently from each other and from mice exposed to SHS both *in utero* and as adults.

2.2 Materials and Methods

Animal protocols. We housed and handled BALB/c mice (Harlan, Indianapolis, IN), as described previously (Penn et al. 2007). The Louisiana State University Institutional Animal Care and Use Committee approved all animal procedures. Pregnant mice were housed in separate cages from Day 20 of pregnancy until weaning (post-natal day 21).

SHS exposures. Sidestream smoke, which comprises 85-90% of SHS, served as a surrogate for SHS (Bowles et al. 2005; Penn and Snyder 1993). Smoke exposures and related measurements were as previously described (Penn et al. 2007) except that 3R4F filtered-research cigarettes (University of Kentucky) were used to achieve a suspended particle density

of 10 mg/m^3. The 3R4F cigarette is a model of a "full flavor" (10 mg tar) commercially available filtered cigarette (2012). Investigations carried out with an earlier version of this model cigarette (1R4F) revealed that the inhalation chamber SHS concentration produced by steady-state combustion of one 1R4F cigarette was exceeded by the SHS concentration in bars where 5 smokers were seated at a table (Penn et al. 1994). In the experiment reported here, pregnant mice, and subsequently, their male offspring, were exposed in inhalation chambers to a steady-state suspended particle level of 10 mg/m^3 and an average carbon monoxide level of 45 ppm, levels 4-10X higher than those generated in the earlier one cigarette steady-state study.

After 5 days of mating, 10-week-old female mice were exposed to SHS mixed with AIR or AIR alone (14 air changes/hr, 5 hr/day, 19 consecutive days) in 1.3-m^3 stainless steel and Plexiglass® dynamic exposure chambers. Male offspring were re-exposed to SHS or AIR from 11-15 weeks of age. There were insufficient numbers of female mice produced by these matings to allow for equivalent size groups of females to be tested. Mice were classified in one of four groups depending on whether SHS (S) or AIR (A) exposures were *in utero* or in adults (AA, N=7; AS, N=8; SA, N=6; SS, N=6). The exposure schedule is presented in Figure 2-1.

Pulmonary function testing. This was carried out as described previously (Penn et al. 2007). In the pulmonary function studies, for each mouse at each methacholine dose level, readings over 5 minutes were averaged. Penh values represent the degree of AHR in each animal. These data were used to generate the graph in Figure 2-2A. The highest Penh value (MaxPenh) recorded for each mouse sampled in the microarray study regardless of the methacholine dose (Figure 2-6B) is presented along with the array results for that mouse. A similar approach was used to calculate minimum breathing frequency (MinF; Figure 2-6A).

In Utero Exposure	Adult Exposure	Symbol	# Male Offspring
AIR	AIR	AA	7
AIR	SHS	AS	8
SHS	AIR	SA	6
SHS	SHS	SS	6

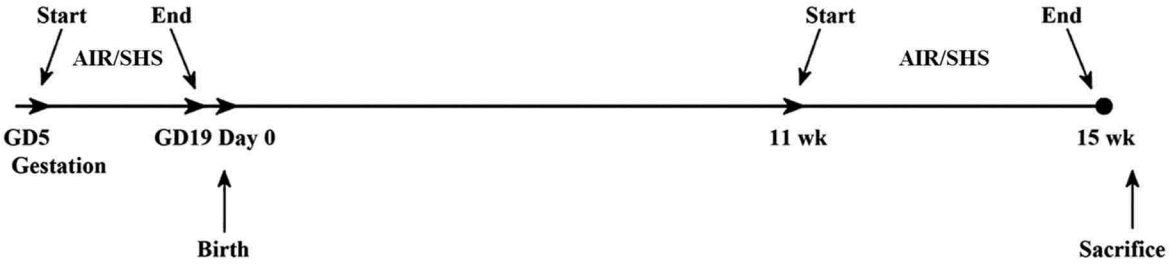

Figure 2–1. Group designation and experimental timeline of SHS-SHS study. The two-letter symbols are assigned to four experimental groups, depending on their exposure status at both time points. Times shown in the experimental timeline are expressed relative to the birthdate of offspring. GD, gestation day.

Cytokine quantitation in BALF. Mouse pro-inflammatory cytokine 7-plex kits (MSD, Meso Scale Discovery, Gaithersburg, MD) were used to measure major pro-inflammatory cytokines in BALF. The cytokines included in the assay were IL-1b, IL-12p70, IFN-γ, IL-6, KC/CXCL1, IL-10 and TNF-α. The manufacturer's stated average limits of detection (based on multiple kit lots) were 0.75, 35, 0.38, 4.5, 3.3, 11 and 0.85 pg/mL, respectively.

Histopathologic analysis of lungs. After BALF collection, lungs were fixed and processed as previously described (Bowles et al. 2005; Penn et al. 2007). We used a six-category scoring system (peribronchial, perivascular, bronchitis, pleuritis, alveolitis, mucus metaplasia) for evaluation of lung inflammation. The sites were scored from 0 (none) - 4 (severe). A board-certified veterinary pathologist, blinded to the treatments, evaluated histopathologic samples. A higher score (maximum score = 24) indicates greater tissue inflammation.

Lung morphometric analysis. Mean linear intercept (MLI) was measured in six 100x random fields/slide. Radial alveolar count (RAC) was measured in six 100x fields, each of

which had a bronchiole termination that could be followed out to the pleura. Each value (MLI or RAC) represents the average of the six fields from each slide (animal) (Ambalavanan et al. 2008). NB: Some RAC measurements had fewer than 6 fields, for we could only identify 4 bronchi in those sections that could be followed out. For vascular morphometry, 20 random arteries accompanying airways were evaluated. Capillaries (<20μm) or large arteries (>150μm) were not evaluated. Wall thickness was calculated using the formula (2x [WT/ED] x100%) where WT = wall thickness; ED = external diameter. We used a Nikon TE2000 microscope equipped with a QImaging cooled high resolution CCD camera and Metamorph image analysis software (v 6.2r4) for measurements.

Statistical analysis. We used the SAS statistical package (version 9.1.3; SAS Institute, Inc., Cary, NC) for data analyses. We performed one-way ANOVA on plethysmograph results, carried out a Kruskal-Wallis test (one-way ANOVA) on the ranks for the cytokine data, in considering limits of detection, and a *t*-test for pairwise-comparison between two combined groups for morphometric analysis. When significant differences were found in the ANOVA model, we conducted *post hoc* pair-wise comparisons with Tukey's HSD (honest significant difference) test. In all cases, we considered comparisons significant at $\boldsymbol{P}<0.05$. All error bars indicate means ± SEMs.

Lung harvest and mRNA extraction. We followed previously described procedures (Penn et al. 2007). We checked RNA samples quantity and purity with a NanoDrop ND-1000 Spectrophotometer (NanoDrop, Wilmington, DE). Values generated from the NanoDrop for all samples fell into the following ranges: 260/280 ratio: 2.13-2.43; 260/230 ratio: 1.95-2.34; concentration: 622-1283 ng/μL. We performed further quality assays on 1:5 dilutions of RNA samples with an Agilent 2100 BioAnalyzer and Agilent RNA 6000 Nano Series II Kits (Agilent

Technologies, Palo Alto, CA). All samples fell into the following ranges: 28S/18S ratio: 1.4-1.6, RNA integrity number: 8.9-9.6.

Microarray assay. We assessed global gene expression in lungs of individual 15-week old mice (four male mice per treatment group) on mouse 430.2 genome arrays (Affymetrix, Santa Clara, CA) representing more than 39,000 transcripts with over 45,000 probe sets. The arrays were processed at the Research Core Facility of LSU Health Science Center-Shreveport, as described previously (Penn et al. 2007).

Gene expression profiling. All analyses were performed in R/bioconductor platform (http://www.r-project.org/; http://www.bioconductor.org/). All 16 arrays were pre-processed with the Robust Multiarray Average (RMA) method to generate comparable expression values across all samples. A linear model for 2X2 factorial design ([*In Utero* Exposure]*[Adult Exposure]) was constructed with the limma package (Smyth 2004) to select those genes that are highly associated with *in utero* and/or adult exposure. Associations between gene expression and phenotypic variables were tested in phenoTest (Planet 2010). Correlation graphs and heat maps were plotted using gclus and Heatplus (Ploner 2011) packages. We adopted a red-yellow color scheme to visualize the relative expression differences across all samples (Figures 2-5, 2-6B), with red indicating relatively low expression and yellow indicating relatively high expression. We used a green-red color scheme to indicate fold-change differences for pairwise-comparisons, (Figure 2-7C). The microarray data have been deposited in NCBIs Gene Expression Omnibus (GEO, http://www.ncbi.nlm.nih.gov/geo/) and are accessible through GEO Series accession number GSE36810.

Gene-set functional analysis and Ingenuity Pathway Analysis (IPA). Gene-lists generated from statistical analyses were analyzed in WebGestalt2 (WEB-based Gene SeT

AnaLysis Toolkit) (Duncan 2010). Degrees of enrichment were calculated based on the gene-lists with assistance from different public databases, including Gene Ontology (GO), KEGG and MSigDB. We analyzed gene expression data with Ingenuity Pathways Analysis 8.7; gene networks and canonical pathways were examined using the Ingenuity Analysis Knowledge Database (Ingenuity Systems, Redwood City, CA). We created custom gene networks to demonstrate the connections between the genes and significantly associated functional and signaling pathways identified in this study.

qRT-PCR. Total RNA was reverse-transcribed with the High Capacity cDNA reverse transcription kit (Applied Biosystems, Foster City, CA). Expression levels of selected genes were measured with TaqMan universal PCR master mix (Applied Biosystems) and predesigned Taqman probes for mouse genes (assay ID: Hprt1, Mm00446968_m1; Gata3, Mm00484683_m1; Cyp1a1, Mm00487218_m1; Adamts9, Mm00614433_m1; Fam107a, Mm01706977_s1; Egr1, Mm00656724_m1; Fos, Mm00487425_m1 ; Btg2, Mm00476162_m1; Zfp36, Mm00457144_m1; Nr4a1, Mm01300401_m1). The expression levels were normalized to Hprt1 levels.

2.3 Results

Pulmonary function testing. Pulmonary function testing revealed significantly elevated AHR in the SS group following methacholine challenge, compared to *in utero* (SA) or adult (AS) SHS exposure alone (Figure 2-2A). A reverse trend was found for breathing frequency (Figure 2-2B). Significant differences (Tukey's, $\boldsymbol{P}<0.05$) were found in enhanced pause (Penh) and breathing frequency (f) between the SS group and the other three groups at the highest methacholine dose (50 mg/ml). At methacholine doses ≤12 mg/ml, both AS and SS groups had higher responses than the SA and AA groups (both exposed to AIR as adults)

whereas further increases in methacholine dose differentiated the SS group from the AS group and even more from the other two groups.

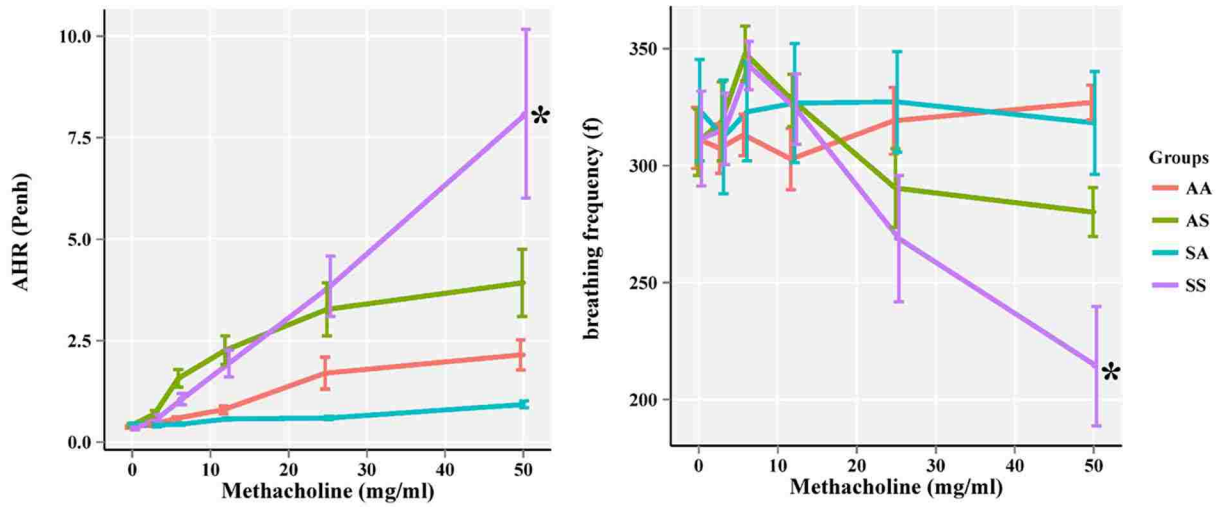

Figure 2–2. The SHS-SHS group exhibited significantly increased AHR and decreased breathing frequency, compared with *in utero* or adult SHS exposure alone. Whole-body plethysmography showed significantly increased AHR (Penh) and decreased breathing frequency (f) in mice twice-exposed to SHS, compared with those exposed either only *in utero* or as adults. Significant differences (ANOVA, $P<0.05$) were found in Penh (all methacholine doses) and f (only 50 mg/ml); *post hoc* Tukey's test indicates the differences are between SS and all other groups when treated with mechacholine 50 mg/ml. Values are represented as the means ± SEMs.

Levels of BALF cytokines. IL-1b, IL-6 and KC/CXCL1 were low, but were significantly increased (Tukey's, $\boldsymbol{P}<0.05$) in the SS group compared to the other three groups (Figure 2-3). IL-10, IL-12p70, TNF- α and IFN-γ were not detected in any samples. Neutrophil levels in cell differentials were very low in all 4 groups and indistinguishable from each other (data not presented).

Lung morphometric analysis. We assessed mean linear intercept (MLI), radial alveolar count (RAC) and vascular morphometric parameters, including arterial wall thickness (WT), artery external diameter (ED), and percentage wall thickness (% WT; Figure 2-4A).

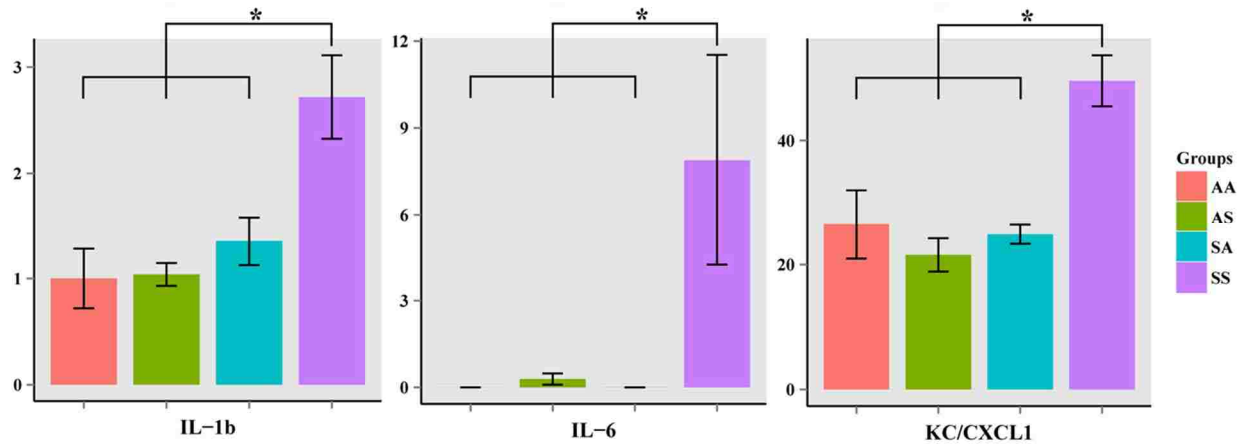

Figure 2–3. The SHS-SHS group had significantly higher levels of BALF cytokines, including IL-1b, IL-6, KC/CXCL1, compared with only *in utero* or adult SHS exposures. Mice in the SS group had significantly higher levels of the cytokines IL-1b, IL-6 and KC/CXCL1, compared with mice in the other three groups (ANOVA on ranks, $P<0.05$; *post hoc* Holm-Sidak's test). There was no detectable IL-10, IL-12p70 or IFN-γ in any group. All bars represent the means ± SEMs.

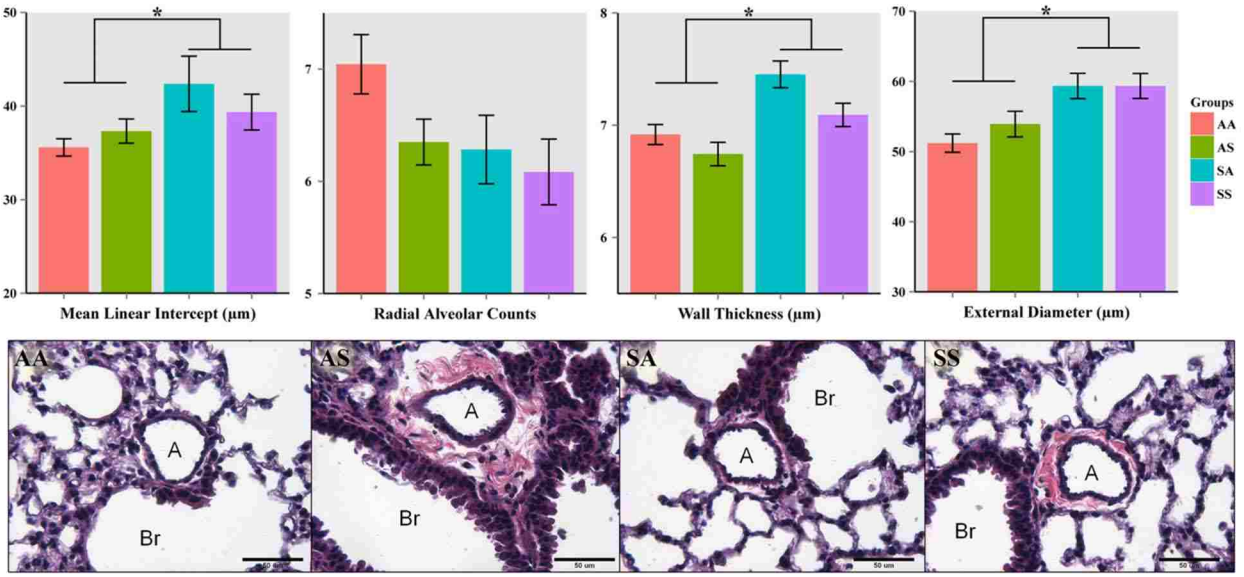

Figure 2–4. *In utero* but not adult exposure, significantly affected lung morphometric results in 15-week male mice. Upper panels showed significantly increased MLI and increased pulmonary arterial WT and ED in groups exposed *in utero* to SHS. Each bar represents the mean ± SEM. Representative slides displayed on the bottom panels showed increased collagen deposition (indicated by pink collagen fibers) around pulmonary arteries in AS and SS groups. A: artery. Br: bronchiole.

We found no statistically significant differences when results for the four individual groups were compared, although there were indications of *in utero* exposure-related responses. After re-grouping the four groups into two groups according to their *in utero* exposure status, there were significant increases in MLI, WT and ED in SX vs AX mice (SX: SA&SS combined, N=12; AX: AA&AS combined, N=15; Tukey's, $\boldsymbol{P}<0.05$). There was evidence of increased perivascular collagen deposition in AS and SS groups (Figure 2-4B).

Gene expression profiling. Via a linear model, gene expression profiling revealed three sets of genes that were uniquely affected by *in utero* SHS exposure (N=232), adult SHS exposure (N=5547) or both *in utero* and adult SHS exposures (N=183), as shown in the Venn diagram in Figure 2-5. All genes in each group had ***P***-values and FDR values<0.05. Adult exposure to SHS yielded 20X more differentially expressed genes than did *in utero* SHS exposure. Relatively low (red) or high (yellow) expression levels across all samples were plotted in heat maps and confirmed that in each case the gene expression patterns were dependent on the timing of SHS exposure (Figure 2-5).

The correlation scatterplot revealed that cytokine levels correlated well with physiological measurements (Figure 2-6A). The measurement with the highest correlation was of MaxPenh ($r_{(IL\text{-}1b,MaxPenh)}=0.66$, $r_{(IL\text{-}6,MaxPenh)}=0.83$). Therefore, we selected MaxPenh to represent AHR, and correlated this set of readings with each gene on the microarray. We found 323 probes, each with ***P***-value and FDR <0.05. All 323 probes were plotted in a heat map, with MaxPenh values also shown below the heat map (Figure 2-6B).

For each of the four gene-lists (*in utero* only; adult only; *in utero*+adult (Figure 2-5); and AHR (Figure 2-6B)), the 10 most up/down-regulated genes (SS vs AA, i.e., doubly exposed to SHS vs never exposed) in each list are presented in Figure 2-7A. Differential expression of

several genes initially identified by microarray analysis, and highlighted in Figure 2-7A, was further confirmed by qRT-PCR. The ΔΔCT values (for the gene of interest compared to the housekeeping gene, Hprt1) are charted in Figure 2-7B. For each comparison, the Hprt1 value is set at zero. An absolute difference of one in the units on the y-axis indicates a 2-fold difference in expression.

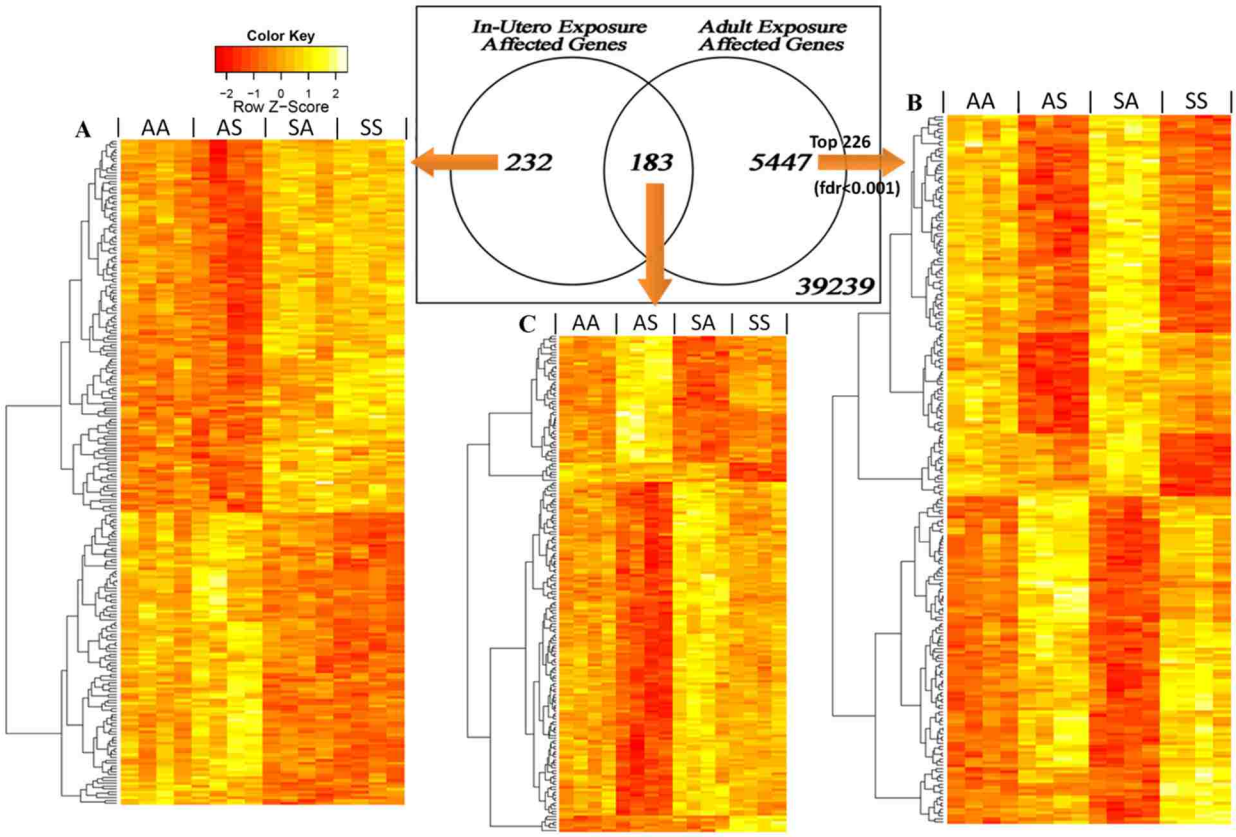

Figure 2–5. Transcriptome screening in lungs of 15-week old male mice revealed subsets of genes that are associated predominantly with A) *in utero* SHS exposure, B) adult SHS exposure and C) mixed effect of both. The Venn diagram shows numbers of probes found significantly expressed for each exposure period (FDR <0.05). Heat maps show the expression pattern of probes in each portion of the Venn diagram. For the adult exposure effect (>5000 probes), 226 gene-probes with FDR <0.001 are presented.

We found a minimum fold-change of two for all the genes charted in Figure 2-7B, including *in utero* exposure-affected genes (Egr1, Fos), both (*in utero* and adult) exposure-affected genes (Btg2, Zfp36, Nr4a1) and AHR-associated genes (Gata3, Fam107a, Cyp1a1,

Adamts9). The high correlation between AHR responses and SS exposures is reflected in the relative expression levels of Fam107, Cyp1a1 and Adamts9.

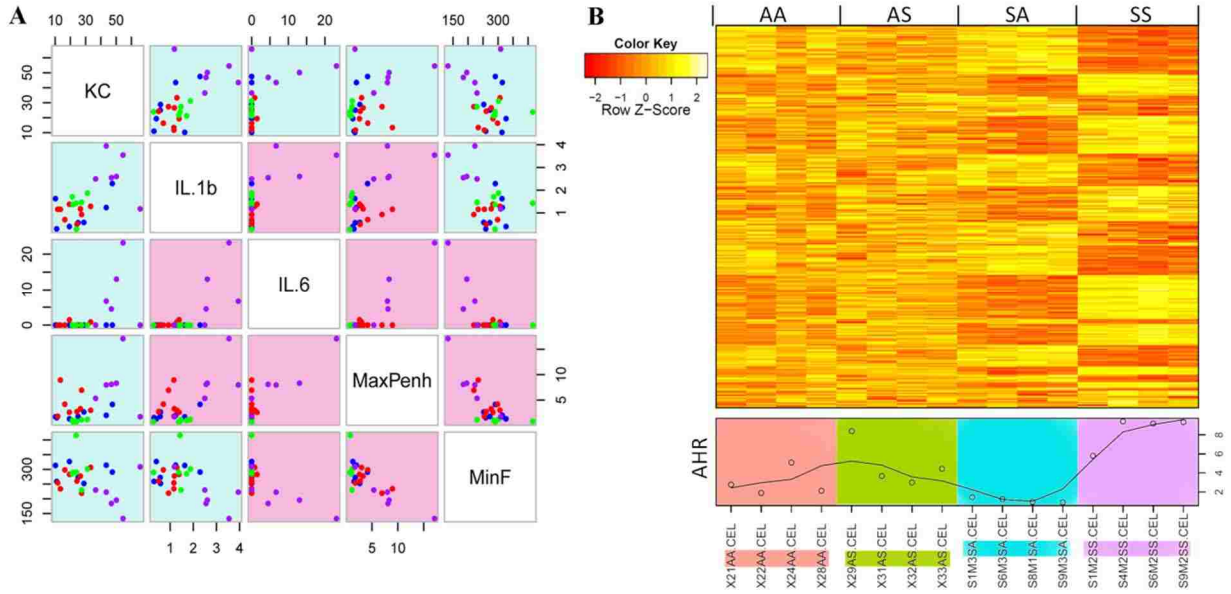

Figure 2–6. The physiological and cytokine measurements were highly correlated and can be associated with subsets of genes through microarray analysis. A) All readings in the same units as in other figures, e.g., pg/mL for cytokines, are plotted to interrogate the correlation between every two parameters (color of each dot: AA=blue, AS=red, SA=green, SS=purple). All measurements had a fairly high correlation with each other (|r|>0.5. The background color of each scatterplot indicates the degree of correlation: blue=moderate; red=high). B) 323 gene-probes, significantly correlated with AHR (represented by MaxPenh values), are shown in a heat map with each animal's MaxPenh values plotted below (actual dots with a smoothed line). The correlation graph was plotted with the gclus package in R/bioconductor (see Methods).

In utero SHS exposure identified genes primarily associated with immune system processes (GO:0002376, ***P***-value=1.18E-8; FDR=5.92E-6), most of which are not responsive to adult SHS exposure. The most striking KEGG pathways of adult exposure-affected genes are "Circadian rhythm–mammal" (***P***-value=2.59E-07; FDR=4.40E-05), "MAPK signaling pathway" (***P***-value=0.0005; FDR=0.0340) and "Pathways in cancer" (***P***-value=0.0006; FDR=0.0340). These significant processess and pathways are listed in Table 2-1 and Table 2-2.

Table 2–1. *In utero* SHS exposure identified genes primarily associated with immune system processes.

biological process----immune system process----GO:0002376 C=720;O=25;E=6.87;R=3.64;rawP=1.18e-08;adjP=5.92e-06			
AffyID	Entrez	GeneSymbol	Description
1417065_at	13653	Egr1	early growth response 1
1419135_at	16994	Ltb	lymphotoxin B
1423135_at	21838	Thy1	thymus cell antigen 1, theta
1439902_at	12273	C5ar1	complement component 5a receptor 1
1422190_at	12273	C5ar1	complement component 5a receptor 1
1417025_at	14969	H2-Eb1	histocompatibility 2, class II antigen E beta
1449580_s_at	15000	H2-DMb2	histocompatibility 2, class II, locus Mb2
1419744_at	15000	H2-DMb2	histocompatibility 2, class II, locus Mb2
1418830_at	12518	Cd79a	CD79A antigen (immunoglobulin-associated alpha)
1456354_at	11438	Chrna4	cholinergic receptor, nicotinic, alpha polypeptide 4
1451383_a_at	12675	Chuk	conserved helix-loop-helix ubiquitous kinase
1418261_at	20963	Syk	spleen tyrosine kinase
1425797_a_at	20963	Syk	spleen tyrosine kinase
1417574_at	20315	Cxcl12	chemokine (C-X-C motif) ligand 12
1425412_at	216799	Nlrp3	NLR family, pyrin domain containing 3
1437304_at	208650	Cblb	Casitas B-lineage lymphoma b
1449127_at	20345	Selplg	selectin, platelet (p-selectin) ligand
1422122_at	14128	Fcer2a	Fc receptor, IgE, low affinity II, alpha polypeptide
1429319_at	74734	Rhoh	ras homolog gene family, member H
1416016_at	16912	Psmb9	proteasome (prosome, macropain) subunit, beta type 9 (large multifunctional peptidase 2)
1448452_at	15900	Irf8	interferon regulatory factor 8
1417867_at	11537	Cfd	complement factor D (adipsin)
1419282_at	20293	Ccl12	chemokine (C-C motif) ligand 12
1416246_a_at	12721	Coro1a	coronin, actin binding protein 1A
1460188_at	15170	Ptpn6	protein tyrosine phosphatase, non-receptor type 6
1435221_at	108655	Foxp1	forkhead box P1
1452514_a_at	16590	Kit	kit oncogene
1415900_a_at	16590	Kit	kit oncogene
1419631_at	22376	Was	Wiskott-Aldrich syndrome homolog (human)

Table 2–2. The most striking KEGG pathways of adult exposure-affected genes are “Circadian rhythm–mammal”, “MAPK signaling pathway” and “Pathways in cancer”.

KEGG pathway----Circadian rhythm - mammal----04710 C=13;O=11;E=2.28;R=4.83;rawP=2.59e-07;adjP=4.40e-05			
AffyID	Entrez	GeneSymbol	Description
1418889_a_at	104318	Csnk1d	casein kinase 1, delta
1435775_at	12753	Clock	circadian locomoter output cycles kaput

(Table 2–2 continued)

AffyID	Entrez	GeneSymbol	Description
1417176_at	27373	Csnk1e	casein kinase 1, epsilon
1417175_at	27373	Csnk1e	casein kinase 1, epsilon
1417602_at	18627	Per2	period homolog 2 (Drosophila)
1417603_at	18627	Per2	period homolog 2 (Drosophila)
1418025_at	20893	Bhlhe40	basic helix-loop-helix family, member e40
1449851_at	18626	Per1	period homolog 1 (Drosophila)
1425099_a_at	11865	Arntl	aryl hydrocarbon receptor nuclear translocator-like
1426383_at	12953	Cry2	cryptochrome 2 (photolyase-like)
1421099_at	79362	Bhlhe41	basic helix-loop-helix family, member e41
1421037_at	18143	Npas2	neuronal PAS domain protein 2
1433733_a_at	12952	Cry1	cryptochrome 1 (photolyase-like)

KEGG pathway----MAPK signaling pathway----04010
C=251;O=65;E=43.98;R=1.48;rawP=0.0005;adjP=0.0340

AffyID	Entrez	GeneSymbol	Description
1460393_a_at	235584	Dusp7	dual specificity phosphatase 7
1440210_at	12300	Cacng2	calcium channel, voltage-dependent, gamma subunit 2
1428473_at	19056	Ppp3cb	protein phosphatase 3, catalytic subunit, beta isoform
1420554_a_at	170758	Rac3	RAS-related C3 botulinum substrate 3
1450698_at	13537	Dusp2	dual specificity phosphatase 2
1417268_at	12475	Cd14	CD14 antigen
1439258_at	11911	Atf4	activating transcription factor 4
1448135_at	11911	Atf4	activating transcription factor 4
1423462_at	68652	Map3k7ip2	mitogen-activated protein kinase kinase kinase 7 interacting protein 2
1459770_at	216965	Taok1	TAO kinase 1
1459996_at	12286	Cacna1a	calcium channel, voltage-dependent, P/Q type, alpha 1A subunit
1454369_a_at	73181	Nfatc4	nuclear factor of activated T-cells, cytoplasmic, calcineurin-dependent 4
1416703_at	26416	Mapk14	mitogen-activated protein kinase 14
1416437_a_at	30957	Mapk8ip3	mitogen-activated protein kinase 8 interacting protein 3
1455597_at	26405	Map3k2	mitogen-activated protein kinase kinase kinase 2
1455758_at	18752	Prkcc	protein kinase C, gamma
1448689_at	66922	Rras2	related RAS viral (r-ras) oncogene homolog 2
1449114_at	56274	Stk3	serine/threonine kinase 3 (Ste20, yeast homolog)
1458226_at	286940	Flnb	filamin, beta
1439004_at	73086	Rps6ka5	ribosomal protein S6 kinase, polypeptide 5
1420584_at	18781	Pla2g2c	phospholipase A2, group IIC
1440619_at	19099	Mapk8ip1	mitogen-activated protein kinase 8 interacting protein 1
1452116_s_at	11909	Atf2	activating transcription factor 2
1434785_at	140723	Cacng5	calcium channel, voltage-dependent, gamma subunit 5
1449839_at	12367	Casp3	caspase 3

(Table 2–2 continued)

AffyID	Entrez	GeneSymbol	Description
1426165_a_at	12367	Casp3	caspase 3
1424852_at	17260	Mef2c	myocyte enhancer factor 2C
1421027_a_at	17260	Mef2c	myocyte enhancer factor 2C
1423478_at	18751	Prkcb	protein kinase C, beta
1460251_at	14102	Fas	Fas (TNF receptor superfamily member 6)
1427853_a_at	15507	Hspb1	heat shock protein 1
1426032_at	18019	Nfatc2	nuclear factor of activated T-cells, cytoplasmic, calcineurin-dependent 2
1419532_at	16178	Il1r2	interleukin 1 receptor, type II
1460420_a_at	13649	Egfr	epidermal growth factor receptor
1436602_x_at	12287	Cacna1b	calcium channel, voltage-dependent, N type, alpha 1B subunit
1421953_at	12929	Crkl	v-crk sarcoma virus CT10 oncogene homolog (avian)-like
1425796_a_at	14184	Fgfr3	fibroblast growth factor receptor 3
1421841_at	14184	Fgfr3	fibroblast growth factor receptor 3
1449545_at	14172	Fgf18	fibroblast growth factor 18
1449117_at	16478	Jund	Jun proto-oncogene related gene d
1454184_a_at	16150	Ikbkb	inhibitor of kappaB kinase beta
1441482_at	26399	Map2k6	mitogen-activated protein kinase kinase 6
1453851_a_at	23882	Gadd45g	growth arrest and DNA-damage-inducible 45 gamma
1420931_at	26419	Mapk8	mitogen-activated protein kinase 8
1416505_at	15370	Nr4a1	nuclear receptor subfamily 4, group A, member 1
1448830_at	19252	Dusp1	dual specificity phosphatase 1
1456467_s_at	18099	Nlk	nemo like kinase
1435970_at	18099	Nlk	nemo like kinase
1429128_x_at	18034	Nfkb2	nuclear factor of kappa light polypeptide gene enhancer in B-cells 2, p49/p100
1422999_at	53859	Map3k14	mitogen-activated protein kinase kinase kinase 14
1421376_at	22034	Traf6	TNF receptor-associated factor 6
1417409_at	16476	Jun	Jun oncogene
1448694_at	16476	Jun	Jun oncogene
1426898_at	66513	Map3k7ip1	mitogen-activated protein kinase kinase kinase 7 interacting protein 1
1451502_at	26565	Pla2g10	phospholipase A2, group X
1431182_at	15481	Hspa8	heat shock protein 8
1415834_at	67603	Dusp6	dual specificity phosphatase 6
1421107_at	58231	Stk4	serine/threonine kinase 4
1434159_at	58231	Stk4	serine/threonine kinase 4
1421925_at	19094	Mapk11	mitogen-activated protein kinase 11
1449901_a_at	53608	Map3k6	mitogen-activated protein kinase kinase kinase 6
1422785_at	114713	Rasa2	RAS p21 protein activator 2
1455181_at	114713	Rasa2	RAS p21 protein activator 2
1418256_at	20807	Srf	serum response factor
1418255_s_at	20807	Srf	serum response factor

(Table 2–2 continued)

AffyID	Entrez	GeneSymbol	Description
1436522_at	26406	Map3k3	mitogen-activated protein kinase kinase kinase 3
1425911_a_at	14182	Fgfr1	fibroblast growth factor receptor 1
1416272_at	56692	Mapksp1	MAPK scaffold protein 1
1418497_at	14168	Fgf13	fibroblast growth factor 13
1446798_at	225028	Map4k3	mitogen-activated protein kinase kinase kinase kinase 3
1420442_at	12292	Cacna1s	calcium channel, voltage-dependent, L type, alpha 1S subunit
1417631_at	17346	Mknk1	MAP kinase-interacting serine/threonine kinase 1
1418401_a_at	70686	Dusp16	dual specificity phosphatase 16
1434295_at	19419	Rasgrp1	RAS guanyl releasing protein 1

KEGG pathway----Pathways in cancer----05200
C=309;O=77;E=54.14;R=1.42;rawP=0.0006;adjP=0.0340

AffyID	Entrez	GeneSymbol	Description
1420554_a_at	170758	Rac3	RAS-related C3 botulinum substrate 3
1455214_at	17342	Mitf	microphthalmia-associated transcription factor
1460657_at	22409	Wnt10a	wingless related MMTV integration site 10a
1436267_a_at	56717	Mtor	mechanistic target of rapamycin (serine/threonine kinase)
1425377_at	22408	Wnt1	wingless-related MMTV integration site 1
1450117_at	21415	Tcf7l1	transcription factor 7-like 2 (T-cell specific, HMG box)
1453134_at	18706	Pik3ca	phosphatidylinositol 3-kinase, catalytic, alpha polypeptide
1425918_at	112407	Egln3	EGL nine homolog 3 (C. elegans)
1455758_at	18752	Prkcc	protein kinase C, gamma
1436791_at	22418	Wnt5a	wingless-related MMTV integration site 5A
1427265_at	110279	Bcr	breakpoint cluster region
1455564_at	110279	Bcr	breakpoint cluster region
1418208_at	18510	Pax8	paired box gene 8
1422912_at	12159	Bmp4	bone morphogenetic protein 4
1428725_at	17344	Pias2	protein inhibitor of activated STAT 2
1456482_at	18710	Pik3r3	phosphatidylinositol 3 kinase, regulatory subunit, polypeptide 3 (p55)
1418587_at	22031	Traf3	TNF receptor-associated factor 3
1428853_at	19206	Ptch1	patched homolog 1
1442884_at	15234	Hgf	hepatocyte growth factor
1451866_a_at	15234	Hgf	hepatocyte growth factor
1449839_at	12367	Casp3	caspase 3
1426165_a_at	12367	Casp3	caspase 3
1423478_at	18751	Prkcb	protein kinase C, beta
1427718_a_at	17246	Mdm2	transformed mouse 3T3 cell double minute 2
1460251_at	14102	Fas	Fas (TNF receptor superfamily member 6)
1450034_at	20846	Stat1	signal transducer and activator of transcription 1
1420915_at	20846	Stat1	signal transducer and activator of transcription 1
1421942_s_at	21802	Tgfa	transforming growth factor alpha

(Table 2–2 continued)

AffyID	Entrez	GeneSymbol	Description
1420888_at	12048	Bcl2l1	BCL2-like 1
1426050_at	12048	Bcl2l1	BCL2-like 1
1443197_at	22412	Wnt9b	wingless-type MMTV integration site 9B
1456529_at	56458	Foxo1	forkhead box O1
1460420_a_at	13649	Egfr	epidermal growth factor receptor
1422162_at	13176	Dcc	deleted in colorectal carcinoma
1422129_at	23805	Apc2	adenomatosis polyposis coli 2
1421953_at	12929	Crkl	v-crk sarcoma virus CT10 oncogene homolog (avian)-like
1441737_s_at	56289	Rassf1	Ras association (RalGDS/AF-6) domain family member 1
1425796_a_at	14184	Fgfr3	fibroblast growth factor receptor 3
1421841_at	14184	Fgfr3	fibroblast growth factor receptor 3
1423886_at	226519	Lamc1	laminin, gamma 1
1449545_at	14172	Fgf18	fibroblast growth factor 18
1416533_at	112406	Egln2	EGL nine homolog 2 (C. elegans)
1450525_at	14634	Gli3	GLI-Kruppel family member GLI3
1420892_at	22422	Wnt7b	wingless-related MMTV integration site 7B
1427640_a_at	12395	Runx1t1	runt-related transcription factor 1; translocated to, 1 (cyclin D-related)
1440310_at	12395	Runx1t1	runt-related transcription factor 1; translocated to, 1 (cyclin D-related)
1448785_at	12395	Runx1t1	runt-related transcription factor 1; translocated to, 1 (cyclin D-related)
1437784_at	12395	Runx1t1	runt-related transcription factor 1; translocated to, 1 (cyclin D-related)
1429428_at	21416	Tcf7l2	transcription factor 7-like 2, T-cell specific, HMG-box
1424113_at	16777	Lamb1-1	laminin B1 subunit 1
1427638_at	235320	Zbtb16	zinc finger and BTB domain containing 16
1439163_at	235320	Zbtb16	zinc finger and BTB domain containing 16
1454184_a_at	16150	Ikbkb	inhibitor of kappaB kinase beta
1420931_at	26419	Mapk8	mitogen-activated protein kinase 8
1436000_a_at	27401	Skp2	S-phase kinase-associated protein 2 (p45)
1460247_a_at	27401	Skp2	S-phase kinase-associated protein 2 (p45)
1437033_a_at	27401	Skp2	S-phase kinase-associated protein 2 (p45)
1418969_at	27401	Skp2	S-phase kinase-associated protein 2 (p45)
1458904_at	14368	Fzd6	frizzled homolog 6 (Drosophila)
1417301_at	14368	Fzd6	frizzled homolog 6 (Drosophila)
1420088_at	18035	Nfkbia	nuclear factor of kappa light polypeptide gene enhancer in B-cells inhibitor, alpha
1420089_at	18035	Nfkbia	nuclear factor of kappa light polypeptide gene enhancer in B-cells inhibitor, alpha
1449731_s_at	18035	Nfkbia	nuclear factor of kappa light polypeptide gene enhancer in B-cells inhibitor, alpha
1448306_at	18035	Nfkbia	nuclear factor of kappa light polypeptide gene enhancer in B-cells inhibitor, alpha

(Table 2–2 continued)

AffyID	Entrez	GeneSymbol	Description
1417360_at	17350	Mlh1	mutL homolog 1 (E. coli)
1429128_x_at	18034	Nfkb2	nuclear factor of kappa light polypeptide gene enhancer in B-cells 2, p49/p100
1418861_at	59004	Pias4	protein inhibitor of activated STAT 4
1418534_at	57265	Fzd2	frizzled homolog 2 (Drosophila)
1421376_at	22034	Traf6	TNF receptor-associated factor 6
1417409_at	16476	Jun	Jun oncogene
1448694_at	16476	Jun	Jun oncogene
1421359_at	19713	Ret	ret proto-oncogene
1420957_at	11789	Apc	adenomatosis polyposis coli
1420956_at	11789	Apc	adenomatosis polyposis coli
1427650_a_at	12394	Runx1	runt related transcription factor 1
1440739_at	22341	Vegfc	vascular endothelial growth factor C
1421107_at	58231	Stk4	serine/threonine kinase 4
1434159_at	58231	Stk4	serine/threonine kinase 4
1447888_x_at	17685	Msh2	mutS homolog 2 (E. coli)
1440764_at	11836	Araf	v-raf murine sarcoma 3611 viral oncogene homolog
1426587_a_at	20848	Stat3	signal transducer and activator of transcription 3
1424272_at	20848	Stat3	signal transducer and activator of transcription 3
1455689_at	93897	Fzd10	frizzled homolog 10 (Drosophila)
1445452_at	22029	Traf1	TNF receptor-associated factor 1
1427567_a_at	59069	Tpm3	tropomyosin 3, gamma
1436983_at	12914	Crebbp	CREB binding protein
1420715_a_at	19016	Pparg	peroxisome proliferator activated receptor gamma
1425911_a_at	14182	Fgfr1	fibroblast growth factor receptor 1
1448861_at	22033	Traf5	TNF receptor-associated factor 5
1418497_at	14168	Fgf13	fibroblast growth factor 13
1455604_at	14367	Fzd5	frizzled homolog 5 (Drosophila)
1434705_at	13017	Ctbp2	C-terminal binding protein 2
1424638_at	12575	Cdkn1a	cyclin-dependent kinase inhibitor 1A (P21)
1421679_a_at	12575	Cdkn1a	cyclin-dependent kinase inhibitor 1A (P21)
1427190_at	72993	Appl1	adaptor protein, phosphotyrosine interaction, PH domain and leucine zipper containing 1
1436116_x_at	72993	Appl1	adaptor protein, phosphotyrosine interaction, PH domain and leucine zipper containing 1
1455886_at	12402	Cbl	Casitas B-lineage lymphoma
1425594_at	23928	Lamc3	laminin gamma 3

We further combined the *in utero* exposure-affected gene-list with the AHR associated gene-list and searched for distinct signaling pathways from the newly generated gene-list in IPA. The enriched canonical pathways found included: "IL-17A Signaling in Fibroblasts" (***P***-

value=2.24E-4) and "Production of Nitric Oxide and Reactive Oxygen Species in Macrophages" (***P***-value=2.09E-3). By connecting genes with reported gene interactions and known biological function, a composite gene network was built and is displayed in Figure 2-7C. The additional two IPA-designated biological functions shown in Figure 2-7C are "Inflammation" (***P***-value=1.02E-8) and "hypersensitive reaction" (***P***-value=1.1E-8). Genes associated with the IL-17A signaling pathway, including Cebpd, Nfkbia, Ccl2 and Fos also appear in the inflammation and reactive oxygen species pathways (Figure 2-7C).

2.4 Discussion

The experiments described here demonstrate that *in utero* exposure to environmentally-relevant levels of SHS modulates adult responses to subsequent SHS exposures. Male BALB/c mice exposed to SHS both *in utero* and as adults exhibited significantly elevated lung morphometry, pulmonary function and gene expression responses compared with the other three groups. Somewhat surprisingly, none of these changes appeared to be driven by inflammatory processes. Although levels of the pro-inflammatory cytokines IL-1b, IL-6 and KC/CXCL1 were significantly elevated in BAL fluid of the SS mice, the levels of each (IL-1b= 2.7; IL-6=7.9; KC/CXCL1=49.5 pg/mL; Figure 2-3) were near the low end of their respective linear response well reflect an overall weak cytokine response to the SHS exposures. The absence of grossly visible inflammation or increased immune cell infiltration in all four groups is consistent with this.

Morphometric analysis provided quantitative values for evaluation of lung structural changes in response to SHS exposures. The lack of significant statistical differences between the 4 groups before pooling likely reflects the relatively low "N"s in each group (6-8). Further statistical analysis identified significant differences after regrouping mice into two groups,

A

In utero exposure affected genes		Both exposure affected genes		Adult exposure affected genes		AHR associated genes	
Up	Down	Up	Down	Up	Down	Up	Down
NTRK2 1.685	FOS -3.154	CYP1A1 2.759	PRR5L -1.560	ZBTB16* 5.391	LRAT* -2.044	ADAMTS9 3.379	CASS4 -2.156
SALL1 1.516	EGR1 -2.916	ERRFI1 1.631	JUNB -1.528	APOLD1 3.646	CCR2* -2.020	CYP1A1 2.759	CXCR4 -1.789
SHROOM2 1.413	CYR61* -2.040	CALCB 1.525	TRIM14 -1.489	FKBP5* 3.449	Iigp1/Iigp1b* -1.901	SORBS1* 2.337	HHEX -1.725
PELI2 1.341	FCER2 -1.944	PER1 1.506	IER2 -1.411	ADAMTS9* 3.379	ELK3* -1.876	MPP3 2.311	PRDM8 -1.715
Glt28d2 1.327	PDE4B -1.900	RASD1 1.431	FOXP1 -1.409	CYP1A1 2.759	IGKC* -1.873	FAM107A* 2.219	GATA3 -1.708
CAMTA1 1.325	CFD -1.774	CSRNP1 1.408	LCP2 -1.332	CDKN1A* 2.509	PTPRC -1.854	UCP2 2.192	Ifi47 -1.690
RGS7BP 1.314	FOSB -1.772	ZHX3 1.378	NR4A1 -1.329	SORBS1* 2.337	MEIS2 -1.821	MAP3K6 2.095	MYCT1 -1.685
PDLIM5 1.302	CCL2 -1.763	FRY 1.362	ZFP36 -1.326	MPP3* 2.311	GPR34 -1.820	Retnla 2.037	PCDH17* -1.670
TTLL7* 1.291	LTB -1.762	BCAR3 1.293	BTG2 -1.297	CREB5* 2.235	CXCR4 -1.789	LMCD1 1.969	SOX4* -1.659
HECW2 1.287	CD79A -1.733	ADRB2 1.281	DUSP1 -1.224	FAM107A* 2.219	NPPA -1.764	CCRN4L 1.963	ANKMY2* -1.633

B

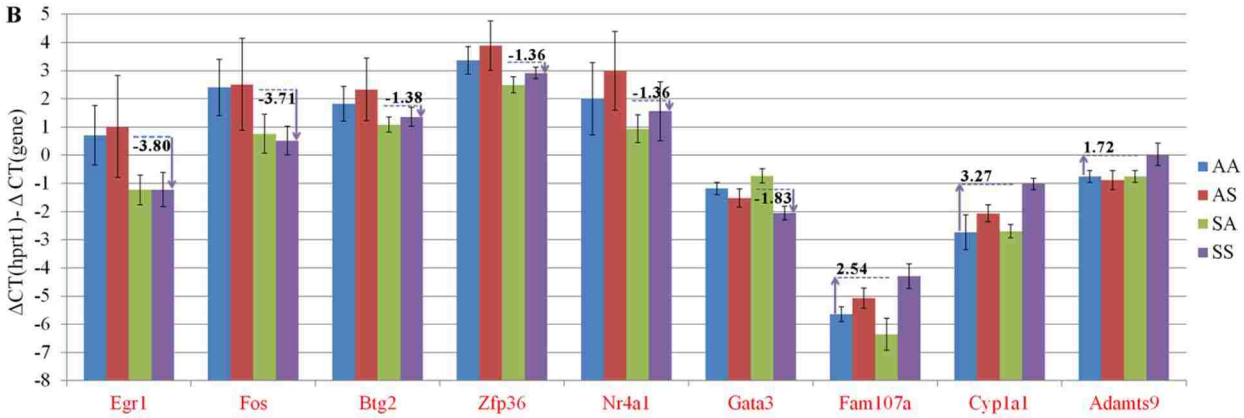

C

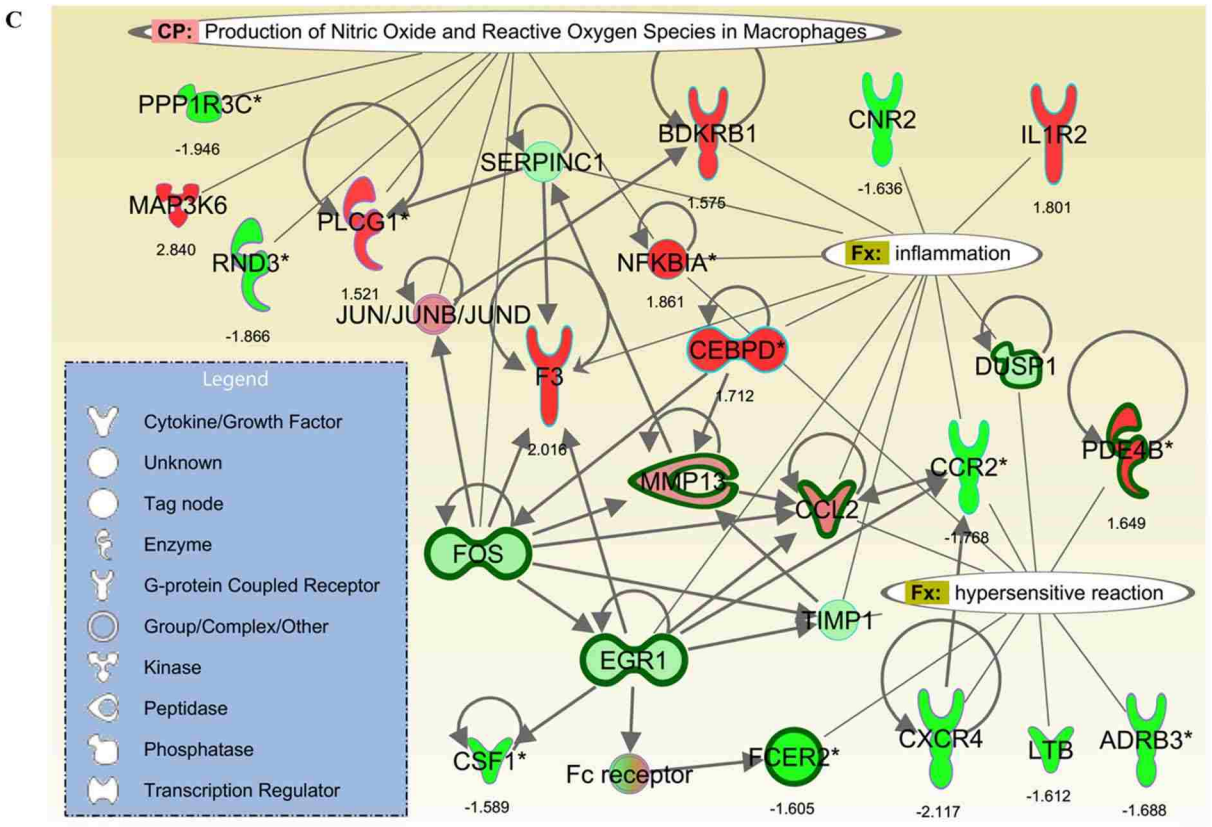

Figure 2–7. Differentially expressed genes were confirmed by qRT-PCR and interrogated by Ingenuity Pathway Analysis. A) Microarray fold-changes between SS and AA (doubly exposed to SHS vs never exposed) are listed for the 10 most up/down-regulated genes that were found in each of the four gene sets. Genes highlighted in red were confirmed by qRT-PCR. B) qRT-PCR

performed on 9 genes confirmed the microarray-based findings. Data (y-axis) are presented as –ΔΔCT values so that calculated values are positively associated with the gene expression levels. For each comparison, the Hprt1 value is set at zero. C) Genes affected by *in utero* exposure and those highly correlated with AHR were inter-connected in IPA Pathway Designer and found to be significantly associated with several known biological functions and canonical pathways ($P<0.05$). Thickened dark green edges indicate significant down-regulation due to *in utero* SHS exposure (SX vs AX); colors inside each node indicate gene expression changes with increased AHR (SS vs SA, red/green=up/down-regulation).

according to their *in utero* exposure status. Mice exposed *in utero* to SHS (SA,SS) had higher MLI values than those exposed to AIR *in utero* (AA,AS); this suggests airspace enlargement in mice exposed *in utero* to SHS. In addition, wall thickness and external diameter of random selected medium-sized arteries were significantly increased in animals exposed *in utero* to SHS. Together, these data indicate a role for *in utero* exposure to SHS on lung development that is sustained into adulthood. In this case, the effects of 2 weeks of *in utero* exposure (SA, SS) outweigh the effects of 4 weeks of adult SHS (AS).

Increased collagen deposition around pulmonary arteries in the AS and SS groups (Figure 2-4) suggests that adult exposure results in production of more ECM proteins, which would ultimately be necessary for development of lung fibrosis and COPD. The pathogenesis of COPD is associated with an imbalance of metalloproteases (MMP, ADAM) and anti-metalloproteases (TIMP, alpha-2M) (Mocchegiani et al. 2011). In the present study, there was notable up-regulation of metalloprotease family genes, including Adamts9 and Mmp3 in the SS and AHR groups (2-4X increase). Up-regulation of both of these genes has been associated with lung fibrosis. Adamts9 up-regulation and associated collagen deposition have been reported in a TGF-beta stimulated model of lung fibrosis (Keating et al. 2006). The collagen-deposition was reduced in alveolar epithelial cells transfected with Adamts9 siRNA. Paraquat-induced lung fibrosis in mice also is associated with Mmp3 up-regulation (Tomita et al. 2007). In addition to lung structural changes, *in utero* SHS exposure may have an effect on COPD pathogenesis. An

epidemiological study in 2009 linked maternal smoke exposure to further impaired lung function in offspring even in late adulthood, when COPD becomes apparent; and further, that maternal smoke exposure aggravates the cumulative effect of active cigarette consumption (Beyer et al. 2009). Together, these results suggest that early life smoke exposure may serve as a risk factor for the pathogenesis of COPD.

Lung function testing revealed that the SS group was more responsive than the other three groups at the highest methacholine dose, 50 mg/ml, in terms of both Penh and breathing frequency. Although Penh does not directly reflect airway mechanical function (Hamelmann et al. 1997), it has been used as an indicator of AHR and has been shown to correlate well with lung resistance in BALB/c mice (DeLorme and Moss 2002; Singh et al. 2003). Together with the observed reduction in breathing frequency, likely an adaptive response to bronchoconstriction (Adler et al. 2004), these results strongly support a significantly enhanced airway response in the group that has been exposed to SHS both *in utero* and as adults. An earlier report described similar results in rats exposed *in utero* and then postnatally to SHS. There was significantly increased lung resistance compared to SHS exposure at one time-point only, at 7-10 weeks of age (Joad et al. 1995).

Gene expression profiling with a linear model, revealed that the most differentially-expressed genes associated with *in utero* SHS exposure are Fos, Egr1 and Cyr61, all of which are down-regulated >2X; these results were confirmed by qRT-PCR (Figure 2-7B). In adults, up-regulation of these three genes has been associated with COPD progression (Ning et al. 2004). Egr1, a zinc finger transcription factor, has been suggested to play a key role in development of cigarette smoke-induced COPD by regulating MMP activity, and then affecting the turnover of ECM proteins during the pathogenesis of COPD (Reynolds et al. 2006). Fos is a

important component of AP-1, a redox-sensitive transcription factor, which interacts with Nrf2 (nuclear factor erythroid-derived 2, like 2) and regulates cytoprotective enzymes, including HO-1 (heme oxygenase) (Baglole et al. 2008). Reduction in Fos expression induced by cigarette smoke may interfere with protection against oxidative stress. Two other genes with ~2-fold down-regulation following *in utero* SHS exposure are Fcer2 and Pde4b, both of which have SNPs linked to increased risks of asthma and COPD. Fcer2 (Fc fragment of IgE, low-affinity II receptor) encodes the low-affinity IgE receptor, CD23, which is a key regulator in the biologic actions of IgE-mediated hypersensitivity commonly found in asthma patients (Tantisira et al. 2007). Pde4b, which encodes the cAMP-specific 3', 5'-cyclic phosphodiesterase 4B, has been identified as an essential molecule for Th2 cell function and development of AHR in allergic asthma (Jin et al. 2010).

The decreased expression here of Fos, Egr1 and Cyr61 in mice exposed *in utero* to SHS contrasts with clinical and experimental findings from adult mainstream smoke exposures, noted in the previous paragraph, that have linked elevated expression of these genes with the progression of asthma or COPD. Clearly, suppressed expression of these genes associated with *in utero* SHS exposure did not protect against indicators of these diseases here, as more airspaces are found in the SA and SS groups and significantly increased AHR is observed in the SS group. In addition, up-regulation of the pro-fibrotic Adamts9 and Mmp3 in lungs of SS-exposed adult mice also is consistent with a COPD-promotion effect.The possibility of a relationship between gestational SHS exposure and subsequent development of COPD has apparently not been previously examined. Alternatively, the unexpected down-regulation of Fos, Egr1 and Cyr61 despite the accompanying increases in airspaces, collagen deposition and AHR in lungs of adult mice exposed *in utero* to SHS may simply be consistent with the view that

there are no good animal models of cigarette smoke-associated COPD (Churg et al. 2011).

Although the approach we adopted successfully selected candidate genes according to how closely they matched the smoke exposure conditions, the gene expression results we observed relating to whole-body plethysmography and cytokine responses were markedly enhanced only in animals exposed to SHS both *in utero* and as adults (Figure 2-6). To identify the genes closely correlated with the prominent SS-response, MaxPenh, the most prominent of the functional lung responses, was selected as the response variable, to which gene expression changes were compared. One of the merits of this approach is that the gene-response correlation values were calculated regardless of the group in which each sample resided, so the in-group variation will not negatively affect the test results. This is illustrated in the sample labeled "29AS" where the high AHR response in an otherwise low AHR group is correlated with levels of gene expression comparable to those found in all 4 mice in the high AHR SS group (Figure 2-6B).

To further investigate how *in utero* SHS exposure may contribute to exacerbated adult responses, we combined the lists of *in utero* only exposure-affected genes with AHR-associated genes and interrogated signaling pathways from this new gene-list. From IPA, the AHR-associated genes were recognized to be significantly associated with increased inflammation, oxidative stress and hypersensitivity reactions. Although the fold-change values (SS vs SA, highest vs lowest AHR, see Figure 2-2 and Figure 2-6B) in the gene network are moderate (1.5X-2.8X), they all are from genes modulated by *in utero* SHS exposure, and retained until 15 weeks of age.

In addition, IL-17 signaling, one of the most significant canonical pathways identified in IPA with *in utero* exposure (***P***-value=6.12E-03) as well as with both exposures (***P***-value=2.05E-

03), may also partially explain the prominent SS-response that originates from *in utero* SHS exposures. As fetal T cells develop during the second trimester of gestation (Papiernik 1970), the cytokine level changes are detected not only in the circulating blood of the pregnant mothers, but also in amniotic fluids with direct contact to the fetal lungs (Mandal et al. 2011). The elevated circulating level of TGF-beta during gestation promotes development of regulatory T cells (Treg cells); however, *in utero* SHS exposure also increases the level of IL-6, and naïve T cells will differentiate into Th17 cells in the presence of both TGF-beta and IL-6 (Bettelli et al. 2006). In addition, the aryl hydrocarbon receptor, which is activated by the polynuclear aromatic hydrocarbons (PAHs) generated by cigarette smoking, was reported to also have regulatory functions in Th17 cell populations (Kimura et al. 2008; Quintana et al. 2008; Veldhoen et al. 2008). During the critical developmental period, the immune cell lineage commitment may greatly affect the lung responses of the offspring even when they become adults (Martino and Prescott 2010).

Summary: We examined lung responses of BALB/c mice to *in utero* and/or adult exposures to environmentally-relevant levels of SHS. There were significant increases in AHR and in pro-inflammatory cytokine production (IL-1b, IL-6, KC/CXCL1), albeit at low levels, in lungs of 15-week old doubly-exposed mice. There were enlarged airspaces and arteries in mice exposed *in utero* to SHS, plus increased collagen deposition in mice exposed to SHS as adults. Unique gene expression patterns were apparent for *in utero*, adult and combined exposures. Overall, the results indicate that *in utero* SHS exposures alter lung structure more severely than do adult SHS exposures of longer duration, aggravate AHR and promote a pro-fibrotic milieu in adult lungs.

CHAPTER 3.
IN UTERO EXPOSURE TO SECOND-HAND SMOKE AGGRAVATES ADULT RESPONSES TO IRRITANTS: ADULT OVALBUMIN[2]

3.1 Introduction

Second-hand smoke (SHS) exposure *in utero* aggravates responses to subsequent post-natal exposures to environmental irritants, including house dust mites (Raherison et al. 2008), *Aspergillus fumigatus* (Singh et al. 2009) and SHS (Xiao et al. 2012). The most common observation among these studies is increased airway hyper-responsiveness (AHR), a hallmark of allergic asthma.

In the murine model of asthma featuring ovalbumin (OVA) sensitization and challenge, OVA-induced lymphocyte infiltration, elevated Th2 cytokine production, and increased AHR mirror several key characteristics of asthma (Kips et al. 2003; Lloyd 2007; Nials and Uddin 2008; Temelkovski et al. 1998). Whether and how *in utero* exposure to SHS affects responses of adults treated with OVA and whether there is a sex bias in the responses are the subjects of the present investigation.

Just as sex differences in response to irritants exist among human asthma patients (Tantisira et al. 2008), studies in animal models have revealed some sex differences in lung responses, particularly those associated with AHR. Male C57BL/6 mice are innately more responsive than females to aerosolized methacholine (Card et al. 2006). In BALB/c mice, however, females were reported to be more responsive than males after OVA challenge (Melgert et al. 2005). Whether sex-associated differences also exist among OVA-challenged mice that

---

[2] Reprinted with permission of the American Thoracic Society. Copyright © 2014 American Thoracic Society. Xiao R, Perveen Z, Rouse RL, Le Donne V, Paulsen DB, Ambalavanan N, Penn AL. *In utero* exposure to second-hand smoke aggravates the response to ovalbumin in adult mice. Am J Respir Cell Mol Biol 2013 Dec;49(6):1102-1109.
Official Journal of the American Thoracic Society.

have been exposed *in utero* to SHS has not been investigated rigorously. An earlier study in our laboratory showed that *in utero* SHS exposure mildly aggravated asthma-associated lung responses to OVA exposure in 15-week-old female BALB/c mice (Penn et al. 2007). We designed the present study to:

- Test whether the effects of *in utero* SHS exposure were sustained in older mice exposed to OVA;
- Examine in greater detail than previously determined (Penn et al. 2007) the range and extent of responses to *in utero* SHS-adult OVA exposure;
- Determine whether sex differences exist in responses of mice to SHS-OVA.

We exposed pregnant BALB/c mice to HEPA-filtered air (AIR) or to SHS diluted with AIR daily from gestation days 6-19 and exposed all offspring to an OVA sensitization/challenge protocol from 19-23 weeks of age. We assessed the following outcomes: pulmonary function (AHR, breathing frequency), lung histopathology (inflammation, structural changes), bronchoalveolar lavage fluid (BALF) cytokine levels and lung gene expression patterns, primarily the identification of SHS-related gene pathways.

3.2 Materials and Methods

Animal protocols, SHS and OVA exposures. We conducted SHS exposures on BALB/c mice (Harlan, Indianapolis, IN), as described previously (Penn et al. 2007; Xiao et al. 2012). Briefly, half of the mated females, randomly-selected, were exposed to SHS generated from 3R4F filtered research cigarettes (University of Kentucky; 10 mg/m^3) mixed with AIR daily, from days 6-19 of gestation. The remaining mated females received 100% AIR exposures instead. All offspring were sensitized by injections of OVA (Grade V >98% pure, Sigma-Aldrich, St. Louis, MO; 80 μg in 2 ml alum) at 19 & 21 weeks of age, followed by OVA aerosol

challenge every other day in weeks 22 & 23, before sacrifice. Mice were classified in one of four groups, depending on *in utero* exposure to SHS (S) or AIR (A), and their sex. All offspring were exposed to OVA. The numbers of animals in each group assessed in each assay are listed with each figure. Mice were housed and handled in accord with the NIH Guide for the Care and Use of Laboratory Animals. All procedures and protocols were approved by the LSU Institutional Animal Care and Use Committee. The group designation and exposure timeline are presented in Figure 3-1.

In Utero Exposure	Adult Exposure	Sex	Symbol
AIR	OVA	Female	AOF
AIR	OVA	Male	AOM
SHS	OVA	Female	SOF
SHS	OVA	Male	SOM

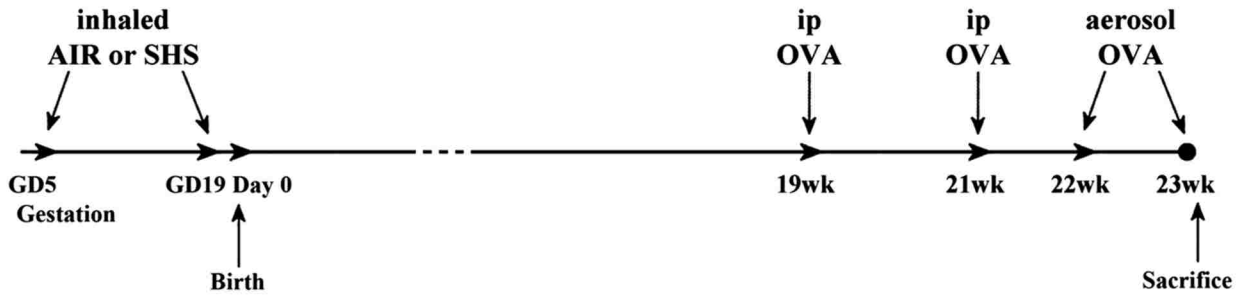

Figure 3–1. Group designation and exposure timeline of the SHS-OVA study. The three-letter symbols were assigned to four experimental groups, depending on the exposure period *in utero* and adult, plus sex of the mice. Times shown in the exposure timeline are expressed relative to birthdate of offspring. GD, gestation day.

Pulmonary function testing. This was carried out as described previously (Penn et al. 2007; Xiao et al. 2012). For each mouse at each methacholine dose level (3-50 mg/ml), readings over 5 minutes were averaged for Penh and breathing frequency. Penh values represent the degree of AHR in each animal.

Histopathologic analysis of lungs. We followed previously published procedures (Penn et al. 2007; Xiao et al. 2012) for BALF collection, fixation, sectioning, staining and scoring of 3-4 μm lung sections, and for lung morphometric analysis (Xiao et al. 2012). Goblet cells and mucin were stained with the routine Periodic acid-Schiff (PAS) stain on 5 μm, paraffin-embedded tissue sections from the same blocks as were used in the H&E stains. 12 males each from the treatment and control groups were evaluated. Slides were scored for estimated percent of linear mucosa that was occupied by goblet cells and given the following scores: 0 for less than 10%, 1 for 10% to 33%, 2 for 34% to 67%, and 3 for greater than 67%. Additionally, lungs were evaluated for the presence (+) or absence (-) of goblet cells in the distal 2 generations of bronchioles in the peripheral lung.

Cytokine quantitation in BALF. Mouse Th1/Th2 9-plex kits (MSD, Meso Scale Discovery, Gaithersburg, MD) & ELISA plates for IL-13 were used to measure 10 major Th1/Th2 cytokines (IFN-γ, IL-1b, IL-2, IL-4, IL-5, IL-10, IL-12, IL-13, KC/CXCL1, TNF-α) in BALF.

Statistical analysis. We used the SAS statistical package (version 9.3; SAS Institute, Inc., Cary, NC) for data analyses. We performed one-way ANOVA and *post hoc* Tukey's HSD (honest significant difference) test for multiple pairwise-comparisons, including SHS-OVA versus AIR-OVA responses in males and females (*) as well as SHS-OVA responses in males versus females (†). Statistical differences between SHS-OVA and AIR-OVA with pooled M and F responses (‡) were calculated by a *t*-test. In all cases, we considered comparisons significant at $P<0.05$. Error bar indicates mean ± SEM.

Lung harvest and mRNA extraction. We followed previously described procedures (Penn et al. 2007; Xiao et al. 2012), including RNA sample quantity and purity assessment with

a NanoDrop ND-1000 Spectrophotometer (NanoDrop, Wilmington, DE), and further assayed 1:5 dilutions of RNA samples with an Agilent 2100 BioAnalyzer and Agilent RNA 6000 Nano Series II Kits (Agilent Technologies, Palo Alto, CA). All samples fell into the following ranges: 260/280 ratio: 2.14-2.19; 260/230 ratio: 1.91-2.34; concentration: 970-2845 ng/μl; 28S/18S ratio: 1.6-2.0, RNA integrity number: 9.2-10.0.

Microarray analysis and Ingenuity Pathway Analysis (IPA). We assessed global gene expression in lungs of individual 23-week old mice (4 mice per group) on mouse 430.2 genome arrays (Affymetrix, Santa Clara, CA). The arrays were processed at the Research Core Facility of Louisiana State University Health Science Center-Shreveport. We performed two pairwise-comparisons on "SOF versus AOF" and "SOM versus AOM" with the limma package (Smyth 2004) in the R/bioconductor platform (www.r-project.org; www.bioconductor.org). Gene probes with at least 2-fold up/down-regulation and FDR<0.05 were considered differentially expressed. The microarray data have been deposited in NCBIs Gene Expression Omnibus (GEO, accession number GSE38409). We performed gene-set functional analyses and generated gene networks with IPA (Ingenuity Systems, Redwood City, CA; www.ingenuity.com).

qRT-PCR. Total RNA was reverse-transcribed with the High Capacity cDNA reverse transcription kit (Applied Biosystems, Foster City, CA). Expression levels of selected genes were measured with TaqMan universal PCR master mix (Applied Biosystems) and predesigned Taqman probes for mouse genes (assay ID: Hprt1, Mm00446968_m1; Cxcl2, Mm00436450_m1; Cxcl5, Mm00436451_g1; Ccl8, Mm01297183_m1; Ccl24, Mm00444701_m1; Il1b, Mm00434228_m1; Il6, Mm00446190_m1; Il13, Mm00434204_m1; Il17b, Mm01258783_m1; Saa1, Mm00656927_g1; Saa3, Mm00441203_m1; Timp1, Mm00441818_m1). The gene expression levels were normalized to Hprt1 levels.

3.3 Results

Pulmonary function testing. Pulmonary function testing revealed significantly increased AHR and decreased breathing frequency in the male and female SHS-OVA groups following methacholine challenge, compared to those in AIR-OVA groups. Among all mice exposed *in utero* to SHS, male offspring exhibited significantly aggravated AHR compared with SHS-exposed females at methacholine doses 3-12 mg/ml (Figure 3-2).

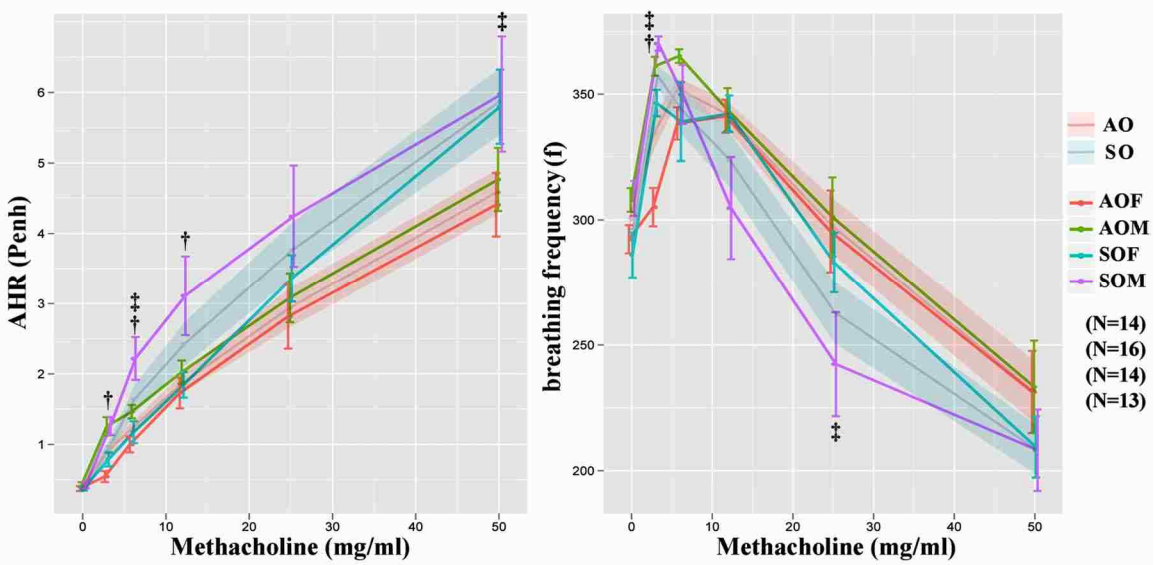

Figure 3–2. The SHS-OVA groups exhibited significantly increased AHR and decreased breathing frequency. Whole-body plethysmography revealed significantly increased AHR (Penh) and decreased breathing frequency (f) in SHS-OVA mice, compared with all mice from AIR-OVA groups [i.e., when we pooled data for females plus males in each exposure set (‡)]. In addition, there was significantly increased AHR in SOM versus all other groups especially at low methacholine doses (†, SOM versus SOF). ‡ (SO vs AO, female and male pooled) @ 6,50 for AHR, @ 25 for f. † (SOM vs SOF, sex difference) @ 3,6,12 for AHR.

Inflammatory cells. Eosinophil counts in BALF were high for all 4 groups. Significant differences were found between SHS-OVA and AIR-OVA for eosinophils and neutrophils. There was a pronounced lung inflammatory response in all four groups (Figure 3-3). The high levels of inflammation made it difficult to reliably quantitate the mean linear intercept and radial

alveolar count values, which we have used previously to assess lung structural changes (Xiao et al. 2012).

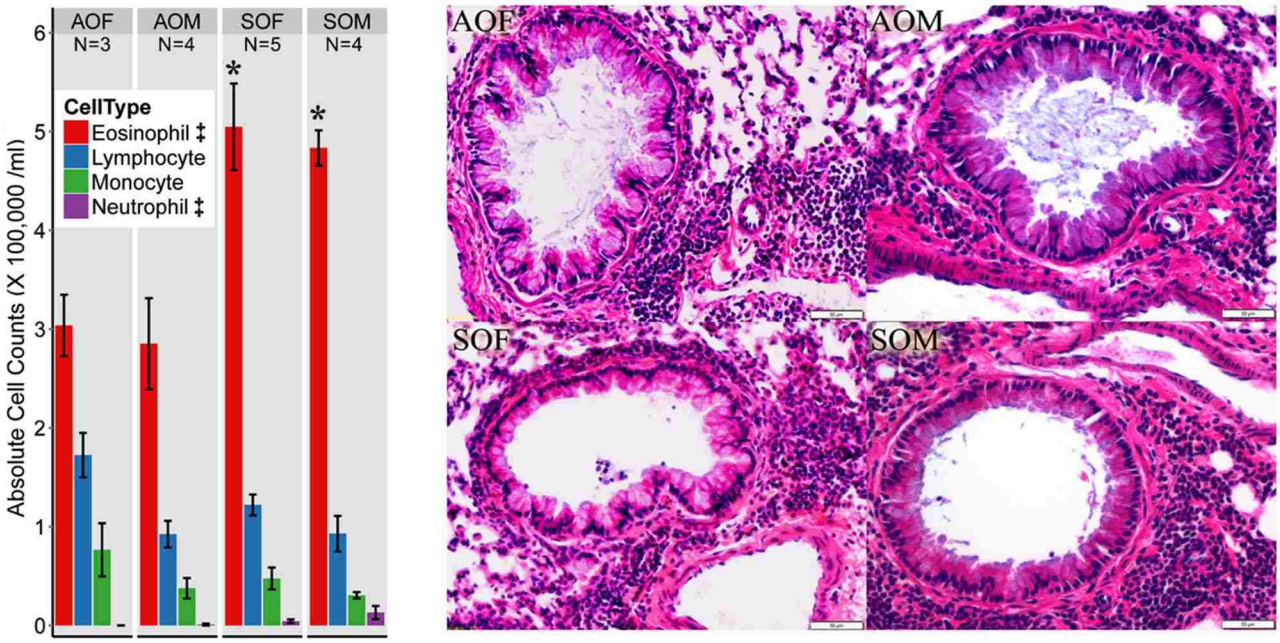

Figure 3–3. There were significantly increased numbers of eosinophils and neutrophils in the SHS-OVA groups. The eosinophil is the major cell type found in BALF for all groups (left panel). There were significantly increased eosinophils and neutrophils in the SHS-OVA groups compared the AIR-OVA groups (‡). Significant differences within either sex (SOF versus AOF & SOM versus AOM) were also found for eosinophils (*). Lung histology of all 4 groups revealed severe inflammation with accumulated inflammatory cells in the airways around bronchioles (right panel). Airspaces in the alveolar region are occupied by inflammatory cells that are stained dark blue. Bar=50 µm.

We also evaluated percent linear mucosa occupied by goblet cells and presence/absence of goblet cells in the distal 2 generations of bronchioles in the peripheral lung. A board-certified veterinary pathologist, blinded to the treatments, evaluated histopathologic samples and found no differences for either set of measurements between males and females or between SHS- and AIR-exposed mice, as shown in Table 3-1.

Table 3–1. There were no significant differences between SHS- and AIR-exposed mice, regarding percent linear mucosa occupied by goblet cells and presence/absence of goblet cells, in the distal 2 generations of bronchioles in the peripheral lung.

Slide	Group	goblet cells, bronchi [0 (none) -3 (numerous)]	goblet cells in distal bronchioles (Y/N)
237B	SOM	3	Y
239W	AOM	2	Y
237A	SOM	3	N
239V	AOM	3	Y
237E	SOM	2	N
239U	AOM	3	N
237F	SOM	2	N
239S	AOM	1	N
237G	SOM	2	Y
239R	AOM	3	Y
237I	SOM	3	N
239J	AOM	3	N
237J	SOM	2	N
239H	AOM	2	N
237M	SOM	2	N
239G	AOM	3	N
237N	SOM	2	Y
239E	AOM	2	N
237O	SOM	3	N
239D	AOM	2	N
237Q	SOM	2	N
239C	AOM	2	Y
237S	SOM	3	Y
238S	AOM	3	N

BALF cytokines. We found significantly elevated cytokine levels in SHS-OVA versus AIR-OVA for 8 of the 10 BALF Th1/Th2 cytokines we assessed (both sexes pooled, Figure 3-4): IFN-γ, IL-1b, IL-4, IL-5, IL-10, IL-13, KC/CXCL1 and TNF-α. IL-2 and IL-12 also were detected but were not significantly different between AIR-OVA and SHS-OVA groups (data not shown). The *post-hoc* Tukey's test among all 4 groups further confirmed the significant

differences between males (SOM versus AOM) for all 8 cytokines and between females (SOF versus AOF) for 5 cytokines (IL-1b, IL-4, IL-5, IL-13, KC/CXCL1). Cytokine levels in BALF from the male SHS-OVA offspring were even higher than corresponding levels in SHS-OVA females and significant differences were found for IFN-γ, IL-1b, IL-5, IL-10 and KC/CXCL1.

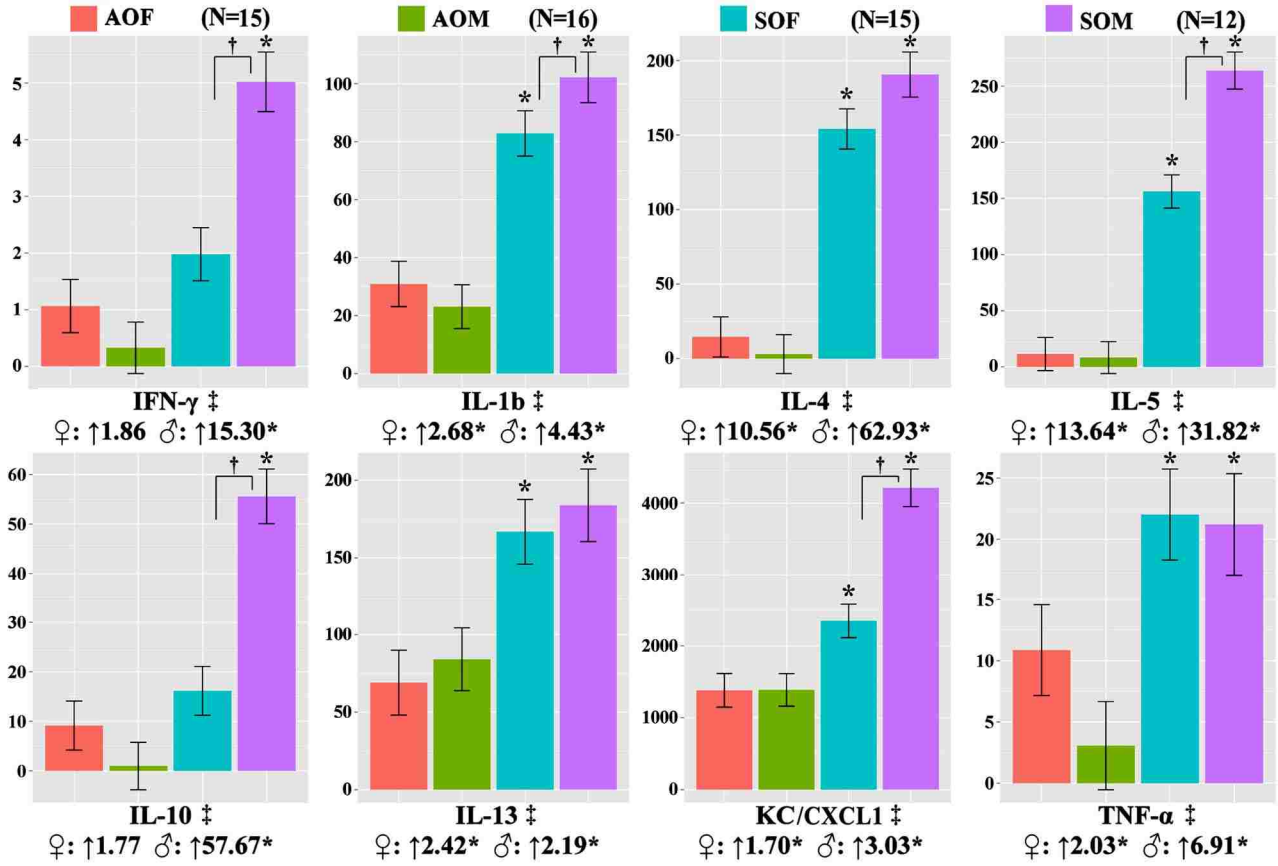

Figure 3–4. BALF cytokines were significantly increased in the SHS-OVA groups. BALF cytokine levels determined by ELISA for the 8 cytokines listed, were increased significantly in SHS-OVA groups compared with AIR-OVA groups (‡). This was also true for all 8 cytokine comparisons between the males (*, ♂, SOM versus AOM) and 6 out of 8 cytokines for females (*, ♀, SOF versus AOF). In the cases of IFN-γ, IL-1b, IL-5, IL-10 and TNF-α, we found significantly elevated responses in the males compared with the females for mice exposed *in utero* to SHS (†, SOM versus SOF). Units on y-axes are pg/ml. ‡: all 8 (SOvsAO); †: 5/8 (SOMvsSOF); *: ♀ 6/8, ♂ 8/8.

Gene expression profiling. With the differential expression threshold for genes in lung homogenates set to a fold change of 2 and FDR<0.05, 65 genes in the females and 86 in the males were differentially expressed between SHS-OVA and AIR-OVA mice (Online Supplement), while 38 genes were shared by both sexes (Figure 3-5A, Table 3-2).

Table 3–2. All 113 differentially expressed genes between SHS-OVA and AIR-OVA groups, shown in Figure 3-5A, are listed with additional information.

Gene Symbol	SOF versus AOF				SOM versus AOM				Affymetrix_ID
	P.Value	FDR	Fold Change	♀	P.Value	FDR	Fold Change	♂	
Cxcl5	6.8E-06	7.1E-03	5.36	*	2.5E-06	1.6E-03	8.64	*	1419728_at
Ddx4	1.8E-03	8.8E-02	8.31		5.7E-04	2.1E-02	7.89	*	1427242_at
Cxcl3	8.9E-10	4.0E-05	10.72	*	4.4E-05	5.5E-03	5.66	*	1438148_at
Sprr2a	2.1E-03	9.6E-02	4.12		7.6E-08	3.8E-04	5.52	*	1450618_a_at
Aldh1a3	1.6E-06	4.5E-03	2.53	*	1.4E-08	1.6E-04	5.40	*	1448789_at
Timp1	3.2E-06	5.2E-03	4.38	*	4.2E-09	1.4E-04	5.38	*	1460227_at
Saa3	4.4E-04	4.7E-02	3.70	*	9.4E-09	1.4E-04	5.19	*	1450826_a_at
Cxcl13	1.6E-02	2.3E-01	2.69		1.8E-06	1.5E-03	4.73	*	1417851_at
Sprr2a	2.3E-03	1.0E-01	3.48		3.0E-07	6.3E-04	4.33	*	1439016_x_at
Ccl24	1.6E-03	8.2E-02	4.97		8.3E-05	7.9E-03	4.25	*	1450488_at
Chl1	5.1E-04	5.0E-02	2.11		8.9E-06	2.6E-03	3.91	*	1435190_at
Cxcl13	1.9E-02	2.5E-01	2.14		7.4E-07	9.7E-04	3.84	*	1448859_at
Fxyd4	2.2E-04	3.2E-02	2.95	*	8.2E-07	9.7E-04	3.74	*	1418207_at
4833422F24Rik	3.5E-04	4.1E-02	5.14	*	8.2E-06	2.5E-03	3.67	*	1425386_at
Arg1	6.6E-04	5.6E-02	6.27		8.9E-05	8.1E-03	3.54	*	1419549_at
Tnfrsf9	2.8E-04	3.7E-02	2.65	*	1.1E-05	2.7E-03	3.43	*	1428034_a_at
Cxcl2	8.1E-07	4.5E-03	3.18	*	2.1E-04	1.2E-02	3.41	*	1449984_at
Reg3g	6.3E-01	8.8E-01	1.16		6.0E-04	2.1E-02	3.39	*	1448872_at
Il6	2.5E-03	1.0E-01	2.22		2.5E-07	6.2E-04	3.19	*	1450297_at
Serpina3n	5.5E-09	1.2E-04	2.78	*	1.2E-07	4.1E-04	3.14	*	1419100_at
Cxcl1	1.3E-05	8.5E-03	2.75	*	4.2E-04	1.8E-02	3.11	*	1419209_at
Selp	9.8E-04	6.6E-02	1.51		3.4E-05	4.8E-03	2.95	*	1440173_x_at
Saa1	1.0E-05	8.1E-03	2.23	*	9.0E-09	1.4E-04	2.85	*	1450788_at
Cxcl1	3.8E-04	4.3E-02	2.15	*	5.1E-04	1.9E-02	2.78	*	1457644_s_at
Ch25h	1.3E-06	4.5E-03	3.35	*	2.5E-08	2.1E-04	2.76	*	1449227_at
Ccl7	2.6E-04	3.5E-02	1.90		4.8E-07	8.0E-04	2.76	*	1421228_at
Cd177	3.0E-02	3.0E-01	1.93		1.3E-05	2.9E-03	2.72	*	1424509_at
Birc5	3.1E-06	5.2E-03	2.59	*	1.3E-07	4.2E-04	2.70	*	1424278_a_at
Cd163	1.2E-03	7.2E-02	1.84		7.9E-08	3.8E-04	2.65	*	1419144_at
Retnlb	1.4E-02	2.2E-01	1.88		6.4E-07	9.7E-04	2.62	*	1418368_at
Ppil5	3.0E-07	3.4E-03	2.64	*	6.0E-05	6.4E-03	2.56	*	1452458_s_at
Ccnb1	4.3E-06	5.9E-03	2.33	*	5.6E-06	2.1E-03	2.53	*	1416076_at

(Table 3–2 continued)

Gene Symbol	SOF versus AOF				SOM versus AOM				Affymetrix_ID
	P.Value	FDR	Fold Change	♀	P.Value	FDR	Fold Change	♂	
Rrm2	5.4E-07	3.5E-03	2.70	*	3.0E-06	1.7E-03	2.52	*	1434437_x_at
Rrm2	1.7E-06	4.5E-03	2.72	*	6.4E-06	2.1E-03	2.50	*	1448226_at
Cdca5	3.5E-07	3.4E-03	2.75	*	7.4E-06	2.3E-03	2.46	*	1416802_a_at
Il4i1	2.2E-03	9.9E-02	2.31		5.9E-06	2.1E-03	2.46	*	1419192_at
Rrm2	5.7E-06	6.3E-03	2.75	*	9.2E-06	2.6E-03	2.44	*	1416120_at
Myom2	3.4E-01	7.2E-01	1.27		7.0E-04	2.3E-02	2.36	*	1457435_x_at
Orm1	1.4E-02	2.2E-01	1.50		1.6E-04	1.1E-02	2.34	*	1451054_at
Cd209e	6.2E-04	5.4E-02	1.81		4.1E-06	1.9E-03	2.32	*	1420582_at
Hist1h2ab	3.1E-05	1.2E-02	2.18	*	8.8E-06	2.6E-03	2.31	*	1438009_at
Ear11	1.0E-04	2.2E-02	2.40	*	7.8E-06	2.4E-03	2.30	*	1425295_at
Ube2c	1.3E-05	8.5E-03	2.54	*	3.0E-05	4.6E-03	2.29	*	1452954_at
Selp	1.3E-04	2.4E-02	1.71		5.1E-08	3.3E-04	2.26	*	1449906_at
Vcan	4.9E-04	4.9E-02	1.68		5.1E-06	2.1E-03	2.24	*	1421694_a_at
Il13ra2	8.1E-04	6.1E-02	1.75		6.1E-05	6.5E-03	2.24	*	1422177_at
LOC632073	3.8E-01	7.4E-01	1.18		1.3E-03	3.2E-02	2.23	*	1423719_at
Fbp1	1.6E-01	5.5E-01	1.42		1.5E-04	1.0E-02	2.23	*	1448470_at
Pdcd1lg2	1.1E-03	6.8E-02	2.72		2.7E-06	1.7E-03	2.22	*	1450290_at
Ccnb1	2.8E-06	5.2E-03	2.06	*	3.7E-05	5.0E-03	2.22	*	1419943_s_at
Afp	9.8E-07	4.5E-03	2.09	*	1.4E-06	1.3E-03	2.21	*	1416645_a_at
Cdca8	1.0E-05	8.1E-03	2.41	*	4.5E-06	2.0E-03	2.20	*	1436847_s_at
Saa1	5.9E-05	1.7E-02	2.24	*	9.5E-05	8.3E-03	2.20	*	1419075_s_at
Guca2a	7.4E-04	5.8E-02	2.48		6.3E-05	6.7E-03	2.19	*	1416905_at
Shcbp1	5.7E-06	6.3E-03	2.49	*	3.1E-06	1.8E-03	2.18	*	1416299_at
Cdca8	1.2E-04	2.4E-02	1.71		9.2E-06	2.6E-03	2.18	*	1428480_at
Cdca8	2.9E-06	5.2E-03	2.02	*	3.3E-06	1.8E-03	2.17	*	1428481_s_at
Gpr109a	2.1E-03	9.5E-02	1.47		2.0E-07	5.3E-04	2.17	*	1419721_at
Ckmt2	9.7E-01	9.9E-01	1.01		2.1E-03	4.1E-02	2.16	*	1428722_at
Aurkb	3.4E-04	4.1E-02	1.92		6.7E-05	6.9E-03	2.15	*	1424128_x_at
Cenpe	1.5E-03	8.1E-02	2.01		3.8E-05	5.1E-03	2.15	*	1439040_at
U46068	4.2E-01	7.7E-01	1.18		1.3E-03	3.2E-02	2.15	*	1439423_x_at
Cdc6	7.3E-06	7.3E-03	2.16	*	3.1E-07	6.3E-04	2.14	*	1417019_a_at
Ccl17	4.4E-03	1.3E-01	1.65		1.5E-03	3.4E-02	2.13	*	1419413_at
Il1r2	7.7E-04	5.9E-02	1.67		2.5E-06	1.6E-03	2.11	*	1419532_at
Ccl2	3.4E-03	1.2E-01	1.65		2.6E-04	1.4E-02	2.09	*	1420380_at
Uhrf1	5.3E-05	1.7E-02	1.82		2.8E-08	2.1E-04	2.09	*	1415810_at
Aurkb	9.2E-06	7.7E-03	1.99		2.4E-05	4.0E-03	2.08	*	1451246_s_at
Top2a	6.4E-06	6.9E-03	2.34	*	5.1E-06	2.1E-03	2.07	*	1454694_a_at
Cep55	3.1E-05	1.2E-02	2.47	*	8.2E-07	9.7E-04	2.06	*	1452242_at
Sprr2a	2.7E-03	1.1E-01	1.82		5.9E-05	6.4E-03	2.06	*	1437258_at
Kif11	1.6E-06	4.5E-03	2.46	*	1.6E-05	3.2E-03	2.04	*	1435306_a_at
Ncapg	1.8E-06	4.5E-03	2.67	*	5.4E-05	6.1E-03	2.04	*	1429171_a_at
Selp	1.8E-06	4.5E-03	1.73		9.6E-07	1.0E-03	2.03	*	1420558_at
Bub1	2.7E-06	5.2E-03	2.27	*	4.7E-06	2.0E-03	2.02	*	1424046_at
Muc4	9.5E-03	1.9E-01	1.29		7.9E-05	7.6E-03	2.02	*	1427398_at

(Table 3–2 continued)

Gene Symbol	SOF versus AOF				SOM versus AOM				Affymetrix_ID
	P.Value	FDR	Fold Change	♀	P.Value	FDR	Fold Change	♂	
Ccnb1	1.2E-05	8.4E-03	2.23	*	2.2E-05	3.9E-03	2.00	*	1448205_at
Cdc2a	4.1E-05	1.5E-02	2.17	*	1.1E-05	2.7E-03	1.99		1448314_at
Mki67	5.3E-06	6.3E-03	2.46	*	6.4E-05	6.7E-03	1.97		1426817_at
Ccna2	2.4E-05	1.1E-02	2.18	*	6.7E-05	6.9E-03	1.95		1417911_at
Ncapg	2.8E-04	3.7E-02	2.07	*	1.8E-04	1.1E-02	1.94		1429172_a_at
Ccna2	7.2E-05	1.9E-02	2.11	*	1.5E-05	3.2E-03	1.93		1417910_at
Cdca3	2.3E-06	5.1E-03	2.12	*	2.1E-05	3.7E-03	1.90		1452040_a_at
2810417H13Rik	2.4E-05	1.1E-02	2.18	*	1.2E-05	2.8E-03	1.90		1419153_at
Rad51	1.2E-05	8.4E-03	2.30	*	6.2E-06	2.1E-03	1.89		1418281_at
Ttk	4.1E-05	1.5E-02	2.01	*	3.2E-04	1.6E-02	1.89		1449171_at
Nusap1	2.9E-05	1.2E-02	2.28	*	2.8E-06	1.7E-03	1.86		1416309_at
Esco2	4.7E-07	3.5E-03	2.30	*	1.6E-05	3.2E-03	1.84		1428304_at
Cks1b	4.3E-05	1.5E-02	2.05	*	1.0E-05	2.7E-03	1.84		1416698_a_at
Hells	5.6E-05	1.7E-02	2.11	*	9.4E-07	1.0E-03	1.80		1417541_at
Nuf2	6.9E-05	1.9E-02	2.16	*	1.0E-04	8.6E-03	1.76		1430811_a_at
Cyp26b1	2.1E-04	3.1E-02	3.10	*	2.6E-01	5.4E-01	1.76		1460011_at
Cenpp	1.6E-04	2.7E-02	2.07	*	7.2E-04	2.3E-02	1.74		1432361_a_at
Aspm	1.7E-05	9.0E-03	2.03	*	3.7E-05	5.0E-03	1.73		1422814_at
Slc7a2	4.3E-05	1.5E-02	2.21	*	6.0E-06	2.1E-03	1.71		1426008_a_at
Kif11	4.9E-05	1.6E-02	2.19	*	2.6E-04	1.4E-02	1.60		1452314_at
Slc7a2	1.8E-04	2.9E-02	2.11	*	1.0E-06	1.0E-03	1.60		1422648_at
Kif20a	2.2E-06	5.1E-03	2.04	*	1.1E-03	2.9E-02	1.54		1449207_a_at
C330027C09Rik	1.3E-05	8.5E-03	2.20	*	6.8E-04	2.3E-02	1.51		1449699_s_at
Tpx2	2.0E-05	9.8E-03	2.12	*	1.1E-05	2.7E-03	1.50		1428104_at
Cep55	9.7E-05	2.2E-02	2.00	*	3.1E-04	1.5E-02	1.48		1453683_a_at
Egr2	8.4E-05	2.0E-02	2.17	*	4.4E-03	6.1E-02	1.35		1427682_a_at
---	1.5E-06	4.5E-03	-2.47	*	6.4E-02	2.6E-01	-1.20		1445238_at
G530011O06Rik	1.2E-05	8.4E-03	2.10	*	2.0E-01	4.7E-01	-1.28		1440342_at
Pon1	8.0E-04	6.1E-02	-2.01		4.8E-04	1.9E-02	-2.10	*	1418190_at
C1qtnf3	1.4E-03	7.7E-02	-1.76		2.3E-04	1.3E-02	-2.14	*	1422606_at
Fmo3	3.2E-04	4.0E-02	-2.36	*	3.2E-05	4.7E-03	-2.16	*	1449525_at
Esm1	2.2E-03	9.8E-02	-2.52		1.0E-04	8.5E-03	-2.32	*	1449280_at
Itgbl1	3.5E-04	4.1E-02	-1.60		1.1E-07	4.1E-04	-2.49	*	1425039_at
Fabp7	1.8E-01	5.8E-01	-1.22		1.9E-06	1.5E-03	-2.68	*	1450779_at
Gpnmb	4.4E-01	7.8E-01	-1.24		2.4E-05	4.0E-03	-3.06	*	1448303_at
Bex1	3.0E-01	6.8E-01	-1.21		2.7E-05	4.3E-03	-3.64	*	1448595_a_at
Igh /// Ighg	6.2E-01	8.7E-01	1.42		1.0E-03	2.8E-02	-4.24	*	1451632_a_at

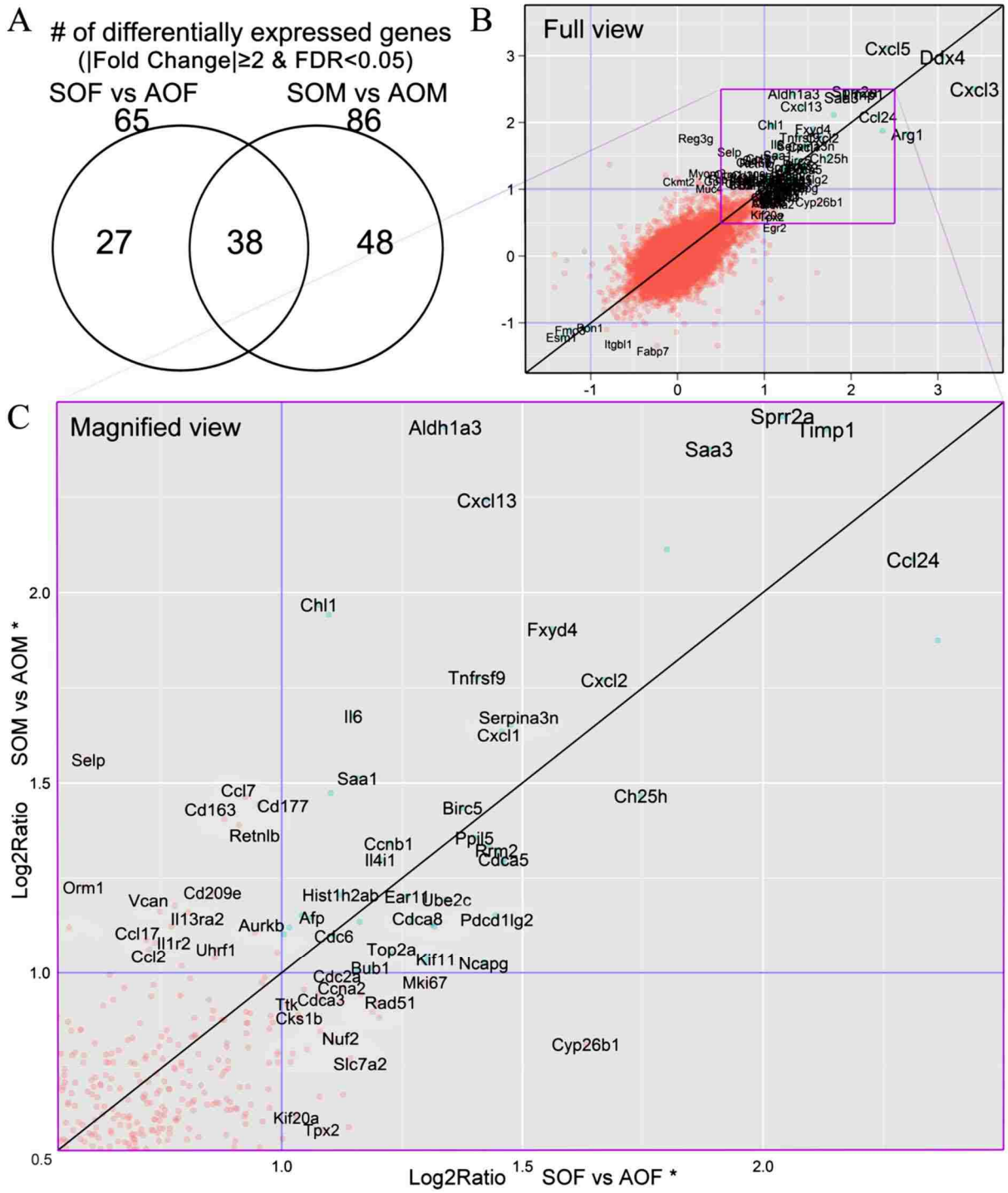

Figure 3–5. Differentially expressed genes were identified for SOF vs AOF and SOM vs AOM. A. Venn diagram shows numbers of differentially expressed genes in two pairwise comparisons. B. Transcriptome screening revealed differentially expressed genes by comparing SHS-OVA and AIR-OVA responses in mice of each sex. We plotted each gene's Log2Ratios from "SOF versus AOF" and "SOM versus AOM" onto the x-axis and y-axis respectively. The "y=x" line indicates the same degree of expression changes in both females and males. All gene symbols shown are

differentially expressed in either male or female mice (|fold change|≥2, FDR< 0.05; N=4 mice in each group). C. Magnified view of box outlined in panel B.

Although the ranges of fold change values are similar for both sexes (Fold change: ↓4.0 - ↑11.3, Log2Ratio: -2.0 - +3.5, Figure 3-5B), not only were there more differentially expressed genes for males than for females (86 versus 65), the majority of the 38 shared genes exhibited higher fold change values in the males than the females (Figures 3-5 & 3-6). This indicated that, on a transcriptional level, males are more responsive than females to OVA as adults after *in utero* exposure to SHS.

This is also evident from Figure 3-5C (in magnified view, Log2Ratios within 0.5 - 2.5 range), where there are more genes located above the "y=x" line that delineates the same degree of up-regulation in both males and females. A few down-regulated genes also were identified, including β1-integrin (Itgb1, ♀: ↓1.60; ♂: ↓2.49) and paraoxonase (Pon1, ♀: ↓2.01; ♂: ↓2.10).

We used IPA to illuminate biological responses and signaling pathways consistent with *in utero* SHS-associated gene expression changes in adult mouse lungs. We focused on the 113 differentially expressed genes found in either or both sexes (Figure 3-5A, 27+38+48=113). We found the most statistically significant diseases and disorders pathways to be "Inflammatory Response", "Cancer" and "Respiratory Disease" (***P***-value≤7.05E-03). The IL-17 signaling pathways (***P***-value≤8.32E-04) were among the most significant canonical signaling pathways. The IPA results are listed in Table 3-3.

We found significant differences by qRT-PCR (Figure 3-6) between SHS-OVA and AIR-OVA for all 11 genes initially identified by BALF cytokine assessment (ELISA) or by microarray analysis. For each of the 11 genes, relative expression levels were significantly higher for SOF versus AOF and for SOM versus AOM. These 11 genes include chemokines (Ccl8, Ccl24, Cxcl2, Cxcl5), cytokines (Il1b, Il6, Il13, Il17b) and acute phase response genes

(Saa1, Saa3) associated with inflammatory responses. In addition, for 3 of the 11 genes (Il1b, Il6 and Timp1), there were significantly increased expression levels in SOM versus SOF. The ΔΔCT values (compared to the house-keeping gene Hprt1) are charted in Figure 3-6. A ΔΔCT difference of one represents a 2-fold difference in expression.

Table 3–3. Ingenuity Pathway Analysis results indicated that the differentially expressed genes affected by *in utero* SHS exposure are significantly associated with inflammatory responses, cancer and respiratory disease, and also are involved in IL-17-associated pathways.

Diseases and Disorders	*P*-value	# Molecules
Inflammatory Response	2.85E-08 - 7.05E-03	29
Cancer	7.69E-08 - 7.05E-03	52
Respiratory Disease	2.12E-07 - 6.99E-03	29
Dermatological Diseases and Conditions	5.19E-07 - 7.05E-03	27
Immunological Disease	5.90E-07 - 7.05E-03	26

Canonical Pathways	*P*-value	Ratio*
Role of IL-17A in Psoriasis	3.92E-05	3/13 (0.231)
LXR/RXR Activation	1.29E-04	6/136 (0.044)
Role of IL-17F in Allergic Inflammatory Airway Diseases	1.57E-04	4/48 (0.083)
Role of IL-17A in Arthritis	4.47E-04	4/63 (0.063)
IL-17A Signaling in Airway Cells	8.32E-04	4/72 (0.056)

Ratio*: Denominator = total # of genes in the pathway; Numerator = # of pathway genes identified in our studies.

We then created a gene network in IPA Pathway Designer, by combining the most differentially expressed genes with the most significant biological functions and canonical pathways, according to the Ingenuity Knowledge Base. These functions and pathways were directly associated with inflammatory responses, AHR, acute phase response signaling and IL-17 signaling (Figure 3-7). The network indicated key information about the gene of interest, including degree of up/down-regulation for either sex (for the two bars in the brackets: females on the left, males on the right), fold change values in males, and each gene's functional

association. With very few exceptions, the left-hand bar (female) is shorter than the right-hand bar (male), further supporting the conclusion that males are more sensitive than females in this SHS-OVA model.

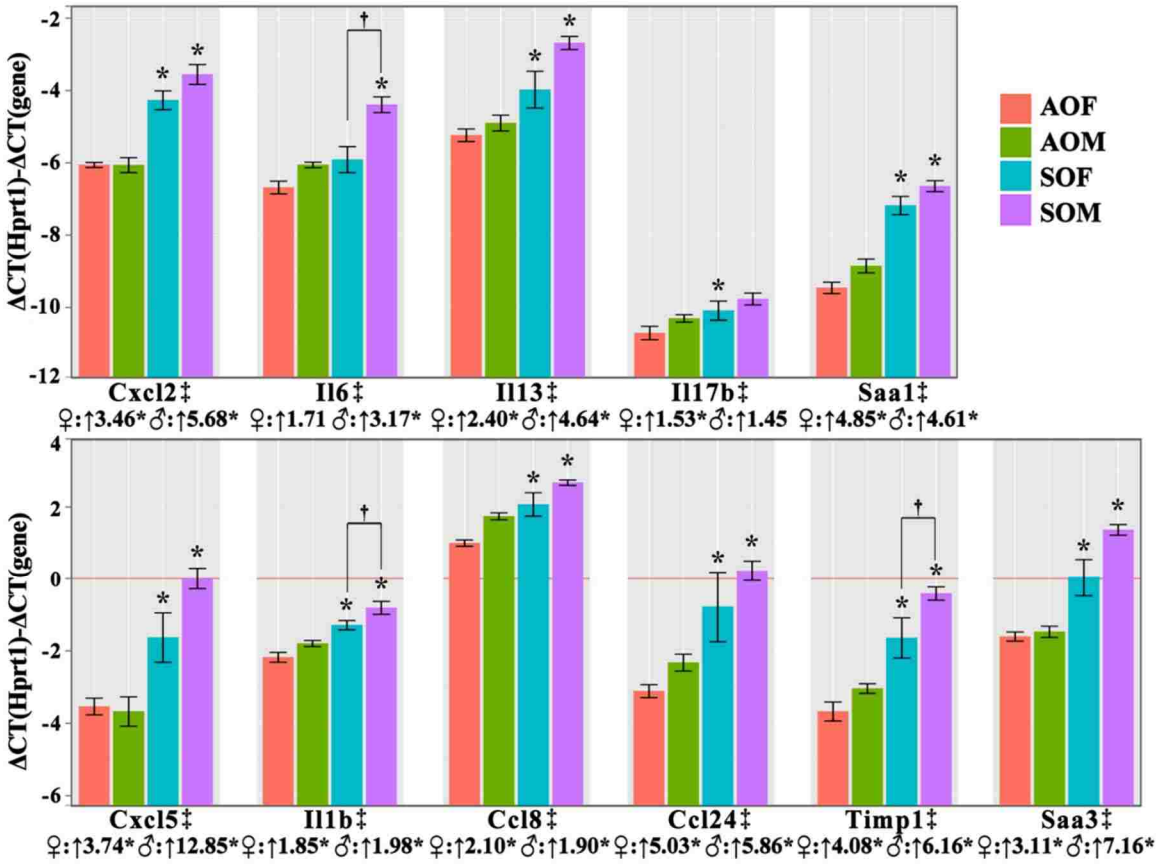

Figure 3–6. Differentially expressed genes identified by BALF cytokine or microarray were confirmed by qRT-PCR. qRT-PCR confirmed 11 differentially expressed genes identified by BALF cytokine assessment or microarray analysis. The y-axis is –ΔΔCT, so the higher the value, the higher the expression level for each group. The line "y=0" represents the level of house-keeping gene (Hprt1) expression. Since the y-axis is calculated from cycle number differences, a difference of one on the y-axis = a 2-fold difference in expression. Beneath each gene symbol, the fold change differences between SHS-OVA and AIR-OVA in either sex are shown, together with asterisks to indicate statistical differences (P<0.05). We carried out qRT-PCR in each of the 4 groups (6 mice/group) except for Ccl24 (N≥5) and Timp1 (N≥4). ‡: all 11 (SOvsAO); †: 3/11 (SOMvsAOF); *: ♀ 10/11, ♂ 10/11.

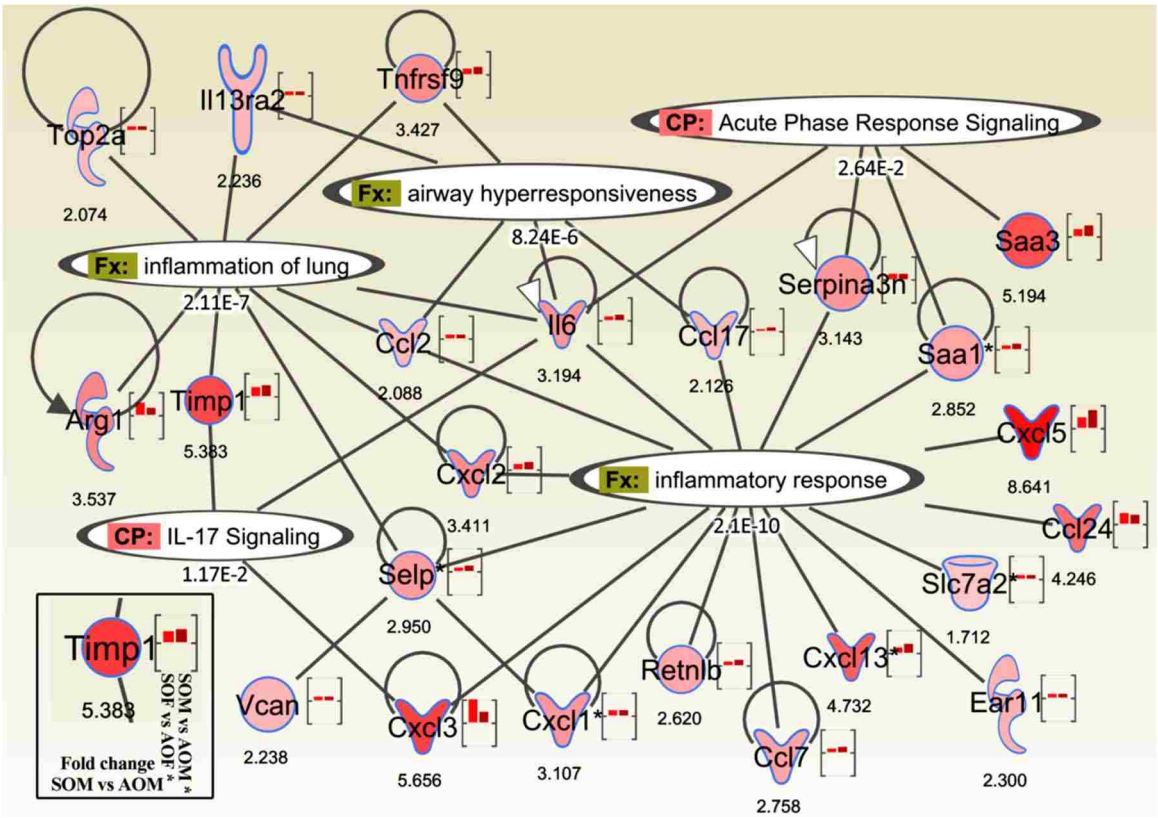

Figure 3–7. Ingenuity Pathway Analysis of microarray results identified biological functions and canonical pathways associated with *in utero* SHS exposure. Ingenuity pathway analysis on microarray results identified several significant biological functions ("Fx:") and canonical pathways ("CP:") associated with *in utero* exposure to SHS in either sex. The color intensity inside each gene symbol and in the right-hand bar inside each bracket is associated with relative fold changes between SOM versus AOM (more saturated red = higher degree of up-regulation). The left-hand bar represents relative level of gene up-regulation in SOF versus AOF. Gene abbreviations: Arg1, arginase (liver); Ear11, eosinophil-associated ribonuclease 11; Retnlb, resistin like beta; Saa 1/3, serum amyloid A; Selp, selectin (platelet); Serpina3n, serine (or cysteine) peptidase inhibitor, clade A, member 3N; Slc7a2, solute carrier family 7 member 2; Timp1, tissue inhibitor of metalloproteinase 1; Top2a, DNA topoisomerase 2-alpha; Vcan, versican.

3.4 Discussion

This study was designed to investigate the effects of *in utero* SHS exposure and of sex differences on adult responses of mice under identical OVA challenge conditions in a mouse asthma model. We used BALB/c mice for three reasons, i) BALB/c mice are a well-accepted strain for asthma studies (Boyce and Austen 2005; Kips et al. 2003; Lloyd 2007; Nials and

Uddin 2008; Temelkovski et al. 1998); ii) a high correlation has been reported for these mice between Penh values and lung resistance (DeLorme and Moss 2002; Hamelmann et al. 1997; Singh et al. 2003), iii) we have established laboratory protocols in BALB/c mice for investigating the effects of *in utero* SHS exposure on adult lung responses to environmental irritants (Penn et al. 2007; Xiao et al. 2012). Control groups without OVA challenge were not included in the study because our previous studies revealed that adult mice exposed *in utero* to SHS, but not exposed as adults to environmental stressors, do not exhibit signs of inflammation compared to the AIR mice (Penn et al. 2007; Xiao et al. 2012).

One consequence of having all groups of adult mice exposed to OVA was that the resulting inflammation masked airway structural changes to which the *in utero* SHS exposure undoubtedly contributed (Xiao et al. 2012). The large numbers of infiltrated inflammatory cells present in the lungs of both male and female mice in all groups made accurate morphometric assessment unachievable (Figure 3-3). In contrast, the results from lung function testing, BALF analysis, and gene expression profiling all demonstrated that *in utero* SHS exposures aggravate responses to adult OVA exposures. In addition, results are more pronouced in male mice than in females..

Lung function testing revealed that there was increased AHR and decreased breathing frequency (f) in SHS-OVA mice, compared to AIR-OVA mice, regardless of sex, at multiple methacholine doses. The males exposed to SHS *in utero* were more responsive than females who were exposed similarly (Figure 3-2). These findings indicate that both SHS *in utero* and sex differentially affect adult lung responses to inhaled environmental stressors.

The prominent lung responses of OVA-exposed adult males that had been exposed *in utero* to SHS were supported by the elevated BALF cytokine levels (Figure 3-4). SHS exposure

in utero markedly increased the levels both of pro-inflammatory cytokines (IFN-γ, IL-1b, KC/CXCL1 and TNF-α) and of Th2 cytokines (IL-4, IL-5, IL-10 and IL-13). This is consistent with the OVA-induced mouse model of asthma. The sex-associated differences described here are associated with two other findings: i) the baseline BALF cytokine levels of male mice were not significantly higher than females; on the contrary, for 6/8 cytokines--IFN-γ, IL-1b, IL-4, IL-5, IL-10 and TNF-α-- female mice exhibited slightly higher baseline BALF cytokine levels than the males, although the difference for each of the cytokines did not reach the level of statistical significance; ii) male mice exposed *in utero* to SHS had much higher BALF cytokine levels than the females.

Results from transcriptome screening supported the findings from lung function testing and BALF cytokine measurements. We performed transcriptome screening on individual whole lung homogenates collected from 4 mice/group for each of the 4 groups, and searched for the differentially expressed genes between SHS-OVA and AIR-OVA in either sex. As shown in Figure 3-5A, we found more differentially expressed genes for the males (N=86 genes, SOM versus AOM) than for the females (N=65 genes, SOF versus AOF). Notably, a large portion of the most differentially expressed genes were chemokines and cytokines involved in inflammatory responses. With only a few exceptions, they exhibited a higher degree of up-regulation in the males than in the females.

To study the biological functions and signaling pathways associated with these differentially expressed genes identified by transcriptome screening, we performed several analyses in IPA of the 113 genes we found differentially expressed in either males or females. “Inflammatory response”, “cancer” and “respiratory disease” are the top 3 diseases/disorders that are significantly associated with these genes. As shown in Figure 3-7, in addition to

inflammation pathways, significantly associated pathways include "airway hyperresponsiveness", "acute phase response signaling" and "IL-17 signaling". There is no doubt that the OVA challenge triggers acute phase response signaling, causes severe inflammation, and increases AHR. However, all mice received identical OVA exposures, indicating that changes in gene expression were due to SHS exposure *in utero* and supporting *in utero* SHS exposure as a potential factor in aggravated adult lung responses.

Despite the fact that most genes affected by *in utero* SHS were up-regulated on microarrays, we identified a few down-regulated genes as well. These genes, including Itgb1 and Pon1, were consistent with data from some human studies. B1-integrin (Itgb1, ♀: ↓1.60; ♂: ↓2.49), initially activated by P-selectin, has been reported to increase during early stages of asthma but to diminish in subjects with severe asthma (Johansson et al. 2012). Pon1 (♀: ↓2.01; ♂: ↓2.10) is decreased in asthmatic versus non-asthmatic children (Cakmak et al. 2009). The decreases in expression of Itgb1 and Pon1 found during asthma exacerbation suggest a protective role for these genes against asthma progression. For instance, integrin $\alpha_9\beta_1$, suppresses exaggerated contraction of the airway smooth muscle through inhibition of IP3-dependent pathways (C Chen et al. 2012). Pon1, on the other hand, may attenuate asthmatic responses via its anti-oxidative properties (Tolgyesi et al. 2009). The down-regulation of these genes resulting from *in utero* exposure to SHS would further impair the defenses against severe asthma.

We observed increased production of Th2 cytokines both transcriptionally (whole lung) and translationally (BALF). The Th2 cytokines, IL-4, IL-5 and IL-13, are believed to mediate isotype switching of allergen-specific B cells into IgE production, promoting airway eosinophilia and inducing AHR (Epstein 2006), the latter two of which were also observed in

this study. Although Th2 responses and eosinophilic inflammation largely explained the observed responses in our earlier study, here the slightly increased BALF neutrophil counts and up-regulation of neutrophil surface antigen Cd177 (♀: ↑1.93; ♂: ↑2.72), suggested early signs of airway neutrophilia in OVA-challenged adult mice that were exposed *in utero* to SHS. As neutrophils accumulate in the airway, which is common in severe allergic asthma (Wang and Wills-Karp 2011), the presence of both eosinophils and neutrophils in the airways have been reported to be associated with lowest lung function, poorest asthma control, and increased exacerbations of asthma patients (Hastie et al. 2010). Recent reports have suggested the possible involvement of IL-17 in neutrophilic inflammation (Hellings et al. 2003; Suzuki et al. 2007; Wilson et al. 2009). IL-17 can induce lung structural cells to secrete pro-inflammatory cytokines, as was found here for TNF-α, IL-1b, IL-6, and chemokines, including CXCL1 (KC), CXCL2 and CXCL8, thereby attracting neutrophils (Laan et al. 1999). According to IPA, the IL-17 signaling pathway is closely associated with Il6, Cxcl3 and Timp1, all of which we found to be significantly up-regulated on microarrays. Microarray analysis also revealed that IL-17B, among all the cytokines in the IL-17 family, showed increased expression in the SHS-OVA groups. In our previous study (Xiao et al. 2012) where we studied recurring SHS exposure to mice that had been to SHS *in utero*, IL-17 signaling also was one of the most significant canonical pathways associated with *in utero* exposure to SHS. Findings from both studies demonstrate that the IL-17 signaling pathway is persistently modulated by *in utero* SHS exposures, independent of the adult irritant. In addition, Th2 cytokines, particularly IL-4 and IL-13, also affect macrophage polarization and induce alternatively activated M2 macrophages (Mills et al. 2000). Although clear evidence was not found for M2 macrophages in the lungs, we found elevated expression of genes that are primarily expressed in M2 macrophages (Nair et al. 2006; Nguyen et al. 2005;

Staples et al. 2012): Arg1 (♀: ↑6.27; ♂: ↑3.54), Ccl17 (♀: ↑1.65; ♂: ↑2.13) and Cd163 (♀: ↑1.84; ♂: ↑2.65). Thus, SHS exposure *in utero* appears to aggravate adult asthmatic responses mediated by a variety of cell types, including eosinophils, neutrophils and macrophages.

The most highly-responsive group, SOM, is of particular interest. The sex bias we report was not apparent unless mice were exposed to SHS *in utero*, which means a) the *in utero* environment selectively modified the male offspring more significantly than the females and b) the differential effects of *in utero* exposure are prolonged to at least 23 weeks of age. Sex-specific effects induced by smoke exposures *in utero* have been shown by other researchers as well. In a study by Ng et al. (Ng et al. 2006), *in utero* exposure to mainstream cigarette smoke significantly reduced cytotoxic T-lymphocyte activity in 5- and 10-week-old male offspring, whereas the females were not affected. In another study, Murphy et al. (Murphy et al. 2012) reported *in utero* cigarette smoke-related increases in DNA methylation of insulin-like growth factor 2, which is more pronounced in the male offspring than the females. Epigenetic alterations induced by *in utero* smoke exposures have been revealed (Breton et al. 2009; Guerrero-Preston et al. 2010), with the potential for these alterations to persist into adulthood and modulate adult responses (Jirtle and Skinner 2007; Tang and Ho 2007). We are currently investigating the epigenetic changes associated with SHS exposure *in utero* to gain more insights into adult disease susceptibility.

CHAPTER 4.
IN UTERO EXPOSURE TO SECOND-HAND SMOKE ACTIVATES ONCOGENIC MICRORNAS IN OVALBUMIN-CHALLENGED ADULT MICE[3]

4.1 Introduction

MicroRNAs (miRNAs) are small non-coding RNAs (19-23 nt), that serve as endogenous sequence-specific regulators of various biological processes. Dysregulation of miRNA expression has been implicated in diverse diseases, including inflammatory lung disease (Oglesby et al. 2010), cardiovascular disease (Small et al. 2010) and cancer (Chen et al. 2012; Melo and Esteller 2011). In recent years, an increasing body of literature has reported dysregulated miRNA expression profiles resulting from direct exposures to various environmental pollutants, including metal-rich particulate matter (Bollati et al. 2010), diesel exhaust particles (Jardim et al. 2009; Yamamoto et al. 2013) and tobacco smoke (Izzotti et al. 2009; Schembri et al. 2009). Among these studies, metal-rich particulate matter and diesel exhaust particle exposures were reported to aggravate systemic oxidative stress and to up-regulate expression of miRNAs, particularly of miR-21 (Bollati et al. 2010; Yamamoto et al. 2013); whereas cigarette smoke exposures, both in vitro (human primary bronchial epithelial cells) and in vivo (rat lungs), down-regulate expression of miRNAs. Although the dysregulated miRNA expression profiles were clearly detectable immediately after exposures to the environmental pollutants ended, whether the influence of the pollutants on miRNA expression remains long after the exposures end has not yet been fully investigated.

Uterine life is one of the most critical periods for developmental programming (Knopik et al. 2012); thus, *in utero* environmental exposures would be expected to have profound

[3] This chapter was submitted to American Journal of Respiratory Cell and Molecular Biology.

influence not only on fetal growth, but on postnatal health and disease conditions as well (Martino and Prescott 2011). Previously, we reported that *in utero* second-hand smoke (SHS) exposure aggravates adult responses to subsequent post-natal exposures to environmental irritants, including ovalbumin (OVA) (Rouse et al. 2007; Xiao et al. 2013) and SHS (Xiao et al. 2012). In the most recent studies (Xiao et al. 2013), where we challenged all adult mice with OVA to induce allergic asthma, we found, in this murine model of asthma (Kips et al. 2003), that the effects of *in utero* SHS exposure persisted into adulthood, further aggravated lung inflammation, increased airway hyperresponsiveness (AHR) and altered gene expression profiles. However, whether *in utero* SHS dysregulates miRNA expression profiles and further modulates target gene expression in adult mice that have been challenged by OVA, remains to be determined.

We used RNA sequencing (RNA-seq) technology to establish the complete expression profiles of miRNAs and mRNAs in adult mouse lungs from 23-week old female and male BALB/c mice, that had been exposed *in utero* to either SHS or filtered air (AIR), and then as adults to OVA. We aimed to answer the following questions:

- Can we identify dysregulated miRNAs in lungs of OVA-challenged adult mice that had been exposed *in utero* to SHS compared to those exposed to AIR? Are there any sex differences in miRNA expression? Are these changes associated with previously observed pro-asthmatic lung responses?
- Are there any connections between the *in utero* SHS dysregulated miRNAs and mRNAs that may lead to better understanding of the regulatory mechanisms underlying the sustained effect of *in utero* SHS exposure?

- Can we identify a miRNA-mRNA regulatory network that may contribute to aggravated asthmatic responses or to other lung diseases?

4.2 Materials and Methods

Animal protocols, SHS and OVA exposures. The RNA samples originated from a previous report (Xiao et al. 2013). Briefly, pregnant BALB/c mice (Harlan, Indianapolis, IN) were exposed 5 hours per day on days 6-19 of pregnancy to SHS (3R4F filtered research cigarettes, University of Kentucky; 10 mg/m^3) mixed with HEPA-filted air (AIR) or AIR alone. All offspring (females and males) were sensitized by OVA (Grade V >98% pure, Sigma-Aldrich, St. Louis, MO; 80 μg in 2 ml alum) injections at 19 & 21 weeks of age, followed by OVA aerosol challenge every other day in weeks 22 & 23, before sacrifice. Mice were divided into 4 groups: AOF, AOM, SOF and SOM, according to exposures *in utero* (A, S) and as adults (O), plus sex (F, M). The 4 individual RNA samples with the highest RIN (RNA Integrity Number) values in each group (collected from 4 different mice, N=4) were selected for RNA-seq analysis. The experimental design is shown in Table 4-1.

Table 4–1. *In utero* exposure to SHS potentiates AHR, elevated BALF cytokine production and altered lung gene expression in OVA-challenged adult mice.

In Utero **(GD 6-19)**	**Adult (19-23wk)**	**Sex**	**Symbol**	**=>**	**AHR**	**BALF Cytokine**	**Lung Gene Expression**
AIR	OVA	Female	AOF		_	_	_
AIR	OVA	Male	AOM		_	_	_
SHS	OVA	Female	SOF	♀	↑	↑	↑
SHS	OVA	Male	SOM	♂	↑↑	↑↑	↑↑

AHR: airway hyperresponsiveness; BALF: bronchoalveolar lavage fluid; GD: gestational day; AIR: HEPA-filted air; SHS: second-hand smoke; ♀: SOF versus AOF; ♂: SOM versus AOM. Data summarized from a previous publication (Xiao et al. 2013).

RNA sequencing analysis. Small RNAs (<150bp, including miRNAs), were purified by gel electrophoresis. Paired-end sequencing (Illumina, 50bp) was performed on these small RNAs (Expression Analysis Inc., Durham, NC). After clipping the adapter sequence, the small RNA sequences matching mature mouse miRNAs (miRBase.org) were categorized and counted. mRNAs with poly(A) tails were purified with oligo-dT magnetic beads and sequenced by the Illumina system (paired-end, 50bp; Expression Analysis Inc.). RNA-seq reads were aligned to the reference genome (UCSC mm9) and quantitated by the RSEM method (RNA-Seq by Expectation Maximization) to provide accurate estimation of mapped transcripts (Li and Dewey 2011).

qRT-PCR. miRNAs were quantitated with predesigned Taqman probes for small RNA controls and mature miRNAs (assay ID: snoRNA234, 001234; miR-155-5p, 002571; miR-541-5p, 002562; miR-511-3p, 453069; miR-21(a)-3p, 002493; miR-298-5p, 002598; miR-18a-5p, 002422; miR-18b-5p, 002466; miR-138-5p, 002284; miR-144-3p, 002676; miR-134-5p, 001186; miR-181c-3p, 464644; miR-146b-5p, 001097; miR-1934-5p, 121185) with the Taqman MicroRNA Reverse Transcription kit and Taqman Universal Master Mix II (NO UNG) kit (Applied Biosystems, Foster City, CA). snoRNA234 was used as an endogenous control to standardize qRT-PCR results for miRNAs.

Statistical analysis. RNA-seq data were analyzed in the R/bioconductor platform (bioconductor.org) with the edgeR package (Robinson et al. 2010). miRNA and mRNA counts were analyzed with the generalized linear model (2*2 factorial design) to test for differentially expressed miRNAs and mRNAs as a result of *in utero* SHS or a sex bias. The chromosome location enrichment analysis was performed with Fisher's exact test on 114 chromosome locations, each consisting of a chromosome name (Chr.1-19,X,Y) and a major cytogenetic band

designation (A,B,…, annotations accessible from UCSC Genome Bioinformatics). In addition, the following R graphics packages: gclus, ggplot2 and Gviz, were used for visual presentation.

miRNA-mRNA pairing and Ingenuity Pathway Analysis (IPA). Target genes of oncomirs were selected only if they were known targets according to at least 2 of the 4 target predicting databases: DIANA-microT, miRanda, miRWalk and TargetScan (Betel et al. 2008; Dweep et al. 2011; Lewis et al. 2003; Maragkakis et al. 2009). All anti-correlations between miRNA and mRNA expression had to meet the following criteria: Pearson's correlation coefficient $r \leq -0.7$, ***P***-value<0.01; and at least 1.5 fold difference in the expression of target genes. Information on 628 mouse tumor suppressor genes was found in the tumor suppressor genes database, accessible from http://bioinfo.mc.vanderbilt.edu/TSGene/ (Zhao et al. 2013). The miRNA-mRNA regulatory network was built in Ingenuity Pathway Designer and connections between each gene and cancer were generated according to the Ingenuity Knowledge Base (Ingenuity Systems, Redwood City, CA; www.ingenuity.com).

4.3 Results

Dysregulated miRNAs. Direct sequencing of small RNAs from lung samples of BALB/c mice detected 504 miRNAs. The Venn diagram in Figure 4-1A shows the number of miRNAs that were either dysregulated by *in utero* SHS exposures or biased by sex, as determined for three levels of filtering thresholds. As shown in the top level of Figure 4-1A, the most rigorous filtering threshold identified nine miRNAs with a significant smoke effect (FDR<0.05). These nine miRNAs are miR-155-5p, miR-541-5p, miR-511-3p, miR-21-3p, miR-298-5p, miR-341-3p, miR-501-5p, miR-18a-5p and miR-18b-5p.

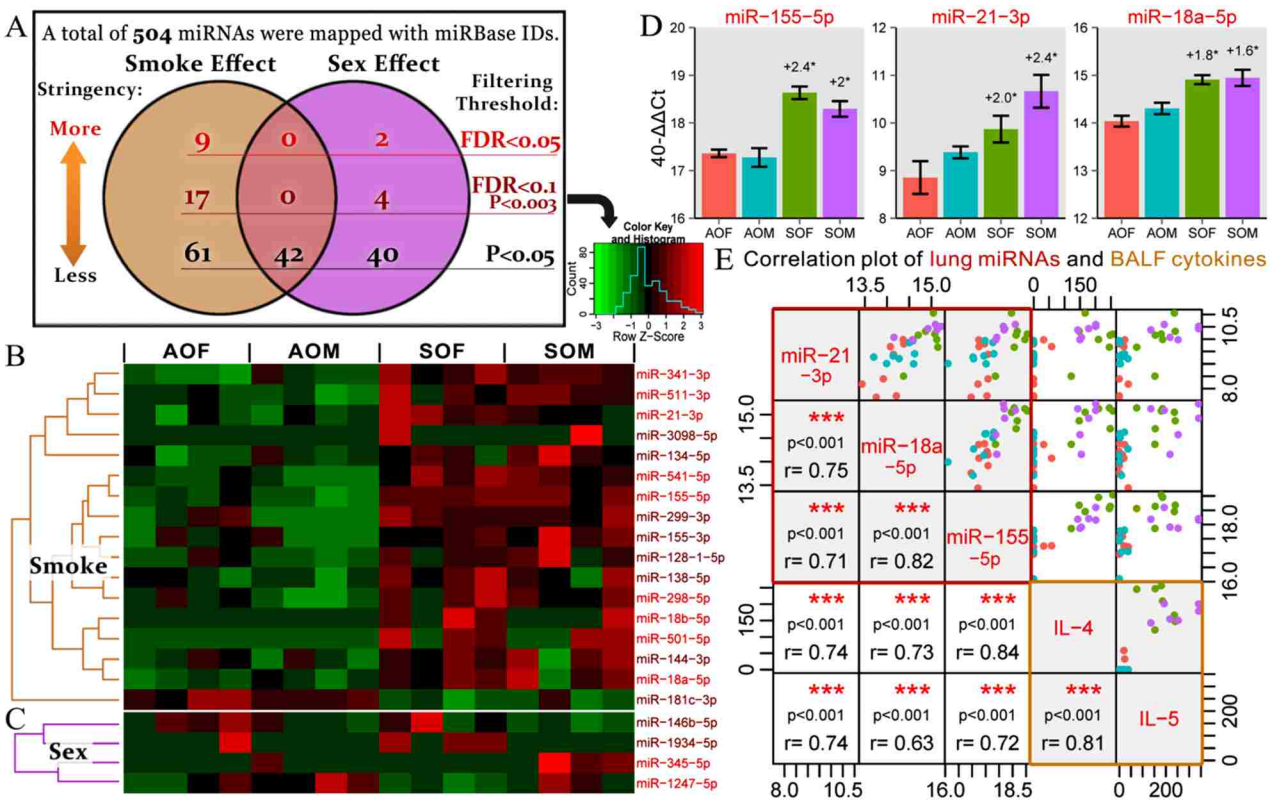

Figure 4–1. *In utero* SHS exposure dysregulates miRNA expression and high correlations were found between elevated miRNA expression and increased inflammatory cytokine levels. miRNA expression profiling (A) revealed more miRNAs significantly dysregulated by *in utero* SHS exposure (B) than those biased by sex (C). The expression levels of miR-155, miR-21 and miR-18a, confirmed by qRT-PCR, were significantly elevated in SO vs AO mice of either sex (D), and were highly correlated with pro-asthmatic Th2 cytokine levels in BALF (E). The Venn diagram (A) lists the numbers of dysregulated miRNAs according to different filtering thresholds (colors of miRNAs: red, FDR<0.05; dark red, FDR<0.1 & *P*-value<0.003). For the color scheme in the heat map, red/green=relative high/low expression. The qRT-PCR results (mean ± SEM) were standardized to the expression of snoRNA234 (housekeeping small RNA) via the ΔΔCt method and subtracted by 40 in order to set the baseline to 40 cycles, which is the detection limit of quantitative PCR; each increment of one on the y-axis represents a 2-fold increase in expression or 1-cycle difference in PCR results. Fold change values of "SOF versus AOF" and "SOM versus AOM" are labeled and marked with asterisks to indicate statistical significance (P<0.05). The units in the correlation plot for miRNA qRT-PCR results are 40-ΔΔCt and pg/ml for cytokine levels. BALF: bronchoalveolar lavage fluid.

All nine of these miRNAs were up-regulated by SHS exposure *in utero*. qRT-PCR analyses were performed on seven of the nine miRNAs and up-regulation of all seven miRNAs was confirmed, as shown in Figure 4-2.

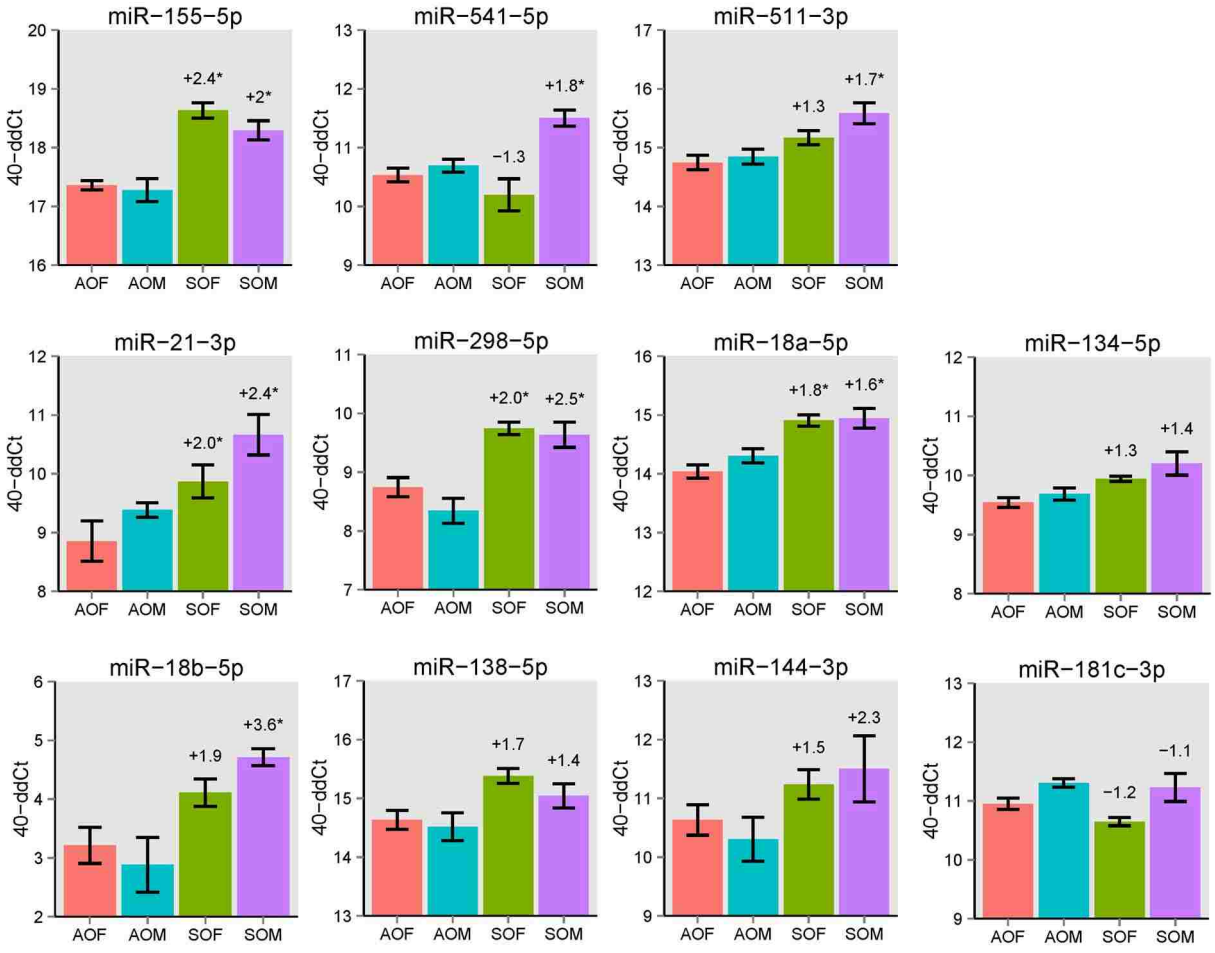

Figure 4–2. The qRT-PCR results confirmed the up-regulation of *in utero* SHS-affected miRNAs. Asterisks indicate significant differences between SHS-OVA and AIR-OVA in either sex ("SOF versus AOF" or "SOM versus AOM"). Significant differences between SHS-OVA and AIR-OVA groups were found for all miRNAs shown above except for miR-181c-3p ($P<0.05$, when females and males were pooled).

In addition, two miRNAs, miR-1247-5p and miR-345-5p, exhibited a significant sex bias; however, as indicated by Figure 4-3, qRT-PCR results did not show significant sex differences in miRNA expression.

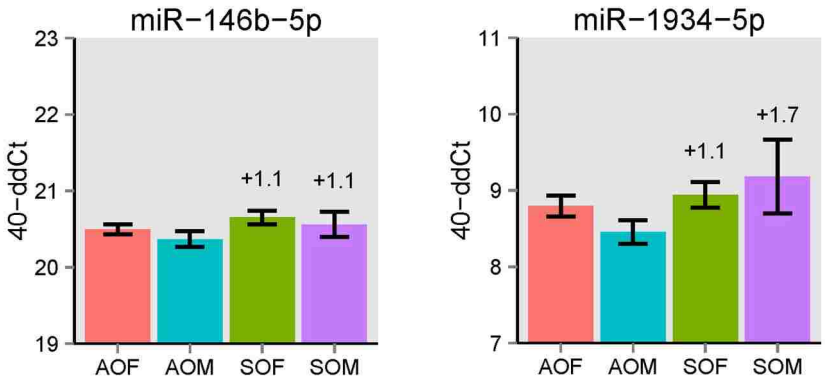

Figure 4–3. The qRT-PCR results did not confirm sex differences in miRNA expression. Significant differences between females and males were not found for either of the miRNAs listed above.

The heat map in Figure 4-1 presents the expression patterns for the top 17 smoke-affected miRNAs and top 4 sex-associated miRNAs among all 4 groups across 16 samples (4 mice/group). These miRNAs meet the criteria of FDR<0.1 and ***P***-value<0.003 (middle level of Figure 4-1A) to allow more miRNAs to be plotted, while the most significantly up-regulated miRNAs are retained. Correlation analysis performed on each sample revealed that the expression levels of 3 miRNAs: miR-155-5p, miR-21-3p and miR-18a-5p (Figure 4-1D), were very highly correlated with expression of the pro-asthmatic Th2 cytokines in BALF (Spearman's r≥0.6, ***P***-value<0.001, Figure 4-1E). Although the up-regulation of these 3 miRNAs correlated with asthma severity in the present study, further analysis revealed surprisingly that these miRNAs (listed in Table 4-2) had been characterized previously as oncogenic miRNAs (oncomirs).

Chromosome locations with increased transcriptional activity. Since the pro-asthmatic genes and oncomirs were both up-regulated by *in utero* SHS exposures and highly-correlated, we investigated whether the increased transcription activity was enriched at any

specific chromosome location. Degree of enrichment on each chromosome location for mRNA only and miRNA only, indicated by $-\log_{10}(\boldsymbol{P}\text{-value})$, is plotted in Figure 4-4A, together with a

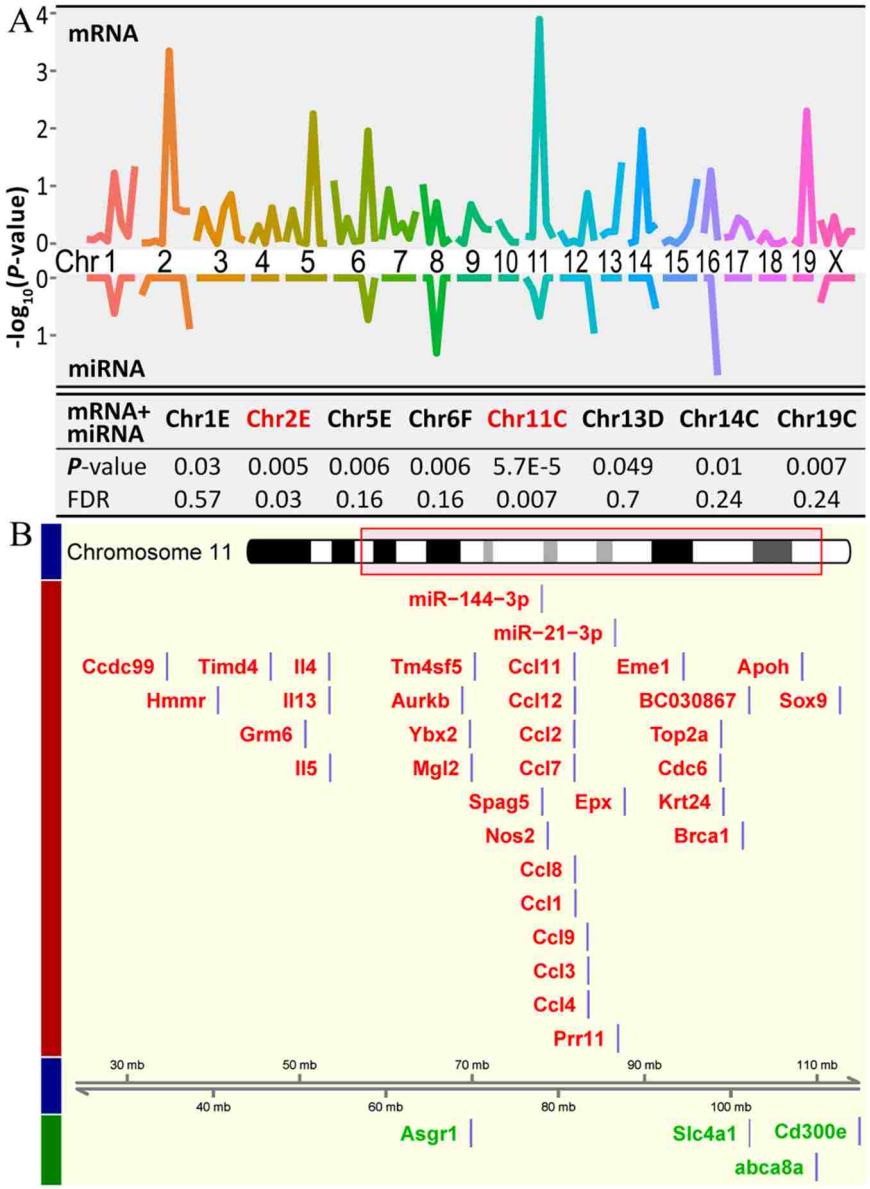

Figure 4–4. Elevated miRNA and mRNA shared common chromosome locations. Differentially expressed miRNAs and mRNAs in lungs of *in utero* SHS exposed BALB/c were found to be enriched primarily at two mouse chromosome locations: Chr11C and Chr2E (A). For the most prominent site, Chr11C, a genome axis along chromosome 11 was plotted with differentially expressed miRNAs and mRNAs aligned accordingly (B). Symbols in red/green = significantly up/down-regulated. A large number of differentially expressed transcripts were aligned to the C region (81.8-90.2Mb, Mb: mega base pairs) of mouse chromosome 11.

list showing the most significant chromosome locations, when miRNA and mRNA were both included. As shown in Figure 4-4A, the 2 most significantly over-represented chromosome locations are Chr11C (FDR=5.7E-5) and Chr2E (FDR=5.9E-4). The most prominent site, a genome axis along chromosome 11, with all differentially expressed miRNAs and mRNAs aligned accordingly, is presented in Figure 4-4B (symbols in red/green = significantly up/down-regulated genes or miRNAs). A large number of differentially expressed transcripts, including the pro-asthmatic Th2 cytokines: Il4, Il5 & Il13, the majority of asthma-associated chemokines, and miR-21 & miR-144, have been aligned adjacent to the C region (81.8-90.2Mb, Mb: mega base pairs) on mouse chromosome 11.

Tumor suppressor genes targeted by oncomirs. With complete transcriptome screening results on miRNA and mRNA, we interrogated the potential target genes of oncomirs, to test whether oncomirs with their transcriptional suppression capability can act to down-regulate tumor suppressor genes. By cross-referencing 4 different miRNA target prediction databases (DIANA-microT, miRanda, miRWalk and TargetScan) and 1 tumor suppressor gene database (Zhao et al. 2013), we identified 16 tumor suppressor genes that i) are targeted by, and ii) show anti-correlation with the oncomirs (Detailed pairing information is available in Supplemental Material). These tumor suppressor genes include Apc, Apc2, Cav2, Crebl2, Grlf1, Il17rd, Kif1b, Lats2, Mtus1, Notch1, Plce1, Reck, Thrb, Timp3, Wif1 and Zfhx3. The anti-correlation pattern between oncomirs and tumor suppressor genes was plotted in heat maps (Figure 4-5A). The miRNA-mRNA regulatory network was built in IPA and the association of the listed genes with cancer was independently confirmed by Ingenuity Knowledge Base (Figure 4-5B).

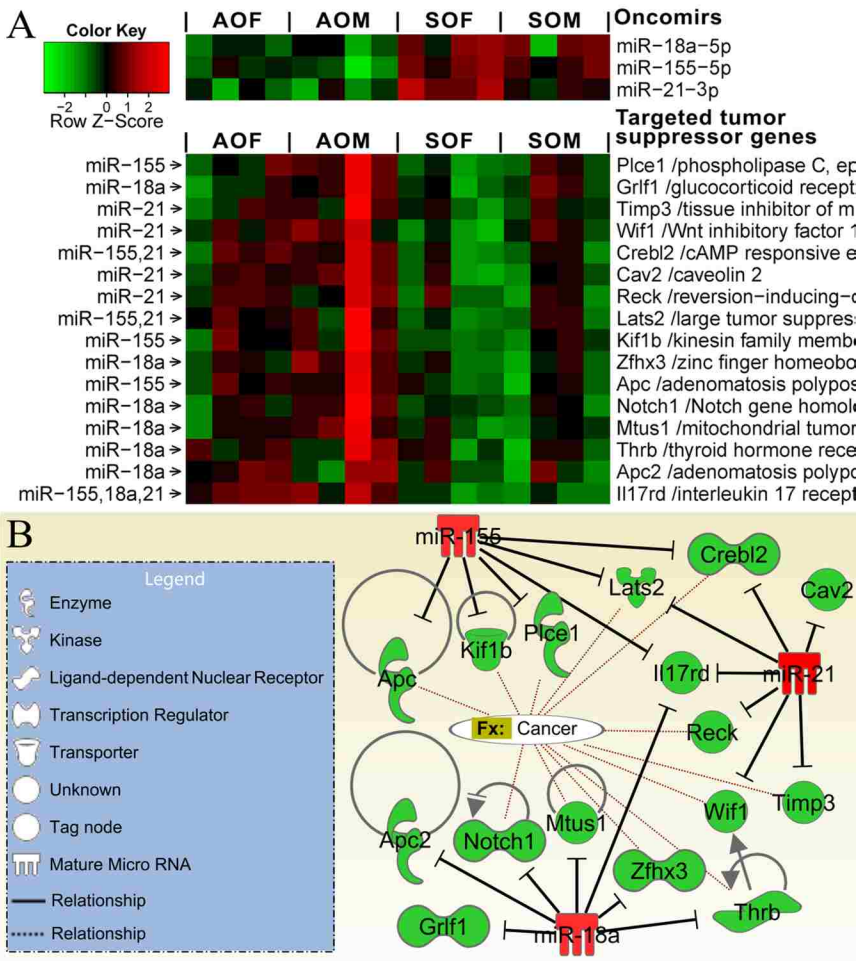

Figure 4–5. Sixteen tumor suppressor genes were targeted by and showed anti-correlation with activated oncomirs. By cross-referencing RNA-seq results for miRNAs and mRNAs, we found 16 tumor suppressor genes that were targeted by, and whose expression was inversely correlated with, the 3 activated oncomirs, miR-155, miR-21 and miR-18a (A). The regulatory network built in Ingenuity Pathway Analysis independently confirmed their association with cancer (B).

4.4 Discussion

This report examines the long-term effects of *in utero* exposure to SHS on modulation of miRNA expression in adult mouse lungs, and addresses implications of this activity on adult pulmonary diseases. The most significantly up-regulated miRNAs, miR-155, miR-21 and miR-18a, also showed high correlation with pro-asthmatic Th2 cytokine levels in the BALF originating from the same samples. In fact, other than miR-21, which has been reported to be up-regulated in allergic airway inflammation and to set the balance between Th1 and Th2

responses (Lu et al. 2011; Lu and Rothenberg 2013), miR-155 and miR-18a have not been discussed in terms of allergic asthma, but rather as well-characterized oncomirs, whose expression has been associated directly with increased lung cancer severity in human (Tang et al. 2013; Volinia et al. 2006; Yang et al. 2013). Whether miR-155 and miR-18a, play important roles in both allergic asthma and lung cancer awaits further investigation. The disease associations of these dysregulated miRNAs were tabulated in Table 4-2.

Table 4–2. *In utero* SHS exposure dysregulates miRNAs that are associated with lung cancer and inflammation.

miRNAs (mmu-)	RNA-seq FDR & (*P*-value)	Associated lung diseases & disorders	qRT-PCR Fold change
miR-155-5p	1.1E-08	Cancer (Tang et al. 2013; Yang et al. 2013) , inflammation (Tili et al. 2007)	♀: ↑2.4* ♂: ↑2.0*
miR-541-5p	2.8E-05		♀: ↓1.3 ♂: ↑1.8*
miR-511-3p	9.8E-04	Cancer (Zhang et al. 2012), inflammation (Squadrito et al. 2012)	♀: ↑1.3 ♂: ↑1.7*
miR-21-3p	1.2E-03	Cancer (Tang et al. 2013; Yang et al. 2013), inflammation (Lu et al. 2009; Moschos et al. 2007)	♀: ↑2.0 ♂: ↑2.4*
miR-298-5p	1.2E-03		♀: ↑2.0* ♂: ↑2.5*
miR-341-3p	1.9E-03		
miR-501-5p	2.1E-03		
miR-18a-5p	1.4E-02	Cancer (miR-17~92 cluster) (He et al. 2005; Hwang and Mendell 2007; Olive et al. 2010)	♀: ↑1.8* ♂: ↑1.6*
miR-18b-5p	1.7E-02		♀: ↑1.8 ♂: ↑3.6*
miR-299-3p	0.05 (1.1E-03)		
miR-138-5p	0.05 (1.2E-03)	Cancer (Seike et al. 2009)	♀: ↑1.7 ♂: ↑1.4
miR-128-1-5p	0.08 (1.9E-03)		
miR-144-3p	0.08 (2.1E-03)		♀: ↑1.5 ♂: ↑2.3

(Table 4–2 continued)

miRNAs (mmu-)	RNA-seq FDR & (*P*-value)	Associated lung diseases & disorders	qRT-PCR Fold change
miR-155-3p	0.08 (2.4E-03)		
miR-134-5p	0.08 (2.4E-03)	Cancer (Chen et al. 2008)	♀: ↑1.3 ♂: ↑1.4
miR-3098-5p	0.09 (2.8E-03)		
miR-181c-3p	0.09 (2.9E-03)		♀: ↓1.2 ♂: ↓1.1

qRT-PCR was performed on eleven miRNAs and significant up-regulation was found for seven of them. *: statistical significance, $P<0.05$, ♀: SOF versus AOF, ♂: SOM versus AOM. N≥5 in each group for qRT-PCR.

In contrast to the primarily down-regulated miRNA expression profiles identified in adults that had been exposed to cigarette smoke (Izzotti et al. 2009; Schembri et al. 2009), the up-regulation of these miRNAs in adult mice suggests that long-term effects of *in utero* SHS exposure may include promotion of a pro-asthmatic and/or oncogenic environment in mice challenged as adults with environmental irritants. This is in part consistent with our previous observations that *in utero* SHS promotes a pro-asthmatic milieu in the adult lungs exposed to OVA (Penn et al. 2007; Xiao et al. 2013).

To identify common chromosome locations where miRNAs and mRNAs might be co-regulated by *in utero* SHS exposure, we screened all the chromosome locations on the mouse genome, separated by major cytogenetic bands. Among these, Chr11C and Chr2E are most significantly enriched for the differentially expressed miRNAs and mRNAs. As shown in Figure 4-4B, a number of asthma- and AHR-associated genes are located on mouse chromosome 11, including Th2 cytokines (Il4, Il5 and Il13), pro-inflammatory chemokines (Ccl2, Ccl3), and significantly up-regulated miRNAs (miR-21, miR-144). Both miR-21 and miR-144 (confirmed

by qRT-PCR, Supplemental Material), are activated by diesel exhaust exposures (Yamamoto et al. 2013). This suggests a miRNA-mRNA co-activation pattern at this chromosome location upon environmental irritant challenge. The increased transcription activity induced by *in utero* SHS exposure at these chromosome locations could be a result of epigenetic modifications, including DNA methylation and specific histone modifications. In addition, the human equivalents of the miRNAs and mRNAs located on mouse chromosome region Chr11C (81.8-90.2Mb) are located on the human chromosome Chr17. With the high degree of homology between mouse and human genomes, further epigenomic study at these chromosome locations should also help to elucidate the mechanisms by which environmental stressors influence early stages in the development of a number of human diseases.

The activation of specific oncomirs raises a new question: are individuals who were exposed to SHS *in utero* at heightened risk as adults for certain cancers? As a first step, we examined the transcriptome responses that contribute to increased chances of developing cancer and that are targeted by the oncomirs. Among the target genes of the 3 major oncomirs identified in the present study, miR-155, miR-21 and miR-18a, we found 16 tumor suppressor genes (12 of them also known to be associated with cancer by IPA), as listed in Table 4-3, that were down-regulated in association with the up-regulated oncomirs. At least eight of the tumor suppressor genes have been implicated directly in lung cancer. These eight genes include the three Wnt/β-catenin signaling inhibitors: Apc, Apc2 & Wif1 (Bonner et al. 2004; Stewart 2014), as well as five other lung cancer-associated genes: Cav2, Lats2, Notch1, Timp3 and Zfhx3 (Kettunen et al. 2004; Minamiya et al. 2012; Strazisar et al. 2009; Wang et al. 2011; Wu et al. 2012). These findings suggest that long-term consequences of *in utero* exposure to SHS include

activation of oncogenic miRNAs in adult lungs, potentially resulting in decreased expression of these tumor suppressor genes.

Table 4–3. According to multiple sources, sixteen tumor suppressor genes are predicted targets of the 3 oncomirs, miR-155, miR-21, and miR-18a, and show anti-correlation with oncomir expression.

miRNA	Gene	DIANA microT	miR anda	miR Walk	Target Scan	Pearson 's r	Fold Change	Description
miR-155	Lats2	1	1	1	1	-0.82	-1.76	large tumor suppressor 2
miR-155	Il17rd	1	1	1	1	-0.81	-1.52	interleukin 17 receptor D
miR-155	Crebl2	1	1	1	1	-0.8	-1.7	cAMP responsive element binding protein-like 2
miR-155	Plce1	1	1	1	0	-0.84	-3.06	phospholipase C, epsilon 1
miR-155	Apc	1	1	0	1	-0.77	-1.77	adenomatosis polyposis coli
miR-155	Kif1b	0	1	1	0	-0.74	-1.61	kinesin family member 1B
miR-18a	Il17rd	0	1	1	1	-0.7	-1.52	interleukin 17 receptor D
miR-18a	Apc2	0	1	1	1	-0.77	-1.97	adenomatosis polyposis coli 2
miR-18a	Thrb	0	0	1	1	-0.72	-3.33	thyroid hormone receptor beta
miR-18a	Grlf1	0	1	1	0	-0.73	-1.58	glucocorticoid receptor DNA binding factor 1
miR-18a	Mtus1	0	1	1	0	-0.74	-1.64	mitochondrial tumor suppressor 1
miR-18a	Notch1	0	1	1	0	-0.75	-1.87	Notch gene homolog 1 (Drosophila)
miR-18a	Zfhx3	0	1	1	0	-0.82	-1.67	zinc finger homeobox 3
miR-21	Cav2	1	1	1	1	-0.75	-1.73	caveolin 2
miR-21	Reck	1	1	1	0	-0.76	-1.84	reversion-inducing-cysteine-rich protein with kazal motifs
miR-21	Timp3	1	1	1	1	-0.8	-1.77	tissue inhibitor of metalloproteinase 3
miR-21	Crebl2	1	1	1	1	-0.75	-1.7	cAMP responsive element binding protein-like 2
miR-21	Wif1	1	1	1	0	-0.81	-2.49	Wnt inhibitory factor 1
miR-21	Il17rd	0	1	1	0	-0.73	-1.52	interleukin 17 receptor D
miR-21	Lats2	0	1	1	0	-0.71	-1.76	large tumor suppressor 2

Tumor suppressor gene database (Zhao et al. 2013); Multiple miRNA-mRNA pairing database (Betel et al. 2008; Dweep et al. 2011; Lewis et al. 2003; Maragkakis et al. 2009).

In addition, the regulatory effects of miRNAs may be largely exerted via translational suppression, which would further decrease final protein products of tumor suppressor genes (Baek et al. 2008; Sonkoly and Pivarcsi 2009). Whether *in utero* exposure to SHS promotes oncogenesis in adult mouse lungs is currently under investigation in our laboratory.

4.5 Conclusion

In utero SHS exposure activates pro-asthmatic and oncogenic miRNAs genes in OVA-challenged adult female and male mice. The results support an environment-epigenome interaction that results from *in utero* SHS exposure and suggests that miRNA expression in adult mice, together with dysregulated gene expression, promotes a pro-asthmatic and oncogenic milieu in adult mouse lungs exposed *in utero* to SHS. The enriched chromosome locations of both mRNA and miRNA suggest that *in utero* SHS exposure may cause epigenetic modifications at these locations that contribute to the increased transcription activity in adult mice. These activated oncogenic miRNAs may promote cancer progression through inhibition of tumor suppressor genes.

CHAPTER 5.
CONCLUDING REMARKS

5.1 Benefits from New Technology Implemented in the Present Study

flexiVent - an improved and direct measurement of lung function. BUXCO's whole-body plethysmography has been routinely implemented as the lung function testing method in our laboratory over the past decade. As a noninvasive method, whole-body plethysmography has two merits: i) it allows large-scale experiments with its decent throughput, i.e., runs simultaneously on 8 mice per experimental session; ii) it also allows longitudinal studies that can follow each individual animal through repeated measurements without losing or traumatizing any of them during the procedure.

Over the years, the accuracy and reliability of measurements made by whole-body plethysmography, particularly for one of the parameters named Penh (enhanced pause), have been questioned by researchers (Alder et al. 2004). Although a high correlation exist between Penh and lung resistance in BALB/c mice (DeLorme and Moss 2002; Hamelmann et al. 1997; Singh et al. 2003) and that is the mouse strain used exclusively in our studies, the parameters interpreted from whole-body plethysmography were largely determined by the spontaneous breathing pattern of each animal, which could be influenced by factors unrelated to lung resistance or AHR, including neural ventilator control or a loss of elastic recoil (Schwarze et al. 2005).

To overcome the short-comings of whole-body unrestrained plethysmography, there is a new forced oscillation technique, and one of the successfully commercialized products using this technique is flexiVent (SCIREQ Inc.; Montreal, QC, Canada). This method completely bypasses the breathing pattern of each mouse by applying a standardized ventilation procedure to each of the anesthetized and intubated mice. This method allows direct and more accurate

assessment of the lung mechanics, including results for lung resistance and dynamic compliance, which are regarded as the "gold standard" for precise and specific determinations of pulmonary mechanics (Drazen et al. 1999; Irvin and Bates 2003; Glaab et al. 2007).

After completing the SHS-SHS and the SHS-OVA studies that are described in Chapter 2 & 3, we had the opportunity to use flexiVent for our lung function testing. In light of the pronounced male response in the SHS-OVA study (Chapter 3; Xiao et al. 2013), we carried out an experiment similar to the SHS-SHS study (Chapter 2; Xiao et al. 2012) but this time included both male and female offspring. As shown in Figure 5-1, the flexiVent was able to distinguish male mice exposed both *in utero* and as adults to SHS from the air-exposed controls, whereas the plethysmography yielded very similar responses for all 4 groups and with differences largely influenced by the sex of the mice. From a statistics perspective, the flexiVent results on ~8 mice per group revealed significant differences ($\boldsymbol{P}<0.05$, unpublished results) between SHS- and AIR-exposed males, while plethysmography results on ~16 mice per group were not able to achieve that.

In conclusion, the flexiVent is a better way of testing lung function, although whole-body plethysmography can still be a good addition, particularly for large scale screening and longitudinal studies that require repeated measurements.

RNA-seq - a sensitive and accurate method for transcriptome screening. Technically, RNA-seq technology innately provides better transcriptome assessment than microarray (Wang et al. 2009), including i) having detailed sequencing information that allows us to examine new transcripts or isoforms not previously identified by microarray, because RNA-seq does not rely upon pre-designed microarray probes; and ii) having exact read counts for each sequence, which provide improved accuracy at estimating gene expression differences.

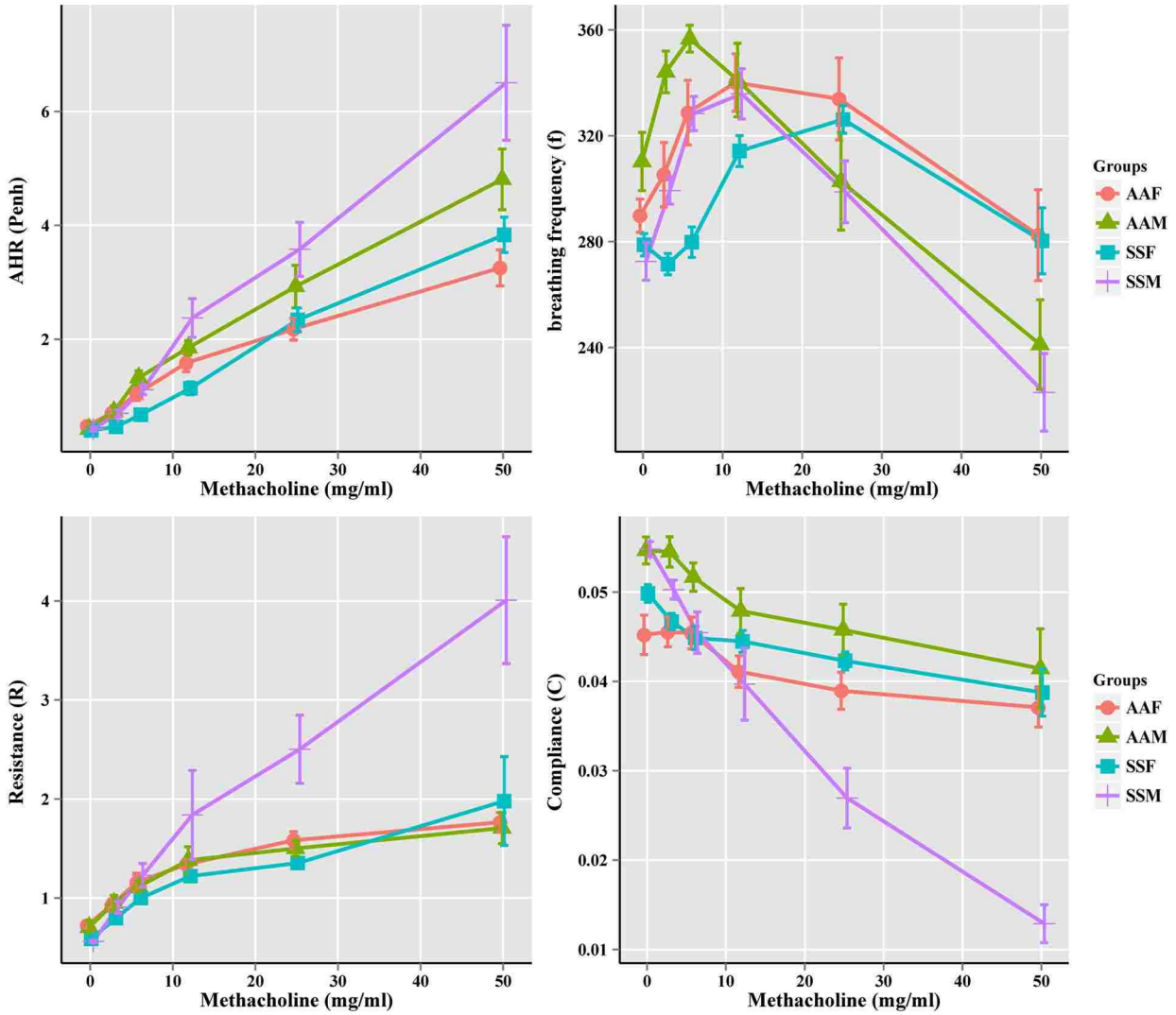

Figure 5–1. flexiVent (lower panels) distinguishes smoke-vs-air-exposed male mice (SSM vs AAM) better than whole-body plethysmography (upper panels), which was primarily influenced by sex. Two upper panels, indicating AHR, determined as Penh values and breathing frequency, are assessed with whole-body plethysmography. Two lower panels, indicating lung resistance and compliance, are measured by flexiVent. SSM, male mice doubly exposed, *in utero* and as adults, to SHS; AAM, male mice without any smoke exposure.

Until recently, RNA-seq had not become a main-stream method for transcriptome screening, in part probably because of the cost and lack of good technical/software support. Now with more affordable prices, better technical support from companies, and a variety of updated software packages available, we started using RNA-seq as a routine transcriptome screening

method in 2013. Other than using RNA-seq for identification and quantification of miRNAs, which was discussed in Chapter 4, we also took the opportunity to compare RNA-seq and microarray results side by side on the same RNA samples.

Not surprisingly, RNA-seq exhibited improved sensitivity compared with microarray for detecting up-regulated pro-asthmatic genes. Among 14090 unique genes with median counts above zero that are annotated by the Reference Sequence (RefSeq) database, by RNA-seq we identified 428 genes, most of which were up-regulated by *in utero* SHS exposure (data not shown). Compared to microarray-based gene expression profiling results (Table 3-2; Figure 3-5; Xiao et al. 2014), RNA-seq identified nearly 4 times more differentially expressed genes (428 versus 113).

More importantly, in the context of a mouse asthma model, the differentially expressed genes that were not detected by microarray are key genes associated with asthma and AHR (Figure 5-2), including major Th2 cytokines (Il4, Il5, Il10 and Il13) and C-C-motif chemokines (Ccl3, Ccl11 and Ccl22). The differential expression of these 7 genes, plus Il33, was confirmed by qRT-PCR, with more than 2-fold up-regulation in the SHS-OVA groups compared to AIR controls (Table 5-1).

Since lung cytokines and chemokines generally are low abundance genes present in the lung, we then compared the sensitivity between RNA-seq and microarray for detecting differentially expressed genes, with regard to each gene's relative abundance (Low, 25%; Medium, 50%; High, 25%). As shown in Figure 5-2, the Pearson's correlation coefficient is highest ($r \approx 0.6$) for high abundance genes while lowest ($r \approx 0.1$, scattered near the vertical line $x=0$) for low abundance genes.

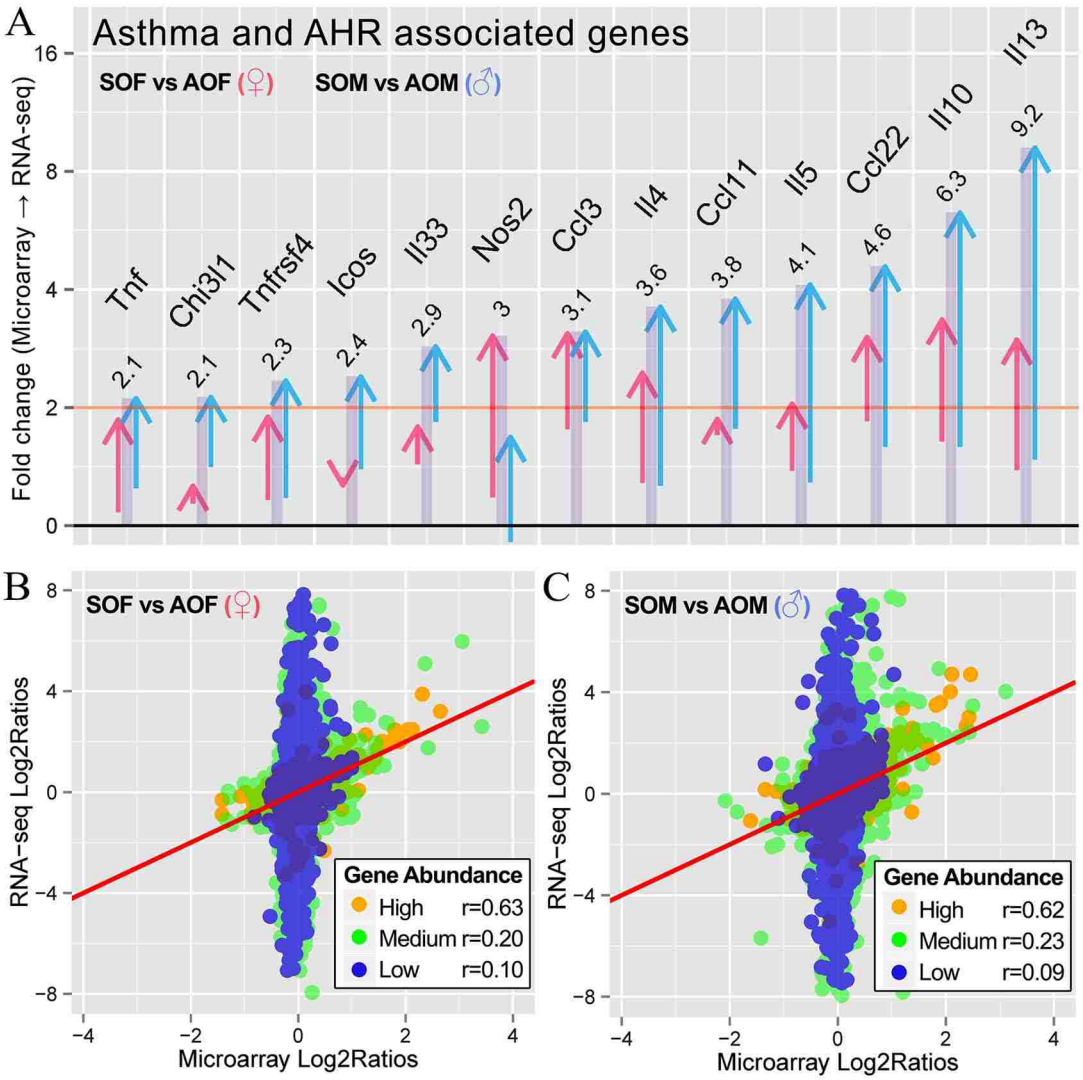

Figure 5–2. RNA-seq provided improved sensitivity for detecting differential expression among pro-asthmatic genes (A). The low abundance genes primarily benefit from improved sensitivity of RNA-seq, as shown for "SOF versus AOF" (B); "SOM versus AOM" (C). The arrows pointing upwards crossing the 2-fold line in panel A (from fold change values estimated by microarray to those via RNA-seq; colored by sex: ♀: red, "SOF versus AOF"; ♂: blue, "SOM versus AOM") indicated that differential expression of the genes listed was detected only by RNA-seq but not by microarray. The low correlation (Pearson's r≈0.1, between RNA-seq and microarray) and more blue dots scattered near the vertical line (x=0) in panel B&C, indicated that the RNA-seq had better sensitivity, particularly among low abundance genes (lowest 25%, in blue dots).

Thus, in the context of this mouse asthma model, these results demonstrate that while the two transcriptome screening methods generate consistent results for high abundance genes, RNA-seq has significantly improved sensitivity for detecting low abundance genes.

Table 5–1. The qRT-PCR results confirmed the differential expression of eight asthma- and AHR-associated genes that are revealed by RNA-seq, but not by microarray.

Asthma and AHR associated genes	qRT-PCR fold change
Il4	♀: ↑1.8* ♂: ↑2.5*
Il5	♀: ↑1.3 ♂: ↑2.1*
Il10	♀: ↑2.7* ♂: ↑4.0*
Il13	♀: ↑2.4* ♂: ↑4.6*
Il33	♀: ↑1.4 ♂: ↑2.0*
Ccl3	♀: ↑1.4 ♂: ↑2.2*
Ccl11	♀: ↑1.4 ♂: ↑2.4*
Ccl22	♀: ↑2.7* ♂: ↑4.3*

Asterisks indicate significant differences between SHS-OVA and AIR-OVA in either sex (P<0.05; “SOF versus AOF” or “SOM versus AOM”).

5.2 Research Summary

These experiments investigate the effects of second-hand smoke (SHS) exposure *in utero* on adult lung responses to inhaled irritants, including SHS and OVA. Results demonstrate:

i) SHS exposures, *in utero* and as adults, act synergistically to aggravate adult lung responses and promote a pro-fibrotic milieu in 15-weeks old adult mice that were exposed *in utero* to SHS;

ii) The effects of *in utero* SHS exposure persist into 23-weeks old adult mice and further aggravate asthmatic responses in lungs of OVA-challenged adult mouse; these responses exhibited a sex bias, which is more pronounced in male offspring;

iii) *In utero* exposure to SHS also modulates the miRNA expression in lungs of 23-weeks old OVA-challenged adult mice, showing overexpression of oncogenic miRNAs, including miR-155-5p, miR-21-3p and miR-18a-5p, which could play a role in allergic asthma

and/or promote an oncogenic milieu in adult mouse lungs via inhibition of miRNA-regulated tumor suppressor genes.

5.3 Critical Thoughts for Future Studies

In addition to adopting new technology, including flexiVent and RNA-seq, to aid in the future experiment, a few more steps could be taken to strengthen and further the subsequent studies:

- Include both sexes to study sex-specific differences

As we discovered a more pronounced lung response in OVA-challenged adult male mice exposed *in utero* to SHS, there are two clear questions that remain to be answered: i) whether this trend continues with other adult irritants? ii) what is the mechanistic explanation underlying this pronounced male response? To better answer these questions, it is advisable to include both female and male offspring for any further study in order to reveal a larger picture and unveil the answers to these questions.

- Expand inhaled irritant challenges to a variety of respiratory disease models

In addition to assessing AHR associated with inhaled irritants, we can expand our horizon to a variety of respiratory disease models. Whether *in utero* SHS exposure accelerates progression of other adult other respiratory disease, including fibrosis, emphysema, or lung cancer, is of great interest.

- Explore diverse epigenetic regulatory mechanisms

As the first step into epigenetics, we have examined the expression of miRNAs. Further exploration on diverse epigenetic regulatory mechanisms, including DNA methylation, histone modifications, and various others, might better explain the sustained effect of *in utero* SHS exposure in adult mice.

REFERENCES

[Anonymous]. 2012. Comments on Draft Guidance Entitled "Reporting Harmful and Potentially Harmful Constituents in Tobacco Products and Tobacco Smoke Under the Federal Food, Drug, and Cosmetic Act" Altria Client Services Inc. Available from http://www.altria.com/en/cms/About_Altria/federal-regulation-of-tobacco/regulatory-filings/pdfs/Reporting-Harmful-and-Potentially-Harmful-Constituents.pdf.aspx?src=search&q=reporting-harmful-and-potentially-harmful-constituents.Pdf.

Adkins B, Bu Y, Guevara P. 2001. The generation of Th memory in neonates versus adults: prolonged primary Th2 effector function and impaired development of Th1 memory effector function in murine neonates. J Immunol 166(2): 918-925.

Adler A, Cieslewicz G, Irvin CG. 2004. Unrestrained plethysmography is an unreliable measure of airway responsiveness in BALB/c and C57BL/6 mice. J Appl Physiol 97(1): 286-292.

Ambalavanan N, Nicola T, Hagood J, Bulger A, Serra R, Murphy-Ullrich J, Oparil S, Chen YF. 2008. Transforming growth factor-beta signaling mediates hypoxia-induced pulmonary arterial remodeling and inhibition of alveolar development in newborn mouse lung. Am J Physiol Lung Cell Mol Physiol 295(1): L86-95.

Baek D, Villen J, Shin C, Camargo FD, Gygi SP, Bartel DP. 2008. The impact of microRNAs on protein output. Nature 455(7209): 64-71.

Baglole CJ, Sime PJ, Phipps RP. 2008. Cigarette smoke-induced expression of heme oxygenase-1 in human lung fibroblasts is regulated by intracellular glutathione. Am J Physiol Lung Cell Mol Physiol 295(4): L624-636.

Bell ML, Davis DL. 2001. Reassessment of the lethal London fog of 1952: novel indicators of acute and chronic consequences of acute exposure to air pollution. Environ Health Perspect 109(Suppl 3): 389–394.

Berndt A, Leme AS, Williams LK, Von Smith R, Savage HS, Stearns TM, Tsaih SW, Shapiro SD, Peters LL, Paigen B, Svenson KL. 2011. Comparison of unrestrained plethysmography and forced oscillation for identifying genetic variability of airway responsiveness in inbred mice. Physiol Genomics 43(1):1-11.

Betel D, Wilson M, Gabow A, Marks DS, Sander C. 2008. The microRNA.org resource: targets and expression. Nucleic Acids Res 36(Database issue): D149-153.

Bettelli E, Carrier Y, Gao W, Korn T, Strom TB, Oukka M, Weiner HL, Kuchroo VK. 2006. Reciprocal developmental pathways for the generation of pathogenic effector TH17 and regulatory T cells. Nature 441(7090): 235-238.

Beyer D, Mitfessel H, Gillissen A. 2009. Maternal smoking promotes chronic obstructive lung disease in the offspring as adults. Eur J Med Res 14 Suppl 4: 27-31.

Blacquiere MJ, Timens W, Melgert BN, Geerlings M. 2009. Maternal smoking during pregnancy. Eur Respir J: 33: 1133–1140.

Boehm M, Slack F. 2005. A developmental timing microRNA and its target regulate life span in C. elegans. Science 310:1954-1957.

Bollati V, Marinelli B, Apostoli P, Bonzini M, Nordio F, Hoxha M, Pegoraro V, Motta V, Tarantini L, Cantone L, Schwartz J, Bertazzi PA, Baccarelli A. 2010. Exposure to metal-rich particulate matter modifies the expression of candidate microRNAs in peripheral blood leukocytes. Environ Health Perspect 118(6): 763-768.

Bonner AE, Lemon WJ, Devereux TR, Lubet RA, You M. 2004. Molecular profiling of mouse lung tumors: association with tumor progression, lung development, and human lung adenocarcinomas. Oncogene 23(5): 1166-1176.

Bowles K, Horohov D, Paulsen D, Leblanc C, Littlefield-Chabaud M, Ahlert T, Ahlert K, Pourciau S, Penn A. 2005. Exposure of adult mice to environmental tobacco smoke fails to enhance the immune response to inhaled antigen. Inhal Toxicol 17(1): 43-51.

Boyce JA, Austen KF. 2005. No audible wheezing: nuggets and conundrums from mouse asthma models. J Exp Med 201(12): 1869-1873.

Breton CV, Byun HM, Wenten M, Pan F, Yang A, Gilliland FD. 2009. Prenatal tobacco smoke exposure affects global and gene-specific DNA methylation. Am J Respir Crit Care Med: 180(185):462–467.

Cakmak A, Zeyrek D, Atas A, Selek S, Erel O. 2009. Oxidative status and paraoxonase activity in children with asthma. Clin Invest Med 32(5): E327-334.

Card JW, Carey MA, Bradbury JA, DeGraff LM, Morgan DL, Moorman MP, Flake GP, Zeldin DC. 2006. Gender differences in murine airway responsiveness and lipopolysaccharide-induced inflammation. J Immunol 177(1): 621-630.

Centers for Disease Control and Prevention. National Center for Health Statistics. National Health Interview Survey Raw Data, 1997-2011. Analysis performed by the American Lung Association Research and Health Education Division using SPSS and SUDAAN software.

Centers for Disease Control and Prevention. Pregnancy Risk Assessment Monitoring System (PRAMS). 2010. CDC's PRAMS Online Data for Epidemiologic Research (CPONDER) V2.0. http://www.cdc.gov/reproductivehealth/TobaccoUsePregnancy/ (accessed April 2014).

Chahwan R, Wontakal SN, Roa S. 2011. The multidimensional nature of epigenetic information and its role in disease. Discov Med 11(58):233-243.

Chen C, Kudo M, Rutaganira F, Takano H, Lee C, Atakilit A, Robinett KS, Uede T, Wolters PJ, Shokat KM, Huang X, Sheppard D. 2012. Integrin alpha9beta1 in airway smooth muscle suppresses exaggerated airway narrowing. J Clin Invest 122(8): 2916-2927.

Chen PS, Su JL, Hung MC. 2012. Dysregulation of microRNAs in cancer. J Biomed Sci 19: 90.

Chen X, Ba Y, Ma L, Cai X, Yin Y, Wang K, Guo J, Zhang Y, Chen J, Guo X, Li Q, Li X, Wang W, Zhang Y, Wang J, Jiang X, Xiang Y, Xu C, Zheng P, Zhang J, Li R, Zhang H, Shang X, Gong T, Ning G, Wang J, Zen K, Zhang J, Zhang CY. 2008. Characterization of microRNAs in serum: a novel class of biomarkers for diagnosis of cancer and other diseases. Cell Res 18(10): 997-1006.

Churg A, Sin DD, Wright JL. 2011. Everything prevents emphysema: are animal models of cigarette smoke-induced chronic obstructive pulmonary disease any use? Am J Respir Cell Mol Biol 45(6): 1111-1115.

Cotes JE. Physiology of the aging lung. In: Crystal JB, West JB, Weibel ER, Barnes PJ (eds). The Lung: Scientific Foundations, 2nd edn. Lipincott-Raven, Philadelphia. 1997; 2193–2203.

DeLorme MP, Moss OR. 2002. Pulmonary function assessment by whole-body plethysmography in restrained versus unrestrained mice. J Pharmacol Toxicol Methods 47(1): 1-10.

DiFranza JR, Aligne CA, Weitzman M. 2004. Prenatal and postnatal environmental tobacco smoke exposure and children's health. Pediatrics 113(4 Suppl): 1007-1015.

Djuardi Y, Wammes LJ, Supali T, Sartono E, Yazdanbakhsh M. 2011. Immunological footprint: the development of a child's immune system in environments rich in microorganisms and parasites. Parasitology 138(12):1508-1518.

Drazen JM, Finn PW, De Sanctis GT. 1999. Mouse models of airway responsiveness: physiological basis of observed outcomes and analysis of selected examples using these outcome indicators. Annu Rev Physiol 61:593-625.

Duncan DT, Prodduturi, N., Zhang, B. 2010. WebGestalt2: an updated and expanded version of the Web-based Gene Set Analysis Toolkit. BMC Bioinformatics 11(Suppl 4): P10.

Durham A, Chou PC, Kirkham P, Adcock IM. 2010. Epigenetics in asthma and other inflammatory lung diseases. Epigenomics 2(4):523-537.

Dweep H, Sticht C, Pandey P, Gretz N. 2011. miRWalk--database: prediction of possible miRNA binding sites by "walking" the genes of three genomes. J Biomed Inform 44(5): 839-847.

Epstein MM. 2006. Targeting memory Th2 cells for the treatment of allergic asthma. Pharmacol Ther 109(1-2): 107-136.

Feinberg AP. 2007. Phenotypic plasticity and the epigenetics of human disease. Nature 447: 433–440.

Fields PE, Kim ST, Flavell RA. 2002. Cutting edge: changes in histone acetylation at the IL-4 and IFN-gamma loci accompany Th1/Th2 differentiation. J Immunol 169, 647–650.

Gilliland FD, Berhane K, Li YF, Rappaport EB, Peters JM. 2003. Effects of early onset asthma and *in utero* exposure to maternal smoking on childhood lung function. Am J Respir Crit Care Med 167(6): 917-924.

Gilliland FD, Berhane K, McConnell R, Gauderman WJ, Vora H, Rappaport EB, Avol E, Peters JM. 2000. Maternal smoking during pregnancy, environmental tobacco smoke exposure and childhood lung function. Thorax 55(4): 271-276.

Gilliland FD, Li YF, Peters JM. 2001. Effects of maternal smoking during pregnancy and environmental tobacco smoke on asthma and wheezing in children. Am J Respir Crit Care Med 163(2): 429-436.

Glaab T, Taube C, Braun A, Mitzner W. 2007. Invasive and noninvasive methods for studying pulmonary function in mice. Respir Res 14;8:63.

Gluckman PD, Hanson MA, Cooper C, Thornburg KL. 2008. Effect of *in utero* and early-life conditions on adult health and disease. N Engl J Med 359(1):61-73.

Guerrero-Preston R, Goldman LR, Brebi-Mieville P, Ili-Gangas C, Lebron C, Witter FR, Apelberg BJ, Hernández-Roystacher M, Jaffe A, Halden RU, Sidransky D. 2010. Global DNA hypomethylation is associated with *in utero* exposure to cotinine and perfluorinated alkyl compounds. Epigenetics 5(6): 539-546.

Guo P, Yokoyama K, Suenaga M, Kida H. 2008. Mortality and life expectancy of Yokkaichi asthma patients, Japan: late effects of air pollution in 1960-70s. Environ Health 7:8.

Hamelmann E, Schwarze J, Takeda K, Oshiba A, Larsen GL, Irvin CG, Gelfand EW. 1997. Noninvasive measurement of airway responsiveness in allergic mice using barometric plethysmography. Am J Respir Crit Care Med 156(3 Pt 1): 766-775.

Hanson MA, Gluckman PD. 2008. Developmental origins of health and disease. New insights Basic Clin Pharmacol Toxicol 102(102):190–193.

Harding, R., Cock, M.L., Louey, S., Joyce, B.J., Davey, M.G., Albuquerque, C.A., Hooper, S.B., Maritz, G.S., 2000. The compromised intra-uterine environment: implications for future lung health. Clin Exp Pharmacol Physiol 27(12):965-974.

Hastie AT, Moore WC, Meyers DA, Vestal PL, Li H, Peters SP, Bleecker ER. 2010. Analyses of asthma severity phenotypes and inflammatory proteins in subjects stratified by sputum granulocytes. J Allergy Clin Immunol 125(5): 1028-1036 e1013.

He L, Thomson JM, Hemann MT, Hernando-Monge E, Mu D, Goodson S, Powers S, Cordon-Cardo C, Lowe SW, Hannon GJ, Hammond SM. 2005. A microRNA polycistron as a potential human oncogene. Nature 435(7043): 828-833.

Heinrich J, Hoelscher B, Wichmann HE. 2000. Decline of ambient air pollution and respiratory symptoms in children. Am J Respir Crit Care Med 161(6): 1930-1936.

Hellings PW, Kasran A, Liu Z, Vandekerckhove P, Wuyts A, Overbergh L, Mathieu C, Ceuppens JL. 2003. Interleukin-17 orchestrates the granulocyte influx into airways after allergen inhalation in a mouse model of allergic asthma. Am J Respir Cell Mol Biol 28(1): 42-50.

Henckel A, Nakabayashi K, Sanz L, Feil R, Hata K, Arnaud P. 2009. Histone methylation is mechanistically linked to DNA methylation at imprinting control regions in mammals. Hum Mol Genet 18: 3375-3383.

Ho SM. 2010. Environmental epigenetics of asthma: an update. J Allergy Clin Immunol 2126(3):453-465.

Hollingsworth JW, Maruoka S, Boon K, Garantziotis S, Li Z, Tomfohr J, Bailey N, Potts EN, Whitehead G, Brass DM, Schwartz DA. 2008. *In utero* supplementation with methyl donors enhances allergic airway disease in mice. J Clin Invest 118:3462–3469.

Hong YC, Lee KH, Son BK, Ha EH, Moon HS, Ha M. 2003. Effects of the GSTM1 and GSTT1 polymorphisms on the relationship between maternal exposure to environmental tobacco smoke and neonatal birth weight. J Occup Environ Med 45(5): 492-498.

Hoymann HG. 2006. New developments in lung function measurements in rodents. Exp Toxicol Pathol 57 Suppl 2:5-11.

Hwang HW, Mendell JT. 2007. MicroRNAs in cell proliferation, cell death, and tumorigenesis. Br J Cancer 96 Suppl: R40-44.

Hylkema MN, Blacquière MJ. 2009. Intrauterine effects of maternal smoking on sensitization, asthma, and chronic obstructive pulmonary disease. Proc Am Thorac Soc: 6(8):660–662.

Inman CF, Haverson K, Konstantinov SR, Jones PH, Harris C, Smidt H, Miller B, Bailey M, Stokes C. 2010. Rearing environment affects development of the immune system in neonates. Clin Exp Immunol 160(3):431-439.

Irvin CG, Bates JH. 2003. Measuring the lung function in the mouse: the challenge of size. Respir Res 4:4.

Izzotti A, Calin GA, Arrigo P, Steele VE, Croce CM, De Flora S. 2009. Downregulation of microRNA expression in the lungs of rats exposed to cigarette smoke. FASEB J 23(3): 806-812.

Jaakkola JJ, Kosheleva AA, Katsnelson BA, Kuzmin SV, Privalova LI, Spengler JD. 2006. Prenatal and postnatal tobacco smoke exposure and respiratory health in Russian children. Respir Res 7: 48.

Jaakkola MS, Piipari R, Jaakkola N, Jaakkola JJ. 2003. Environmental tobacco smoke and adult-onset asthma: a population-based incident case-control study. Am J Public Health 93(12):2055-2060.

Janson PC, Winerdal ME, Winqvist O. 2009. At the crossroads of T helper lineage commitment – epigenetics points the way. Biochim Biophys Acta 1790(9), 906–919.

Jardim MJ, Fry RC, Jaspers I, Dailey L, Diaz-Sanchez D. 2009. Disruption of microRNA expression in human airway cells by diesel exhaust particles is linked to tumorigenesis-associated pathways. Environ Health Perspect 117(11): 1745-1751.

Jin SL, Goya S, Nakae S, Wang D, Bruss M, Hou C, Umetsu D, Conti M. 2010. Phosphodiesterase 4B is essential for T(H)2-cell function and development of airway hyperresponsiveness in allergic asthma. J Allergy Clin Immunol 126(6): 1252-1259 e1212.

Jirtle RL, Skinner MK. 2007. Environmental epigenomics and disease susceptibility. Nat Rev Genet 8(4): 253-262.

Joad JP, Ji C, Kott KS, Bric JM, Pinkerton KE. 1995. *In utero* and postnatal effects of sidestream cigarette smoke exposure on lung function, hyperresponsiveness, and neuroendocrine cells in rats. Toxicol Appl Pharmacol 132(1): 63-71.

Johansson MW, Han ST, Gunderson KA, Busse WW, Jarjour NN, Mosher DF. 2012. Platelet activation, P-selectin, and eosinophil beta1-integrin activation in asthma. Am J Respir Crit Care Med 185(5): 498-507.

Joubert BR, Håberg SE, Nilsen RM, Wang X, Vollset SE, Murphy SK, Huang Z, Hoyo C, Midttun Ø, Cupul-Uicab LA, Ueland PM, Wu MC, Nystad W, Bell DA, Peddada SD, London SJ. 2012. 450K epigenome-wide scan identifies differential DNA methylation in newborns related to maternal smoking during pregnancy. Environ Health Perspect 120(10):1425-1431.

Kajekar R. 2007. Environmental factors and developmental outcomes in the lung. Pharmacol Ther 114(2): 129-145.

Keating DT, Sadlier DM, Patricelli A, Smith SM, Walls D, Egan JJ, Doran PP. 2006. Microarray identifies ADAM family members as key responders to TGF-beta1 in alveolar epithelial cells. Respir Res 7: 114.

Kettunen E, Anttila S, Seppänen JK, Karjalainen A, Edgren H, Lindström I, Salovaara R, Nissén AM, Salo J, Mattson K, Hollmén J, Knuutila S, Wikman H. 2004. Differentially expressed genes in nonsmall cell lung cancer: expression profiling of cancer-related genes in squamous cell lung cancer. Cancer Genet Cytogenet 149(2): 98-106.

Kimura A, Naka T, Nohara K, Fujii-Kuriyama Y, Kishimoto T. 2008. Aryl hydrocarbon receptor regulates Stat1 activation and participates in the development of Th17 cells. Proc Natl Acad Sci U S A 105(28): 9721-9726.

Kips JC, Anderson GP, Fredberg JJ, Herz U, Inman MD, Jordana M, Kemeny DM, Lötvall J, Pauwels RA, Plopper CG, Schmidt D, Sterk PJ, Van Oosterhout AJ, Vargaftig BB, Chung KF. 2003. Murine models of asthma. Eur Respir J 22(2): 374-382.

Knopik VS, Maccani MA, Francazio S, McGeary JE. 2012. The epigenetics of maternal cigarette smoking during pregnancy and effects on child development. Dev Psychopathol 24(4): 1377-1390.

Laan M, Cui ZH, Hoshino H, Lötvall J, Sjöstrand M, Gruenert DC, Skoogh BE, Lindén A. 1999. Neutrophil recruitment by human IL-17 via C-X-C chemokine release in the airways. J Immunol 162(4): 2347-2352.

Lajunen TK, Jaakkola JJ, Jaakkola MS. 2013. The synergistic effect of heredity and exposure to second-hand smoke on adult-onset asthma. Am J Respir Crit Care Med 188(7):776-782.

Lewis BP, Shih IH, Jones-Rhoades MW, Bartel DP, Burge CB. 2003. Prediction of mammalian microRNA targets. Cell 115(7): 787-798.

Li B, Dewey CN. 2011. RSEM: accurate transcript quantification from RNA-Seq data with or without a reference genome. BMC Bioinformatics 12: 323.

Li YF, Gilliland FD, Berhane K, McConnell R, Gauderman WJ, Rappaport EB, Peters JM. 2000. Effects of *in utero* and environmental tobacco smoke exposure on lung function in boys and girls with and without asthma. Am J Respir Crit Care Med 162(6): 2097-2104.

Lindfors A, van Hage-Hamsten M, Rietz H, Wickman M, Nordvall SL. 1999. Influence of interaction of environmental risk factors and sensitization in young asthmatic children. J Allergy Clin Immunol 104(4 Pt 1): 755-762.

Lloyd CM. 2007. Building better mouse models of asthma. Curr Allergy Asthma Rep 7(3): 231-236.

Lu TX, Hartner J, Lim EJ, Fabry V, Mingler MK, Cole ET, Orkin SH, Aronow BJ, Rothenberg ME. 2011. MicroRNA-21 limits in vivo immune response-mediated activation of the IL-12/IFN-gamma pathway, Th1 polarization, and the severity of delayed-type hypersensitivity. J Immunol 187(6): 3362-3373.

Lu TX, Munitz A, Rothenberg ME. 2009. MicroRNA-21 is up-regulated in allergic airway inflammation and regulates IL-12p35 expression. J Immunol 182(8): 4994-5002.

Lu TX, Rothenberg ME. 2013. Diagnostic, functional, and therapeutic roles of microRNA in allergic diseases. J Allergy Clin Immunol 132(1): 3-13; quiz 14.

MacNee W. 2009. Accelerated lung aging: a novel pathogenic mechanism of chronic obstructive pulmonary disease (COPD). Biochem Soc Trans. 37(Pt 4):819-823.

Mandal M, Marzouk AC, Donnelly R, Ponzio NM. 2011. Maternal immune stimulation during pregnancy affects adaptive immunity in offspring to promote development of TH17 cells. Brain Behav Immun 25(5): 863-871.

Mannino DM, Homa DM, Akinbami LJ, Moorman JE, Gwynn C, Redd SC. 2002. Surveillance for asthma--United States, 1980-1999. MMWR Surveill Summ 51(1): 1-13.

Mannino DM, Moorman JE, Kingsley B, Rose D, Repace J. 2001. Health effects related to environmental tobacco smoke exposure in children in the United States: data from the Third National Health and Nutrition Examination Survey. Arch Pediatr Adolesc Med 155(1): 36-41.

Maragkakis M, Reczko M, Simossis VA, Alexiou P, Papadopoulos GL, Dalamagas T, Giannopoulos G, Goumas G, Koukis E, Kourtis K, Vergoulis T, Koziris N, Sellis T, Tsanakas P, Hatzigeorgiou AG. 2009. DIANA-microT web server: elucidating microRNA functions through target prediction. Nucleic Acids Res 37(Web Server issue): W273-276.

Martino DJ, Prescott SL. 2010. Silent mysteries: epigenetic paradigms could hold the key to conquering the epidemic of allergy and immune disease. Allergy 65(1): 7-15.

Martino D, Prescott S. 2011. Epigenetics and prenatal influences on asthma and allergic airways disease. Chest 139(3): 640-647.

Masoli M, Fabian D, Holt S, Beasley R. 2003. Global burben of asthma. http://www.ginasthma.org/local/uploads/files/GINABurdenSummary_1.pdf (accessed March 2014).

Mathews TJ. 2001. Smoking during pregnancy during the 1990s. Natl Vital Stat Rep 49(7):1-14.

McManus MT. 2003. MicroRNA and cancer. Semin Cancer Biol: 13:253-258.

Melgert BN, Postma DS, Kuipers I, Geerlings M, Luinge MA, van der Strate BW, Kerstjens HA, Timens W, Hylkema MN. 2005. Female mice are more susceptible to the development of allergic airway inflammation than male mice. Clin Exp Allergy 35(11): 1496-1503.

Melo SA, Esteller M. 2011. Dysregulation of microRNAs in cancer: playing with fire. FEBS Lett 585(13): 2087-2099.

Miller RL, Ho SM. 2008. Environmental epigenetics and asthma: current concepts and call for studies. Am J Respir Crit Care Med 15;177(6):567-573

Miller RL. 2008. Prenatal maternal diet affects asthma risk in offspring. J Clin Invest 118(10):3265-3268.

Mills CD, Kincaid K, Alt JM, Heilman MJ, Hill AM. 2000. M-1/M-2 macrophages and the Th1/Th2 paradigm. J Immunol 164(12): 6166-6173.

Minamiya Y, Saito H, Ito M, Imai K, Konno H, Takahashi N, Motoyama S, Ogawa J. 2012. Suppression of Zinc Finger Homeobox 3 expression in tumor cells decreases the survival rate among non-small cell lung cancer patients. Cancer Biomark 11(4): 139-146.

Mocchegiani E, Giacconi R, Costarelli L. 2011. Metalloproteases/anti-metalloproteases imbalance in chronic obstructive pulmonary disease: genetic factors and treatment implications. Curr Opin Pulm Med 17 Suppl 1: S11-19.

Moschos SA, Williams AE, Perry MM, Birrell MA, Belvisi MG, Lindsay MA. 2007. Expression profiling in vivo demonstrates rapid changes in lung microRNA levels following lipopolysaccharide-induced inflammation but not in the anti-inflammatory action of glucocorticoids. BMC Genomics 8: 240.

Murphy SK, Adigun A, Huang Z, Overcash F, Wang F, Jirtle RL, Schildkraut JM, Murtha AP, Iversen ES, Hoyo C. 2012. Gender-specific methylation differences in relation to prenatal exposure to cigarette smoke. Gene 494(1):36-43.

Nair MG, Guild KJ, Artis D. 2006. Novel effector molecules in type 2 inflammation: lessons drawn from helminth infection and allergy. J Immunol 177(3): 1393-1399.

Ng SP, Silverstone AE, Lai ZW, Zelikoff JT. 2006. Effects of prenatal exposure to cigarette smoke on offspring tumor susceptibility and associated immune mechanisms. Toxicol Sci 89(1): 135-144.

Nguyen TT, Schwartz EJ, West RB, Warnke RA, Arber DA, Natkunam Y. 2005. Expression of CD163 (hemoglobin scavenger receptor) in normal tissues, lymphomas, carcinomas, and sarcomas is largely restricted to the monocyte/macrophage lineage. Am J Surg Pathol 29(5): 617-624.

Nials AT, Uddin S. 2008. Mouse models of allergic asthma: acute and chronic allergen challenge. Dis Model Mech 1(4-5): 213-220.

Ning W, Li CJ, Kaminski N, Feghali-Bostwick CA, Alber SM, Di YP, Otterbein SL, Song R, Hayashi S, Zhou Z, Pinsky DJ, Watkins SC, Pilewski JM, Sciurba FC, Peters DG, Hogg JC, Choi AM. 2004. Comprehensive gene expression profiles reveal pathways related to the pathogenesis of chronic obstructive pulmonary disease. Proc Natl Acad Sci U S A 101(41): 14895-14900.

Oglesby IK, McElvaney NG, Greene CM. 2010. MicroRNAs in inflammatory lung disease--master regulators or target practice? Respir Res 11: 148.

Olive V, Jiang I, He L. 2010. mir-17-92, a cluster of miRNAs in the midst of the cancer network. Int J Biochem Cell Biol 42(8): 1348-1354.

Osei-Kumah A, Ammit AJ, Smith R, Ge Q, Clifton VL. 2006. Inflammatory mediator release in normal bronchial smooth muscle cells is altered by pregnant maternal and fetal plasma independent of asthma. Placenta 27(8):847-852.

Papiernik M. 1970. Correlation of lymphocyte transformation and morphology in the human fetal thymus. Blood 36(4): 470-479.

Pearce N, Sunyer J, Cheng S, Chinn S, Bjorksten B, Burr M, Keil U, Anderson HR, Burney P. 2000. Comparison of asthma prevalence in the ISAAC and the ECRHS. ISAAC Steering Committee and the European Community Respiratory Health Survey. International Study of Asthma and Allergies in Childhood. Eur Respir J 16(3): 420-426.

Penn A, Chen LC, Snyder CA. 1994. Inhalation of steady-state sidestream smoke from one cigarette promotes arteriosclerotic plaque development. Circulation 90(3): 1363-1367.

Penn A, Snyder CA. 1993. Inhalation of sidestream cigarette smoke accelerates development of arteriosclerotic plaques. Circulation 88(4 Pt 1): 1820-1825.

Penn AL, Rouse RL, Horohov DW, Kearney MT, Paulsen DB, Lomax L. 2007. *In utero* exposure to environmental tobacco smoke potentiates adult responses to allergen in BALB/c mice. Environ Health Perspect 115(4): 548-555.

Phaybouth V, Wang SZ, Hutt JA, McDonald JD, Harrod KS, Barrett EG. 2006. Cigarette smoke suppresses Th1 cytokine production and increases RSV expression in a neonatal model. Am J Physiol Lung Cell Mol Physiol 290(2): L222-231.

Planet E. 2010. phenoTest: Tools to test association between gene expression and phenotype in a way that is efficient, structured, fast and scalable. We also provide tools to do GSEA (Gene set enrichment analysis) and copy number variation.

Ploner A. 2011. Heatplus: Heatmaps with row and/or column covariates and colored clusters.

Quintana FJ, Basso AS, Iglesias AH, Korn T, Farez MF, Bettelli E, Caccamo M, Oukka M, Weiner HL. 2008. Control of T(reg) and T(H)17 cell differentiation by the aryl hydrocarbon receptor. Nature 453(7191): 65-71.

Raherison C, Pénard-Morand C, Moreau D, Caillaud D, Charpin D, Kopferschmitt C, Lavaud F, Taytard A, Maesano IA. 2008. Smoking exposure and allergic sensitization in children according to maternal allergies. Ann Allergy Asthma Immunol 100(4): 351-357.

Rahman I, Adcock IM. 2006. Oxidative stress and redox regulation of lung inflammation in COPD. Eur Respir J 28(1):219-242.

Reynolds PR, Cosio MG, Hoidal JR. 2006. Cigarette smoke-induced Egr-1 upregulates proinflammatory cytokines in pulmonary epithelial cells. Am J Respir Cell Mol Biol 35(3): 314-319.

Robinson MD, McCarthy DJ, Smyth GK. 2010. edgeR: a Bioconductor package for differential expression analysis of digital gene expression data. Bioinformatics 26(1): 139-140.

Rouse RL, Boudreaux MJ, Penn AL. 2007. *In utero* environmental tobacco smoke exposure alters gene expression in lungs of adult BALB/c mice. Environ Health Perspect 115(12): 1757-1766.

Schembri F, Sridhar S, Perdomo C, Gustafson AM, Zhang X, Ergun A, Lu J, Liu G, Zhang X, Bowers J, Vaziri C, Ott K, Sensinger K, Collins JJ, Brody JS, Getts R, Lenburg ME, Spira A. 2009. MicroRNAs as modulators of smoking-induced gene expression changes in human airway epithelium. Proc Natl Acad Sci U S A 106(7): 2319-2324.

Schick S, Glantz S. 2005. Philip Morris toxicological experiments with fresh sidestream smoke: more toxic than mainstream smoke. Tob Control 14(6):396-404.

Schick S, Glantz S. 2006. Sidestream cigarette smoke toxicity increases with aging and exposure duration. Tob Control 14(6):396-404.

Schwarze J, Hamelmann E, Gelfand EW. 2005. Barometric whole body plethysmography in mice. J Appl Physiol (1985) 98(5):1955-1957.

Seike M, Goto A, Okano T, Bowman ED, Schetter AJ, Horikawa I, Mathe EA, Jen J, Yang P, Sugimura H, Gemma A, Kudoh S, Croce CM, Harris CC. 2009. MiR-21 is an EGFR-regulated anti-apoptotic factor in lung cancer in never-smokers. Proc Natl Acad Sci U S A 106(29): 12085-12090.

Sethi JM, Rochester CL. 2000. Smoking and chronic obstructive pulmonary disease. Clin Chest Med 21(1): 67-86, viii.

Singh SP, Barrett EG, Kalra R, Razani-Boroujerdi S, Langley RJ, Kurup V, Tesfaigzi Y, Sopori ML. 2003. Prenatal cigarette smoke decreases lung cAMP and increases airway hyperresponsiveness. Am J Respir Crit Care Med 168(3): 342-347.

Singh SP, Gundavarapu S, Peña-Philippides JC, Rir-Sima-ah J, Mishra NC, Wilder JA, Langley RJ, Smith KR, Sopori ML. 2011. Prenatal secondhand cigarette smoke promotes Th2 polarization and impairs goblet cell differentiation and airway mucus formation. J Immunol 187(9): 4542-4552.

Singh SP, Mishra NC, Rir-Sima-Ah J, Campen M, Kurup V, Razani-Boroujerdi S, Sopori ML. 2009. Maternal exposure to secondhand cigarette smoke primes the lung for induction of phosphodiesterase-4D5 isozyme and exacerbated Th2 responses: rolipram attenuates the airway hyperreactivity and muscarinic receptor expression but not lung inflammation and atopy. J Immunol 183(3): 2115-2121.

Skinner MK, Guerrero-Bosagna C. 2009. Environmental signals and transgenerational epigenetics. Epigenomics 1(1): 111-117.

Small EM, Frost RJ, Olson EN. 2010. MicroRNAs add a new dimension to cardiovascular disease. Circulation 121(8): 1022-1032.

Smyth GK. 2004. Linear models and empirical bayes methods for assessing differential expression in microarray experiments. Stat Appl Genet Mol Biol 3: Article3.

Sonkoly E, Pivarcsi A. 2009. Advances in microRNAs: implications for immunity and inflammatory diseases. J Cell Mol Med 13(1): 24-38.

Squadrito ML, Pucci F, Magri L, Moi D, Gilfillan GD, Ranghetti A, Casazza A, Mazzone M, Lyle R, Naldini L, De Palma M. 2012. miR-511-3p modulates genetic programs of tumor-associated macrophages. Cell Rep 1(2): 141-154.

Staples KJ, Hinks TS, Ward JA, Gunn V, Smith C, Djukanovic R. 2012. Phenotypic characterization of lung macrophages in asthmatic patients: Overexpression of CCL17. J Allergy Clin Immunol 130(6):1404-1412.e7.

Stewart DJ. 2014. Wnt signaling pathway in non-small cell lung cancer. J Natl Cancer Inst 106(1):djt356.

Stocks J, Hislop A, Sonnappa S. 2013. Early lung development: lifelong effect on respiratory health and disease. Lancet Respir Med: 1(9):728-742.

Strazisar M, Mlakar V, Glavac D. 2009. LATS2 tumour specific mutations and down-regulation of the gene in non-small cell carcinoma. Lung Cancer 64(3): 257-262.

Suzuki S, Kokubu F, Kawaguchi M, Homma T, Odaka M, Watanabe S, Ieki K, Matsukura S, Kurokawa M, Takeuchi H, Sasaki Y, Huang SK, Adachi M, Ota H. 2007. Expression of interleukin-17F in a mouse model of allergic asthma. Int Arch Allergy Immunol 143 Suppl 1: 89-94.

Szyf M. 2007. The dynamic epigenome and its implications in toxicology. Toxicol Sci: 100(101):107–123.

Tamaru H, Selker E. 2001. A histone H3 methyltransferase controls DNA methylation in Neurospora crassa. Nature 414: 277-283.

Tang D, Shen Y, Wang M, Yang R, Wang Z, Sui A, Jiao W, Wang Y. 2013. Identification of plasma microRNAs as novel noninvasive biomarkers for early detection of lung cancer. Eur J Cancer Prev 22(6):540-548.

Tang WY, Ho SM. 2007. Epigenetic reprogramming and imprinting in origins of disease. Rev Endocr Metab Disord 8(2): 173-182.

Tantisira KG, Colvin R, Tonascia J, Strunk RC, Weiss ST, Fuhlbrigge AL. 2008. Airway responsiveness in mild to moderate childhood asthma: sex influences on the natural history. Am J Respir Crit Care Med 178(4): 325-331.

Tantisira KG, Silverman ES, Mariani TJ, Xu J, Richter BG, Klanderman BJ, Litonjua AA, Lazarus R, Rosenwasser LJ, Fuhlbrigge AL, Weiss ST. 2007. FCER2: a pharmacogenetic basis for severe exacerbations in children with asthma. J Allergy Clin Immunol 120(6): 1285-1291.

Temelkovski J, Hogan SP, Shepherd DP, Foster PS, Kumar RK. 1998. An improved murine model of asthma: selective airway inflammation, epithelial lesions and increased methacholine responsiveness following chronic exposure to aerosolised allergen. Thorax 53(10): 849-856.

Tili E, Michaille JJ, Cimino A, Costinean S, Dumitru CD, Adair B, Fabbri M, Alder H, Liu CG, Calin GA, Croce CM. 2007. Modulation of miR-155 and miR-125b levels following lipopolysaccharide/TNF-alpha stimulation and their possible roles in regulating the response to endotoxin shock. J Immunol 179(8): 5082-5089.

Tölgyesi G, Molnár V, Semsei AF, Kiszel P, Ungvári I, Pócza P, Wiener Z, Komlósi ZI, Kunos L, Gálffy G, Losonczy G, Seres I, Falus A, Szalai C. 2009. Gene expression profiling of experimental asthma reveals a possible role of paraoxonase-1 in the disease. Int Immunol 21(8): 967-975.

Tomita M, Okuyama T, Katsuyama H, Miura Y, Nishimura Y, Hidaka K, Otsuki T, Ishikawa T. 2007. Mouse model of paraquat-poisoned lungs and its gene expression profile. Toxicology 231(2-3): 200-209.

U.K. Ministry of Health. 1954. Mortality and Morbidity during the London Fog of December 1952. Reports on Public Health and Medical Subjects No. 95. London: Ministry of Health.

Veldhoen M, Hirota K, Westendorf AM, Buer J, Dumoutier L, Renauld JC, Stockinger B. 2008. The aryl hydrocarbon receptor links TH17-cell-mediated autoimmunity to environmental toxins. Nature 453(7191): 106-109.

Volinia S, Calin GA, Liu CG, Ambs S, Cimmino A, Petrocca F, Visone R, Iorio M, Roldo C, Ferracin M, Prueitt RL, Yanaihara N, Lanza G, Scarpa A, Vecchione A, Negrini M, Harris CC, Croce CM. 2006. A microRNA expression signature of human solid tumors defines cancer gene targets. Proc Natl Acad Sci U S A 103(7): 2257-2261.

Wang NJ, Sanborn Z, Arnett KL, Bayston LJ, Liao W, Proby CM, Leigh IM, Collisson EA, Gordon PB, Jakkula L, Pennypacker S, Zou Y, Sharma M, North JP, Vemula SS, Mauro TM, Neuhaus IM, Leboit PE, Hur JS, Park K, Huh N, Kwok PY, Arron ST, Massion PP, Bale AE, Haussler D, Cleaver JE, Gray JW, Spellman PT, South AP, Aster JC, Blacklow SC, Cho RJ. 2011. Loss-of-function mutations in Notch receptors in cutaneous and lung squamous cell carcinoma. Proc Natl Acad Sci U S A 108(43): 17761-17766.

Wang YH, Wills-Karp M. 2011. The potential role of interleukin-17 in severe asthma. Curr Allergy Asthma Rep 11(5): 388-394.

Weaver IC, Szyf M, Meaney MJ. 2002. From maternal care to gene expression: DNA methylation and the maternal programming of stress responses. Endocr Res 28(4):699.

Wang Z, Gerstein M, Snyder M. 2009. RNA-Seq: a revolutionary tool for transcriptomics. Nat Rev Genet 10(1):57-63.

Wignarajah, D., Cock, M.L., Pinkerton, K.E., Harding, R., 2002. Influence of intrauterine growth restriction on airway development in fetal and postnatal lung. Pediatr Res 51(6):681-688.

Williams AE, Moschos SA, Perry MM, Barnes PJ, Lindsay MA. 2006. Maternally imprinted microRNAs are differentially expressed during mouse and human lung development. Dev Dyn: 236:572-580.

Williams AE, Perry MM, Moschos SA, Lindsay MA. 2007. microRNA expression in the aging mouse lung. BMC Genomics 8:172.

Wilson RH, Whitehead GS, Nakano H, Free ME, Kolls JK, Cook DN. 2009. Allergic sensitization through the airway primes Th17-dependent neutrophilia and airway hyperresponsiveness. Am J Respir Crit Care Med 180(8): 720-730.

Wright RJ. 2010. Perinatal stress and early life programming of lung structure and function. Biol Psychol 84(1):46-56.

Wu DW, Tsai LH, Chen PM, Lee MC, Wang L, Chen CY, Cheng YW, Lee H. 2012. Loss of TIMP-3 promotes tumor invasion via elevated IL-6 production and predicts poor survival and relapse in HPV-infected non-small cell lung cancer. Am J Pathol 181(5): 1796-1806.

Xiao R, Perveen Z, Paulsen D, Rouse R, Ambalavanan N, Kearney M, Penn AL. 2012. *In utero* exposure to second-hand smoke aggravates adult responses to irritants: adult second-hand smoke. Am J Respir Cell Mol Biol 47(6): 843-851.

Xiao R, Perveen Z, Rouse RL, Le Donne V, Paulsen DB, Ambalavanan N, Penn AL. 2013. *In utero* exposure to second-hand smoke aggravates the response to ovalbumin in adult mice. Am J Respir Cell Mol Biol 49(6):1102-1109.

Yamamoto M, Singh A, Sava F, Pui M, Tebbutt SJ, Carlsten C. 2013. MicroRNA expression in response to controlled exposure to diesel exhaust: attenuation by the antioxidant N-acetylcysteine in a randomized crossover study. Environ Health Perspect 121(6): 670-675.

Yang M, Shen H, Qiu C, Ni Y, Wang L, Dong W, Liao Y, Du J. 2013. High expression of miR-21 and miR-155 predicts recurrence and unfavourable survival in non-small cell lung cancer. Eur J Cancer 49(3): 604-615.

Yoshida K. 1984. Air Pollution and its Transition in Yokkaichi (review). Report of the Environmental Science of Mie University, 9,93-1

Zhang C, Chi YL, Wang PY, Wang YQ, Zhang YX, Deng J, Lv CJ, Xie SY. 2012. miR-511 and miR-1297 inhibit human lung adenocarcinoma cell proliferation by targeting oncogene TRIB2. PLoS One 7(10): e46090.

Zhao M, Sun J, Zhao Z. 2013. TSGene: a web resource for tumor suppressor genes. Nucleic Acids Res 41(Database issue): D970-976.

Zlotkowska R, Zejda JE. 2005. Fetal and postnatal exposure to tobacco smoke and respiratory health in children. Eur J Epidemiol 20(8): 719-727.

APPENDIX.
REPRINT PERMISSION FROM AMERICAN THORACIC SOCIETY.

Gmail by Google

Rui Xiao <ruixiao85@gmail.com>

Request permission to reprint two red journal articles in my dissertation.

2 messages

Rui Xiao <rxiao1@tigers.lsu.edu> Wed, Jan 8, 2014 at 11:58 AM
To: permissions@thoracic.org

Dear Ms. Gern:

My name is Rui Xiao, a student member of ATS, who has two first-author publications on the red journal (AJRCMB) in the past two years. Now I am completing my doctoral dissertation at Louisiana State University entitled "*In utero* exposure to second-hand smoke aggravates adult responses to inhaled irritants." I would like your permission to reprint in full, the following articles in my dissertation:

1. *In utero* exposure to second-hand smoke aggravates the response to ovalbumin in adult mice.

Xiao R, Perveen Z, Rouse RL, Le Donne V, Paulsen DB, Ambalavanan N, Penn AL.

Am J Respir Cell Mol Biol. 2013 Dec;49(6):1102-9.

PMID: 23898987

2. *In utero* exposure to second-hand smoke aggravates adult responses to irritants: adult second-hand smoke.

Xiao R, Perveen Z, Paulsen D, Rouse R, Ambalavanan N, Kearney M, Penn AL.

Am J Respir Cell Mol Biol. 2012 Dec;47(6):843-51.

PMID: 22962063

LSU is a member of the Networked Digital Library of Theses and Dissertations (http://www.ndltd.org/). The requested permission extends to any future revisions and editions of my dissertation, including non-exclusive world rights in all languages, and to the prospective publication of my dissertation by UMI Company. These rights will in no way restrict republication of the material in any other form by you or by others authorized by you.

If these arrangements meet with your approval, could you please confirm the ATS copyright ownership of the above-described material and grant me the reprint permission? Thank you very much.

Sincerely,

Rui Xiao

PhD Candidate

CBS Department, School of Veterinary Medicine,

Skip Bertman Dr., Baton Rouge, LA 70803

ATS Permission Requests <permissions@thoracic.org> Wed, Jan 8, 2014 at 3:54 PM
To: Rui Xiao <rxiao1@tigers.lsu.edu>

Dear Rui,

You are free to re-use the articles in your dissertation, so long as the copyright is clearly noted, as follows:

Reprinted with permission of the American Thoracic Society. Copyright © 2014 American Thoracic Society.

Cite: Author(s)/Year/Title/Journal Title/Volume/Pages.

Official Journal of the American Thoracic Society.

In addition, if the dissertation is to be posted publicly on an electronic repository, you must wait until 6 months after the initial publication of the article; in this case, as the most recent article appeared on December 1st, that will be June 1st, 2014.

Best,

Dan Fallon

dfallon@thoracic.org

American Thoracic Society

VITA

Rui Xiao was born in Wuhu, Anhui province, China, in the winter of 1985. He is the only child to a family of a kind father, a high school teacher, and a strict mother, a physician. As his father became more accomplished in his career as a teacher, the whole family moved to the city of Shanghai, soon after Rui went through middle school. A few years later, he went to Shanghai Jiao Tong University and majored in animal biotechnology. By the time for him to get the Bachelor's degree in the year 2008, one of his graduate school applications went through and he finally got in touch with Dr. Arthur Penn, who then provided him the opportunity to join the laboratory and work towards a PhD degree at LSU School of Veterinary Medicine. Now in the Spring of 2014, Rui Xiao is completing his PhD degree and will pursue a postdoc position at Columbia University Medical Center.